THE CURRENT SITUATION OF VEHICLE CRASH COMPATIBILITY IN JAPAN AND ITS IMPROVEMENT

July, 1999

Koji Mizuno

ABSTRACT

In car-to-car collisions, the injury risks to the driver in each car differ due to the differences of mass, stiffness and geometry of both vehicles. This compatibility problem was firstly discussed in the 1970's, however, it has not been solved yet. There has been no research on vehicle compatibility considering the traffic situations in Japan. Therefore, this thesis focuses on the compatibility in Japan, and its countermeasures are examined. Total compatibility including cars, trucks, pedestrians and road environments was investigated by a combination of accident data analysis and computer simulations.

The compatibility of cars is influenced by the difference in the mass, stiffness and geometry. As the vehicle mass has the largest effect on the vehicle compatibility, the injury risk was formulated based on the average mass of the car. The stiffness and geometry compatibility was examined by accident analysis.

In traffic situations in Japan, it was shown based on accident data, that the high aggressivity of trucks and the poor self-protection of mini cars have to be improved to accomplish total compatibility. Irrespective of low self-protection of mini cars due to its small mass and low stiffness, this type of car is increasing. Two countermeasures for poor self-protection of the mini car were analyzed using MADYMO. The first is to stiffen the mini car and to install an optimum restraint system, and the second is to provide a large car with additional crush space designed for a crash with a mini car. Either method can reduce the injury risk to the driver in the mini car.

Current test procedures for frontal impact were examined to evaluate the vehicle compatibility. The full rigid barrier and offset deformable crash tests which are currently adopted in the regulations, can not reproduce the injury risks of the driver in car-to-car crashes even by changing the impact velocity. In order to evaluate the compatibility performance of the car correctly, it is necessary that the MDB test procedures is introduced and self- and partner-protection of the car are measured.

In a car-to-truck collision, the injury risk of the driver in the car is extremely high. Accident analysis shows that the geometry incompatibility leads to large intrusion into the car compartment, which results in a high injury risk to the driver in the car. The effectiveness of the underrun guard of the truck was examined by mathematical simulation and the optimal force levels to reduce the injury risk were proposed.

In the present study, the car-pedestrian compatibility was also examined. Based on the results from the accident analyses and simulations, it is found that the vehicle shape has large effects on the injury risk to the pedestrian. In order to clarify the head injury risk with impact with various parts of the car, the headform impact tests were carried out. The HICs in the impact of the car including windscreen regions were clarified.

Key Words: Safety, Traffic accident, Compatibility, Injury risk, Car-to-car collision, Car-to-truck collision, Pedestrian accident, Single-car crash, Crash test procedure, Accident analysis, Multi-body simulation

CONTENTS

ABBREVIATIONS

AIS	Abbreviated Injury Scale
AM50	American Male 50 percentile
CTP	Component Test Procedure
EBS	Equivalent Barrier Speed
ECE	Economic Commission for Europe
EEVC	European Experimental Vehicle Committee
ESV	Experimental (Enhanced) Safety of Vehicles
FARS	Fatality Analysis Reporting System
FMVSS	Federal Motor Vehicle Safety Standards
FUPS	Front Underrun Prevention System
GEBOD	Generator of Body Data
GVW	Gross Vehicle Weight
HIC	Head Injury Criteria
HPC	Head Performance Criteria
IIHS	Insurance Institute for Highway Safety
IHRA	International Harmonized Research Activities
ITARDA	Institute for Traffic Accident Research and Data Analysis
ISO	International Standard Organization
JAMA	Japan Automobile Manufactures Association
LMV	Low Mass Vehicle
LTV	Light Trucks and Vans
MADYMO	Mathematical Dynamic Model
MAIS	Maximum AIS
MDB	Moving Deformable Barrier
MEBS	Mass-related Equivalent Barrier Speed
NCAP	New Car Assessment Program
NHTSA	National Highway Traffic Safety Administration
ODB	Offset Deformable Barrier
PDOF	Principal Direction of Force
SID	Side Impact Dummy
SUV	Sports Utility Vehicle
TTI	Thoracic Trauma Index
WAD	Wrap Around Distance

1. INTRODUCTION

1.1. TRAFFIC SAFETY

1.1.1. The Scope of the Problem

In the world, about 15 million people are injured each year in traffic accidents, five million require in-patient hospital treatment and half a million die [IRF 1995]. In Japan, about 10 thousand people are fatally injured and one million are injured in traffic accidents every year [ITARDA 1998]. However, it is generally recognized that the injury is a problem that can be controlled by injury prevention strategies.

In the USA, the number of deaths due to heart diseases is a quarter of a million, and those due to cancer are half a million, which is far larger than that due to traffic injuries [Injury in America 1984]. However, when one estimate the preretirement years of life lost, traffic accidents are about twice that of cancer and heart disease. Judging by the level of research expenditure for the causes and countermeasures, the importance of traffic accidents is too underestimated.

1.1.2. Injury Control Strategies in Traffic Accidents

Traffic injury problems and its countermeasures are very difficult to investigate because the problem is large and wide. One useful approach is to consider the traffic injury problems as resulting from an interaction of different factors that consist of time and space. Haddon (1981) developed a matrix to consider the traffic injury problem by factors which occurred in different phases in time and space (see Figure 1.1). The time can be classified as before the injury-producing event, during the event and after the event. The space which causes injuries are divided into three factors: the human being, the vehicles and equipment, and the environment. For developing a program of injury reduction, we should discuss the problems and countermeasures through each cell of the Haddon's matrix in a systematic manner.

The precrash category consists of all actions related to the occurrences of the accidents. For example, anti-lock brakes are included in this category. The crash category includes only the time during impact. The crashworthiness, seatbelts and airbags are included in this crash category. The postcrash category consists of all the time after impact, and treatment and rehabilitation of the victim are included.

		Factors		
		HUMAN	VEHICLE AND EQUIPMENT	ENVIRONMENT
Phases	PRECRASH			
	CRASH			
	POSTCRASH			

Figure 1.1. Haddon's matrix.

Though traffic safety has been discussed as if the only goal in creating traffic system were safety, the goal is mobility [Evans 1992]. Traffic injury is a side effect of mobility. Safety measures such as speed restrictions, driver licensing and drunk driver laws reduce the mobility. Active and passive protection devices, vehicle safety improvements and improved emergency medicine do not affect mobility. On the other hand, safety measures such as upgrading roads, improving vehicle handling and brakes can increase mobility. The injury reduction strategy should be adopted so as not to interfere with traffic mobility.

The increased safety is sometimes in conflict with other human activities. The use of a restraint system restricts the freedom of the human. However, the mandatory use of restraint system has more merit. It is society that pays the cost of the injuries of the unbelted occupants.

Five categories of strategy for injury reduction can be counted [Trinca, G. et al 1988].

- Exposure control
- Behavior modification
- Crash prevention
- Injury control
- Post-injury management

The approach to adopt these strategies varies with traffic situations in each country.

Exposure control

Traffic safety can be accomplished by reducing the amount of travel, or moving by safer forms of travel. Exposure can be controlled by the vehicle, roadway and user restrictions. The measures which limit the highest risk forms of travel are particularly effective.

The modal shift from personal transport to the mass transit like trains and buses will be useful to reduce injury exposure. Electronic communication also has the potential to be an alternative for transport. Another way of exposure control is achieved by vehicle restrictions. The control of car sales, licensing, taxation and insurance procedures can control the use of vehicles. Roadway restrictions are also commonly performed for exposure control. The vehicle mix problems such as the car/truck segregation and pedestrians/vehicle separation are important roadway restrictions. The exposure

control by user restrictions can be achieved through licensing. The most common method is the control of the age for user license since young people are particularly at high risk.

Behavior modification

Human behavior is considered important to achieve traffic safety. Many researchers report that more than 90% of injury causes are due to human factors. Education and the law are important strategies for behavior modification. The traffic laws can control behavior and punish activities like speeding, jay walking and driving under the influence of alcohol which may lead to collisions.

Training of human performance is quite effective for behavior that occurs frequently and where there is time to decide on behavior, like wearing a seatbelt. On the other hand, people are less skillful for behavior in situations that occur infrequently. However, it is indicated that the education about panic braking is effective for shortening the stopping distance in an emergency situation. Education is important for pedestrians, bicyclists and drivers to recognize their responsibilities to each other. Licensing is an education process as well as exposure control, which can be accomplished by issuing, controlling and withdrawing a license.

The human behavior is difficult to improve. Therefore, the viewpoint has been advanced that the vehicle and roadway itself are equally important to prevent accidents. Improving the vehicle and road environment so as to be more tolerant to human errors means that the number of accidents can be reduced.

Crash prevention

The vehicle engineering such as the design, construction and maintenance of vehicles, and the road engineering influence the occurrence of traffic accidents.

The road systems in the road design and construction are fundamental to the reduction of traffic injuries. High quality signing and street lighting facilitate safe travel for road users. It is also important to separate traffic for trucks, buses, cars, motorcycles, cycles and pedestrians.

For vehicle engineering, design and operating characteristics influence the crash prevention. There are two basic vehicle characteristics that lead to crash avoidance. The ability of the driver to see and be seen is fundamental for safe traffic flow. This calls for adequate lights and reflectors. The other fundamental category of crash prevention is the ability to stop the vehicle. Anti-lock brake system serves to keep stability of the vehicles direction of travel and steerability by preventing wheel locking during emergency braking.

The electronics and information technology of both the road systems and the vehicle will prevent crash occurrences. The Intelligent Transport System (ITS) is a new transport system which is comprised of an advanced information and telecommunications network for users, roads and vehicles. The ITS is intended to enhance the advances in navigation systems, establishment of electronic toll collection, assistance for safe driving, optimization of traffic management and increasing efficiency in road management. Advanced Safety Vehicles (ASV) is a project of the Japanese Ministry of Transport,

which forms a part of the technological platform of ITS as a vehicle [Ministry of Transport 1997]. This project aims to promote research and development of safe vehicle technology for the future, taking into consideration the possibility of autonomous driving as well.

Injury control

It is difficult to prevent accidents because humans make mistakes by their very nature. Although the accidents are difficult to prevent, the injuries can be prevented by improving the vehicle design and the road environment. Injury control is based on recognition that injury risk can be reduced if the actual conditions of the impact are modified. It is a powerful strategy for reducing the severity and frequency of injuries to all road users.

It is necessary to clarify the injury causes and the mechanisms of crash injury, and to design systems to reduce crash injuries. For this research, detailed data collection of the collisions should be conducted. The data should be examined from the viewpoint of vehicle engineering, biomechanics and human behavioral science.

For vehicle design, the crashworthiness principles can be applied to all road users, though they are adapted only to passenger cars. Crashworthiness designs are controlled by international standards of vehicle safety. The optimal crashworthiness of cars, and the restraint system such as seatbelts and airbags can reduce the injury severity of the occupants in the car.

The first attempt of injury control to reduce the number of fatalities and injuries occurring as a result of frontal crashes was introduced by the National Highway Traffic Safety Administration (NHTSA) in the USA in 1972 by promulgating the Federal Motor Vehicle Safety Standard (FMVSS) No. 208, Occupant Crash Protection. This standard requires occupant safety in a frontal impact crash test into a rigid barrier at 30 mph (48.3 km/h).

The crashworthiness of cars has been improved by this crash test requirement. However, side effects of this test procedure were also indicated because only self-protection of cars has been considered in the regulations, and it does not always lead to the safety of the occupants in the other vehicle. The crash test into a rigid barrier does not reflect the safety of the vehicle that the subject car collides with. This full rigid barrier test may lead to a stiffer front end of a heavier car than a lighter car so as to protect the integrity of the car compartment from its large inertial force [Prasad et al. 1995].

Both light and heavy cars meet the rigid barrier crash test of the FMVSS because there are no mass effect in this type of test. The crashworthiness of the car has attained to a high level due to the optimal car structure and the safety devices, irrespective of vehicle mass. Whereas, in the real world in head-on collision, the consequences for light cars are still likely to be severe. Although there is law to prevent high vehicle speeds, no considerations are given to heavy cars which are also aggressive to other cars. The safety of both cars in collisions (compatibility) should be considered for the total safety of the vehicles.

One of the complexities of traffic safety is the great variation in vehicle fleet. Crash compatibility between different classes of vehicles is also an important issue of the injury control strategy. Conflicts between cars, trucks, pedestrians, motorcyclists and cyclists can be reduced by application of appropriate technologies and standards. However, currently the safety standards are applied only to passenger cars. In a car-to-truck collision, the consequence is serious for the car. The safety benefits of all road users including car occupant, motorcyclist, cyclist and pedestrians should be considered in order to reduce the total number of fatalities.

Crash energy management principles can also be applied to the road environment. When a vehicle goes off the road and strikes an object, the injury risks of the occupants are affected by the size and stiffness of the object. The design of signs and signal supports, bridge structures, guardrails and rigid poles affect the probability of injury in a crash. The road authorities and organizations that manage these objects are partly responsible for the outcome of crashes with these objects. The design of these objects can change the consequence of these crashes.

Post-injury management

If the accidents cannot be prevented and injuries cannot be eliminated, recovery, treatment and rehabilitation measures can reduce the severity of injuries. Survival and the extent of recovery depend on the initial care in the accidents because 50% of fatalities occur within minutes, and 35% of fatalities are within two hours after accidents.

1.2. CAR COMPATIBILITY

In car-to-car collisions, the injury risks to the occupants are affected not only by their cars but also by the partner cars. However, cars have been designed mainly to improve self-protection, which is referred to as crashworthiness. The frontal and side impact tests do not consider the compatibility problems. This leads to individual cars with different structure, size and mass.

The topics of compatibility were first discussed at the Conference on the Experimental (Enhanced) Safety Vehicles (ESV) in 1970 when the concept of car aggressivity emerged. The compatibility was first discussed in side collisions [Chillon 1971] and later in head-on collisions [Appel 1971]. However, during 20 years, compatibility has not been considered by car manufactures, while performance of restraint system has been greatly improved. In the 15th ESV, the compatibility has become one of the 6 subjects of the International Harmonized Research Activities (IHRA) of ESV, where the EC/EEVC has a leading responsibility [NHTSA 1996]. In IHRA the aim of the effort is to develop the internationally agreed test procedures designed to improve the compatibility of car structures in front to front and side car-to-car impacts. The report will be published in the 17th ESV conference in 2001. Recently in the highly-motorized countries, the vehicle population variation has increased and car types with different shapes such as the SUV and the pickup are also increasing. In the United States,

the NHTSA has started a research program on this subject [Hollowell and Gabler 1996]. In Japan, there is little research on the subject of vehicle compatibility.

Most projects have focused on the compatibility in car-to-car frontal collisions. Therefore, in the following paragraphs, the compatibility of this crash configuration is reviewed from Parts 1.2.1 to 1.2.8, that of side collisions in 1.2.9, and that of single-car crash in 1.2.10.

1.2.1. Definition of Compatibility

Compatibility is defined as the vehicle combination that ensures a high level of occupant safety in both vehicles in vehicle-to-vehicle collisions. Therefore, the compatibility ensures that passenger vehicles of disparate size provide an equal level of occupant protection. The compatibility consists of *self-protection* and *partner-protection*. Self-protection is protection of the occupants in the subject car when involved in a crash (*crashworthiness*), while partner-protection is protection of the occupants in the other vehicle. The opposite of partner-protection is *aggressivity*, which causes a high probability of death in the other car. The crashworthiness and aggressivity are two different aspects of vehicle safety and they are not necessarily consistent. The goal of vehicle compatibility is to minimize the number of fatalities while the injury rates of the occupants in each vehicle remain the same.

The compatibility of the car in car-to-car collisions has been considered most important because the number of injuries in these collisions is large. On the other hand, since the injury risk to the occupants in cars is much higher than that in trucks, car-to-truck compatibility is also important.

In a larger sense, the compatibility can be extended to single-car crashes since the partner-protection of the fixed objects is important in terms of crush energy absorption. The impact of vehicles with vulnerable road users such as pedestrians and cyclists can also be included in the concept of compatibility because in these types of accidents the partner-protection of the vehicle is important [Appel 1995, Schimmelpfenning 1996, Tarrière 1997]. We define *total compatibility* as the combination of vehicle and its crash-partner which has a high level of protection of all vehicle occupants and vulnerable road users involved in all types of crashes including car-to-car, car-to-truck, single-car and also car-to-pedestrian impacts.

1.2.2. Factors Affecting Compatibility

In general, crash compatibility can be attributed to the following three causes resulting from three characteristics of vehicle design as follows (see Figure 1.2) [Ventre 1972]:

- *Mass compatibility*
- *Stiffness compatibility*
- *Geometry compatibility*

The larger the difference of mass, stiffness and geometry become between two-vehicles, the more the vehicles are incompatible. The difference of the vehicle mass has the largest effects on the occupant injury risk in car-to-car crashes. The incompatibility of stiffness leads to large intrusions into the

compartment of the less-stiff car. Due to the geometry incompatibility, the subject car underrides the other car, and the car body can not absorb the crush energy as it was designed to.

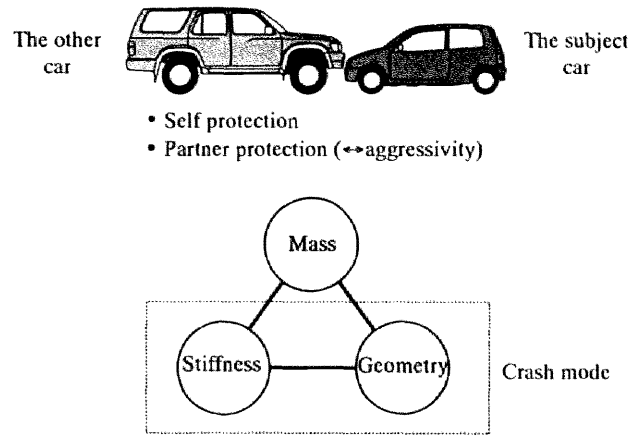

Figure 1.2. Factors which affect compatibility.

The *collision type* (*crash mode*) of frontal, offset frontal, oblique, side and rear affects the stiffness and geometry compatibility due to the change of the force interaction between two vehicles. Collision type is an important factor governing vehicle crashworthiness because it determines how the two car's structures interact. Therefore, collision type has a modifying influence on the effect of compatibility parameters such as geometry and stiffness [Wykes 1998].

1.2.3. Mass Compatibility

Cars of unequal mass

Accident data from many countries show that the occupants in a lighter vehicle have a higher risk of injury than those in a heavier vehicle. Campbell and Reifnfurt (1973) were among the first to undertake to identify the safety consequences according to vehicle model and weight from police reported crashes. They reported an inverse relationship between vehicle weight and relative injury frequency in car-to-car collisions. This relationship was also found in the analysis of accident data in many countries: The United States [Evans 1983], Germany [Ernst et al 1991], France [Fontaine 1992, Tarrière 1994], the United Kingdom [Grime and Hutchinson 1982], Sweden [Aldman 1984], Australia [Cameron 1992]. However, in Japan, there are no publications which indicate the relation between vehicle mass and injury risk.

The magnitude of the mass effect on the occupant injury rate is different among the various studies. Grime and Hutchinson (1982) reported that when cars with a mass ratio of two collide head-on, the percentage of driver death was about 7 times larger in the lighter vehicle. The influence of the mass effect on injury rates increased with increasing injury severity. For serious injury, the ratio of percentages was about 3 for a mass ratio of two.

Aldman et al. (1984) described trends in vehicle safety in terms of the frequency and severity of injuries in passenger cars in Sweden. The severity of injuries decreased significantly with increasing

car weight, and this was true from slightly injured to fatally injured occupants. The frequency of driver death in cars of the smallest class (less than 950 kg) was 1.9 times higher than that in the largest class (more than 1250 kg).

Evans has many publications on the effects of the vehicle mass on the injury risk of the occupants using accident data. He (1983) reported that in crashes between 900 kg cars and 1800 kg cars, eight times as many occupants of the smaller cars were killed in comparison to the larger cars. In accident analysis, there is an exposure problem such that the heavier cars are more inclined to be involved in severe accidents. To solve this problem, Evans used the number of pedestrian fatalities for a measure of exposure [Evans 1991b]. He assumed that the number of pedestrian is independent of the vehicle mass and it can reflect the car velocity. Thus, the number of driver fatalities divided by that of pedestrian fatalities in the same mass categories was examined. Based on the analysis of head-on collisions using the Fatality Analysis Reporting System (FARS), he concludes that when 900 kg and 1800 kg cars crash into each other, the risk of driver death in the small car is about 14 times what it is in the large car. The correctness of using pedestrian fatalities as an exposure measure has not been confirmed yet.

Delta-V is defined as the velocity change of the car passenger compartment during an impact and is used as an indicator of impact severity. Generally, the injury severity of the occupant in a car is strongly related to delta-V. In two-car crashes, the ratio of delta-V is inversely proportional to the mass ratio of the cars. Evans (1993, 1994) showed that the ratio of the driver fatality risk in the lighter car to the risk in the heavier car increases as a power function of the mass ratio as follows:

$$\frac{R_1}{R_2} = \left(\frac{m_2}{m_1}\right)^k \tag{1.1}$$

He determined the parameter k for various crash configurations. For example, the parameter k is 3.53 for all driver fatalities. Since the FARS that he used for the analysis includes only fatalities without including the data of the injuries and no-injuries, the absolute injury rate of the occupant could not be evaluated.

Cars of similar mass

When cars with identical mass crash, the mass does not influence the crash dynamics. However, some analyses using accident data have shown that the injury risk is lower when two heavy cars crash compared with two light cars [Evans 1987, Ernst et al 1991], and vice versa [Dreyer 1981]. This problem is difficult to analyze using accident data because heavy cars in general travel at higher velocity than smaller cars.

Evans and Waielewsk (1987) evaluated the likelihood of driver fatalities in head-on collisions using the estimating exposure approach, in which they used pedestrian fatalities as a measure of accident involvement. A driver in a 900 kg car crashing head-on into another 900 kg car was 2.0 times as likely to be killed as was a driver in an 1800 kg car crashing head-on into another 1800 kg car. They

concluded that this could be interpreted as a size effect where crush material and space are different between small and large cars.

On the other hand, there have been some investigations which indicated that there is not a significant difference of the injury risks in collisions of vehicles with identical mass [Grime and Hutchinson 1982, Thomas et al. 1990, Fontaine 1992, Bloch 1994]. However, the basic theory has not been presented up to now on whether the vehicle mass has effects on the injury risk of the driver in a crash of two cars with equal mass.

1.2.4. Stiffness Compatibility

Stiffness and deformation

The stiffness of the car front structures also has a large effect on the vehicle compatibility. Since the accident data have shown that the intrusion into the compartment is one of the main causes of death of the occupants, the stiffness is an important factor for compatibility.

From a frontal crash test into a rigid barrier, it was found that the force-deflection characteristics of the car can be approximated by a line [Emori 1968] and its coefficient is called linear stiffness. Gabler and Hollowell (1998) reported that there is a wide variation in relations between linear stiffness and car aggressivity compared with factors of mass. Because the stiffness of a vehicle is related to its mass, stiffness may not be proved to be a factor as dominant as mass for compatibility.

In general, the stiffness of a car is lower for a lighter car. Based on the results of full rigid barrier crash tests, the linear stiffness of the car k (kN/m) is proportional to the car mass m (kg) to the power of 1/3 as follows [Ishikawa 1990].

$$k = 78\, m^{1/3} \tag{1.2}$$

This situation is not desirable for the safety of a small car because intrusion is larger for a smaller car in a crash into a larger car. In crashes between small and large cars, when the force-deflection curve of the small car has a plato region, the deformation of the small car becomes particularly large [Marumo 1974]. Therefore, it is suggested that for small car the force-deformation curve has a triangular shape without the plato region.

The countermeasures for the vehicle compatibility have been mainly focused on modifying the stiffness to compensate for the mass difference. The compatibility between two cars is measured by the energy absorbed by each car. There are several proposed ways for the relationship between the absorbed energy and the car mass m to accomplish compatibility, as follows [NHTSA 1975, Tarrière 1997]:

I. $$E_2 / E_1 = m_2 / m_1 \tag{1.3}$$

II. $$E_2 / E_1 = \frac{3(m_2 / m_1) - 1}{(m_2 / m_1) + 1} \tag{1.4}$$

III. $$E_2 / E_1 = 1 \tag{1.5}$$

IV. $$E_2 / E_1 = (m_1 / m_2)^{1/3} \tag{1.6}$$

(I) This condition can be said to be complete compatibility [Tarrière 1997]. At a certain velocity, a heavier car has larger kinetic energy than a lighter car. The assumption that the car should absorb the kinetic energy by the mass ratio yields this equation. When equivalent barrier speed *EBS* is considered, the internal energies of car 1 and 2 can be expressed as:

$$E_1 = 1/2 m_1 (EBS_1)^2 \tag{1.7}$$

$$E_2 = 1/2 m_2 (EBS_2)^2 \tag{1.8}$$

where EBS_1 and EBS_2 is the *EBS* of car 1 and 2, respectively. When the *EBS* is the same for each car $EBS_1 = EBS_2$, the equation of condition (I) can be obtained. Car 1 and 2 will be compatible if the absorbed energy during car-to-car collision is the same as that against the rigid barrier.

(II) This condition comes from the idea that the upper limit of the closing speed is 2 times the *EBS* of car 1.

(III) If the stiffness of each car is the same, the absorbed energies for light and heavy cars are the same. In this case, the deformation of the cars is equal for both cars. This design condition is easier to realize than the above two conditions.

(IV) Using Eq. (1.2), the ratio of the absorbed energy for both cars in the current car population is obtained as condition (IV).

Figure 1.3 shows the compatibility scenario based on the force-deformation characteristics according to conditions (I) to (IV). In this analysis, the ratio of car mass is two, the slope of the heavier car (car 2) is varied and the stiffness of the lighter car is constant (car 1). In order to accomplish the complete compatibility of (I), the deformation of the heavier car is two times larger than that of the lighter car. In the situation of the current car (IV), the deformation of the lighter car is larger compared to the heavier car, though in general the crushable zone is limited for the lighter car.

There have been some investigations into the effects of the car stiffness on the deformation in car-to-car frontal crashes using basic theory, however, there are only a few that investigated these effects on the risk to occupant injuries by accident, experiment or simulation.

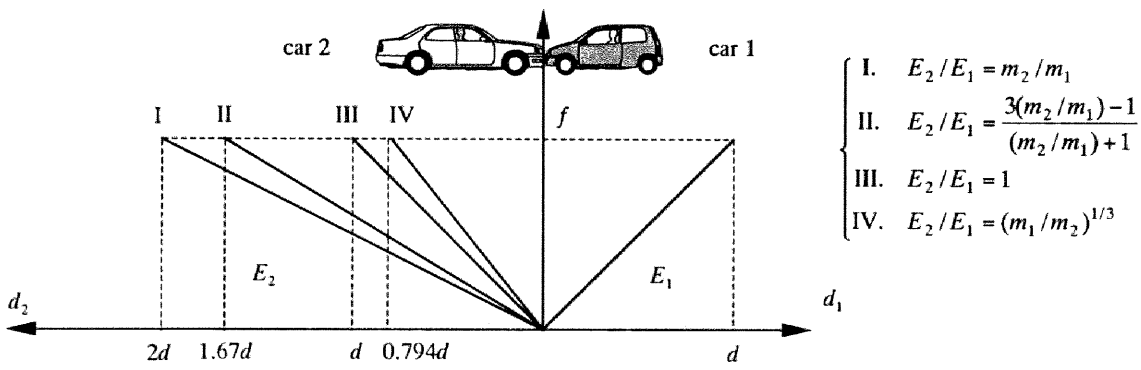

Figure 1.3. The force-deformation characteristics for various compatibility scenario (m_2/m_1=2.0).

Local stiffness

The stiffness uniformity is also important since the stiff parts of one vehicle penetrate the weaker part of the other. This may result in penetration fork effect or over-ride. Thus, the stiffness uniformity is also related to the geometry compatibility. There is a case when the poor structural interaction has a dominant effect on over-ride compared to stiffness and mass.

From the offset deformable crash test, Bloch (1994) indicated that the deformation of the barrier element can be used as an evaluation of aggressivity. High uniform deformation shape shows that the investigated vehicle is compatible with other cars. (Figure 1.4). High local stiffness parts such as longitudinal beams penetrate the honeycomb of the deformable barrier (Figure 1.5). Bloch (1996) also suggested that the aggressivity due to the combination effect of mass and stiffness may be estimated by this type of crash. He also tried to use car stopping time or energy loss for this estimator. However, the effectiveness of this measure is not confirmed.

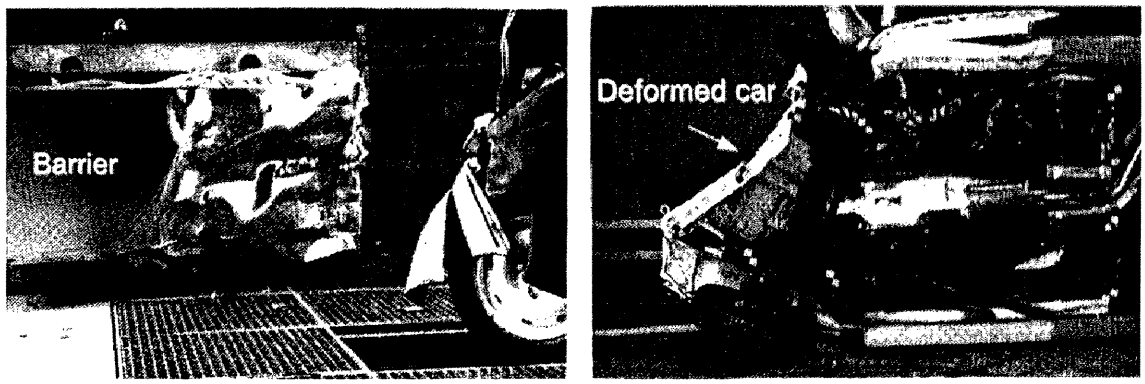

(a) (b)

Figure 1.4. Deformable element hit by a soft vehicle [Bloch and Chevalier 1996]. Left figure (a) shows the barrier face, and right figure (b) shows the deformed car.

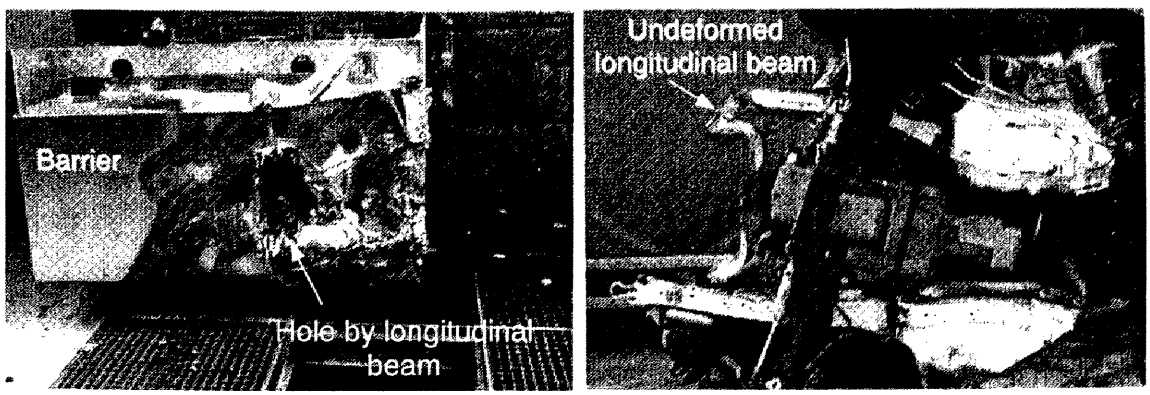

(a) (b)

Figure 1.5. Deformable element hit by a vehicle with very stiff front parts [Bloch and Chevalier 1996]. Left figure (a) shows the barrier face, and right figure (b) shows the deformed car.

Geometry Compatibility

The geometry difference, especially the height of the main energy-absorbing elements influences compatibility. If the front side member of the heavier vehicle is higher than that of lighter vehicle, both vehicles' member will not absorb the crash energy. One vehicle will override the other, diminishing the effective energy absorption.

The geometry incompatibility between a car and a Sports Utility Vehicle (SUV) is often discussed [Gabler and Hollowell 1998, IIHS 1998]. The heights of bumper and front side members of the SUVs are higher than those of cars. This creates a mismatch in the structural load paths in frontal impacts by override of the SUV.

Usually geometry compatibility is discussed together with mass and stiffness compatibility. Wykes et al. (1998) showed by two-crash tests that the geometry interaction is important for car compatibility. They indicated that in a frontal crash the upper load stiffness should be increased to prevent underride. They also performed the FE analysis for a side collision changing the stiffness distribution and geometry of the MDB (Moving Deformable Barrier). They recommended for a side collision that the upper load path of the striking car should be reduced for the safety of the occupant in the struck car. However, both requirements for frontal and side collision are contradictory.

1.2.5. Compatibility by Combined Mass, Stiffness and Geometry

Mass, stiffness and geometry incompatibility can be combined, and lead to a worse outcome. An example of combined incompatibility can be seen in light trucks and vans (LTV). LTV consists of SUV, pickup and vans. The difference in weight between passenger cars and LTVs is increasing and currently over 454 kg [NHTSA 1998]. Using crash data from the New Car Assessment Program (NCAP), it was shown that in general SUVs are stiffer than passenger cars (see Figure 1.6) [Kubota and Kokubu 1995].

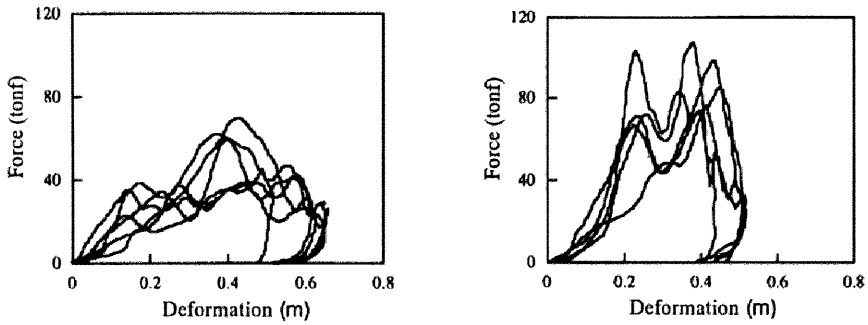

Passenger cars (Front wheel drive) SUVs

Figure 1.6. Force-deformation characteristics of passenger cars and SUVs [Kubota and Kokubu 1995].

From Figure 1.6, Kubota and Kokubu (1995) calculated the crush energy (E) based on the deformation (δ) of a passenger car and a SUV as follows:

$$E = 27465\delta^2 + 4948\delta + 210 \quad \text{for passenger car (front wheel drive)} \tag{1.9}$$

$$E = 50143\delta^2 + 4637\delta + 107 \quad \text{for SUV.} \tag{1.10}$$

In the US, the population of LTVs is growing and occupies over 1/3 of all light vehicle registrations [Gabler and Hollowell 1998]. The rapid growth in LTV population in recent years in the US has raised the problem of "vehicle aggressivity".

There are two characteristics of LTVs that have the potential to increase fatalities: compatibility and rollover propensity. Gabler and Hollowell (1998) showed that the risk of fatal injury of the drivers in passenger car is higher than that in the LTV in car-LTV frontal crashes. They examined the ratio of driver fatalities in the subject vehicle to driver fatalities in its collision partner for car-to-car frontal impacts (Figure 1.7). In collisions between full-size vans and cars, six drivers died in the car for one driver killed in a van.

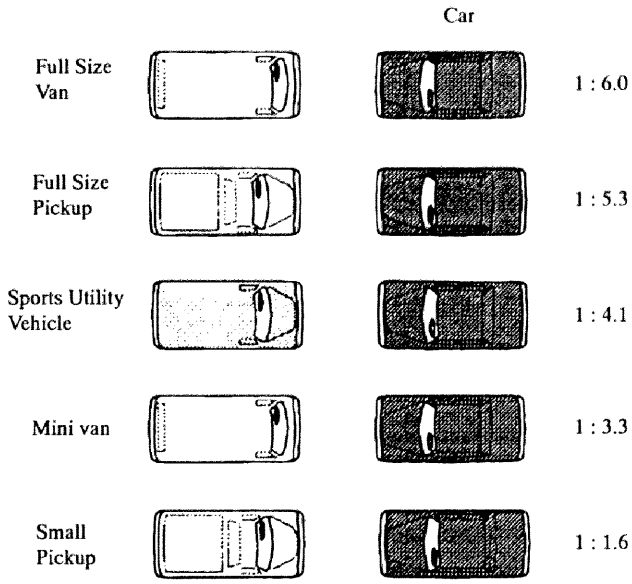

Figure 1.7. Ratio of fatally-injured drivers in LTV-to-Car Frontal Collisions. FARS 1992-96 [Gabler and Hollowell 1998].

1.2.6. Current Test Procedures for Frontal Crash

It is necessary that the car compatibility is evaluated from crash tests. There are several established crash tests for evaluating occupant injury risk in frontal crashes (see Table 1.1). However, the crash test procedures to evaluate the compatibility of cars in frontal crashes are currently under investigation by several researchers.

The full frontal crash test into a rigid barrier is currently adopted in the US, Japan and Australian regulations. The head and chest accelerations of the dummy are high due to high acceleration of the car because the car crashes into the rigid barrier with a full overlap. Thus, this crash test is useful for evaluating life saving injuries. This full rigid barrier crash test is a more severe evaluation of restraint

Table 1.1. Test procedures in frontal crashes.

Test procedures	Organization	Impact velocity (km/h)	Configuration
Full rigid barrier crash test 	US regulation Japan regulation Australia regulation US NCAP Japan NCAP Australia NCAP	48 km/h 50 km/h 50 km/h 56 km/h 55 km/h 56 km/h	Overlap ratio 100%
Offset deformable barrier (ODB) crash test 	EU regulation Euro-NCAP Australia NCAP IIHS ADAC (Automobile club)	56 km/h 64 km/h 64 km/h 64 km/h 60 km/h	Overlap ratio 40%
Oblique crash test 	US regulation ECE Proposal (1983)	48 km/h 50 km/h	Impact angle 0°-30° Impact angle 30°
Offset rigid barrier crash test 	AMS (Auto Motor Sports)	55 km/h	Overlap ratio 50% Barrier R=190 mm (ISO/DIS 3560)
MDB crash test 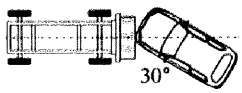	NHTSA (1998) Sugimoto et al. (1998)	112 km/h 112 km/h (Closing velocity)	Impact angle 0°, 20°, 30° MDB 1360 kg, 950 kg

system performance than the offset deformable barrier crash test to be mentioned below [Planath et al. 1994, IIHS 1995, Hackney et al. 1996, NHTSA 1997].

The EU developed an offset deformable barrier (ODB) crash test procedure and has started to use it for car approval since 1998 [Lowne 1994]. This test is designed to duplicate the crush patterns and compartment intrusion of offset frontal collisions seen in the real world since the intrusion into the passenger compartment is considered the major cause of fatal and serious injuries. Thus, this test address intrusion-induced injuries like lower leg injuries that are currently not evaluated by a full frontal crash test [Lowne 1994, NHTSA 1997].

In order to evaluate the stiffness compatibility, the test procedure based on the ODB crash has been proposed [ISO 1999]. The tests will be carried out in two procedures with different crash velocities. In crush capacity procedure with high crash velocity, the crush force (F1) is measured to estimate the self-protection. In energy control procedure with low crash velocity, the crush force (F2) is measured to estimate the aggressivity. The force F1 should be higher and F2 should be lower than the prescribed force based on compartment collapse. Further research will be necessary to determine the parameters such as F1, F2 and crash velocities. This test procedure will not be able to evaluate the mass compatibility.

In rigid barrier crash at a constant velocity, a heavy car has to absorb more energy than a small car because the car structure has to absorb the whole of the kinetic energy ($1/2mv_0^2$). In addition, in an offset deformable crash test the heavy car has to absorb more energy because the energy absorption capacity of a deformable barrier is constant (40 kJ) and the net energy should be absorbed by the car structure. Since the heavy car has to absorb more energy, these test procedures may have the potential to make a heavy car stiffer than a light car [NHTSA 1997, Sugimoto et al. 1998, Kallina 1998]. Thus, these test procedures may increase the incompatibility of the car and make for an incompatible car fleet.

NHTSA has conducted a crash test program to develop a crash test procedure for the car compatibility [Ragland et al. 1991, NHTSA 1997, Ragland 1998]. According to the results of the test program, the MDB test procedure was found to give closer crash pulse and dummy response to a car-to-car crash test than the offset crash test [Ragland 1998]. In the EU test procedure, the peak acceleration comes later and shows a much lower dummy response including leg injury parameters. The MDB test seems to be a good method to assure better front-to-front compatibility [Ragland 1998, Sugimoto et al. 1998]. Though the MDB impact angles of 0°, 20° and 30° have been examined, they have not been fixed yet. It is necessary to discuss further whether this crash configuration of impact angle and overlap ratio can be representative of the car-to-car frontal collisions. Since the MDB tests have been carried out for medium and large cars in the US, small cars have not been tested yet for evaluating the compatibility in Japan.

Though the MDB test procedure has several advantages for reproducing the car-to-car crashes, some research has indicated several problems like the override or the stiffness of the MDB. Sugimoto et al. (1998) suggested that the force-stroke characteristic of currently used honeycombs of the MDB is not suitable for car-to-car crash tests in view of the bottoming out problem in particular. Compatibility consists of the self-protection and partner-protection, however, only injury risks of the driver in the subject car have been evaluated in this test procedure. It should be considered that not only self-protection but also aggressivity should be estimated in this crash test procedure.

Because a crash test using a single car is simple and reliable compared with the MDB test procedure, single-car crashes into a fixed barrier were examined in the IHRA as the alternative of MDB test procedure. In this test procedure using a single-car, the mass difference in a car-to-car crash is reflected by changing the crash velocity of the car. The possibility of this alternative has not been clarified yet.

1.2.7. Countermeasure for Compatibility of Mini Car

To achieve the compatibility of a mini car, a low mass vehicle (LMV) with a mass of 600-650 kg and length of 2.5-3.0 m was proposed [Waltz 1991, Kaeser 1992, 1995, Frei 1997]. The front structure of a LMV is designed to be stiff in order to reduce the intrusion into the passenger compartment. As the acceleration of a LMV becomes high due to the stiff structure, it needs a specially designed restraint

system to ensure the occupant's safety. Optimum restraint systems were analyzed using the crash victim simulation program MADYMO [Muser 1996]. The crush force level of 400 kN for the front structures and optimum restraint (seatbelt force limiter, seatbelt pretensioner and energy absorbing steering system) were recommended.

A small car, Daimler-Benz A-class, was developed taking compatibility aspects into consideration [Kallina 1998]. The A-class is stiff and the front end is homogenous in height and width to withstand a car-to-car collision with a heavier car. In a crash test with an A-class against a SUV with a mass ratio 1:1.7 and an overlap degree of 50% at 50 km/h each, the load for the dummies in the A-class is less than the injury criteria level (HIC: 410, chest 3 ms: 49g, femur force: 1.8 kN). However, the A-class weight is more than 1000 kg, which is only 100 kg less than average mass of the passenger cars in Japan. This stiff car with average weight may be aggressive to lighter cars than the A-class, especially to mini cars in Japan.

The compatibility of the mini car may be also accomplished by changing the stiffness of the opposite car. Using a simple mass-spring model, Tarrière et al. (1994) suggested that the maximum crush force of a large car in a given impact be limited in order to reduce the deformation of a small car. However, the influences of this partner-protection on the injury risks to both drivers have not been examined.

1.2.8. Vehicle Population

It was shown that the homogeneous car fleet will be most compatible when compared to the car fleet with various sized cars using the accident rate, car registrations and the injury risk by delta-V [Marumo et. al 1974, Buzeman 1998a]. Using accident data for the driver and the pedestrian fatalities of FARS to measure exposure, Evans et al. (1991a) examined the effect of car population on the number of fatalities of the driver. He showed that driver fatalities increases if:

- Any car in the population is replaced by a lighter car.
- One population of identical cars is replaced by another population of lighter identical cars.
- The car population becomes of uniform mass while maintaining the average mass constant.

As the exposure evaluation by the pedestrian fatalities has not been confirmed, it is difficult to be sure of these results. The effect of vehicle fleet has not been analyzed using the domestic accident data in Japan.

Down-sizing of the vehicle in the USA occurred between 1970 and 1980 and was motivated by the fuel crisis. The regulation of vehicle emissions may also cause downsizing of the vehicle. Small cars have environmental benefits of a reduced need for materials, reduction of cost of manufacturing, reduction in fuel consumption, reductions in road maintenance cost, reduced parking requirements, and less emissions [Filders et al. 1993]. Downsizing of cars during ten years has not led to an increase in the number of fatalities. The influences of downsizing of the car on the number of fatalities have not been shown clearly.

1.2.9. Side Collision

There are insufficient research projects on the compatibility for side collisions. Dalmotas (1983) conducted an analysis of injuries in a passenger car occupant in near- and far-side impacts in which restrained occupant was injured at AIS 2 or greater severity. Injury severity and injury probabilities were inversely related to the mass of the vehicle for occupants on the near-side. However, the mass of the striking vehicle had no significant effects for occupants on the far-side. On the other hand, Watanabe et al. (1989) carried out side impact tests and found that the mass of the struck car has little effects on the injury parameters of the Side Impact Dummy (SID).

Since the stiffness of the front of cars is generally higher than that of the side structure of the car, the struck car absorbs more energy in a side collision [Tarrière 1984]. Yonezawa et al. (1994) examined the energy consumption in side impact tests, and 63% of the deformation energy was absorbed by the struck car and 37% by the striking car. A less-stiff front structure of the striking car is preferable to improve the compatibility in side collisions [Tarrière 1984].

The incompatibility of geometry in a side collision of the car struck by the SUV has been reported [Shearlaw and Thomas 1996, IIHS 1998]. The front bumpers of the SUV impacted above the side sill of the struck car, and causes large door intrusion which results in a high injury risk to the occupants in the struck car.

In Japan, the regulations of side impact tests have been introduced in 1998. The US and EU also prescribe the injury parameters in side impact tests (see Table 1.2). Although the US and EU employ different test procedures, the MDB are used in both tests. The MDB mass, stiffness and geometry (height of the deformable barrier) are based on the average car. So only self-protection from impact by an average car can be evaluated. The compatibility of the car in a side impact can not be evaluated based on these test procedures.

Table 1.2. Test procedures for side impact.

Country	Japan, EU	US
Impact Velocity	50 km/h	54 km/h
Impact Angle	90 deg.	90 deg. (Crab 27deg)
MDB Mass	950 kg	1366 kg
Width	1500 mm	1676 mm
Length	500 mm	559 mm
Depth	500 mm	483 mm
Ground Clearance	300 mm	279 mm
Stiffness (Dfl 100 mm)	60-110 kN	245 kN
(Dfl 200 mm)	140-190 kN	380 kN
(Dfl 300 mm)	210-260 kN	380 kN
Dummy	EUROSID-1	SID
Dummy Sitting Position	Front seat (impact side)	Front & Rear seat (impact side)
Injury Criteria	HPC (1000) Rib Deflection (42 mm) Viscous Criterion (1.0 m/s) (Not in Japan regulation) Abdomen Force (2.5 kN) Pelvis Force (6.0 kN)	TTI (d) (85g for four doors and 90g for two doors) Pelvis Acceleration (130g)

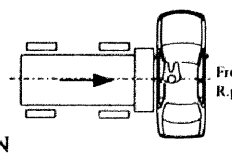

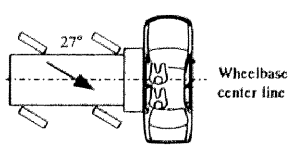

1.2.10. Single-Car Accident

Single-vehicle crashes give the best indication of vehicle protection for occupants because no other vehicles are involved. Campbell and Reinfurt (1973) found that for single-vehicle crashes, there are insignificant differences for injury frequency by vehicle weight. However, many studies [Stewart and Stutts 1978, Evans 1982, Partyka 1989] found that in single-vehicle crashes, the fatality rate decreases with increasing car mass if we consider the exposure such as vehicle velocity and registration. Many factors such as driver age, sex and vehicle velocity are associated with the effect of vehicle properties. Based on the corrected fatality rate using car velocity, it can be found that the fatality rate decreases with car mass. High injury risk to the occupants in small cars can be explained from the fact that heavier cars are more likely to destroy the struck object than smaller cars [Evans 1991b]. However, the reduction of the fatality rate by increasing car mass is smaller than that in car-to-car crashes.

In 1984, Joksch and Thoren conducted an analysis of FARS (1981-1982). By correcting the data, they found that only the smallest cars (subcompact) differed significantly from any other size class. In single-vehicle accidents, large cars (wheelbase greater than 3048 mm) were found to have no more protection than small compacts (wheelbase between 2565 and 2692 inches). They found that plotting death rate as a function of wheelbase showed a much smoother relationship than plotting death rate as a function of mass. Joksch and Thoren concluded that wheelbase and crush space is needed for protection rather than vehicle mass. However, increasing the wheelbase beyond that of the small compact did not appear to provide increased protection.

Fontaine (1992) and Tarrière et al. (1994a) reported that in single-vehicle crashes, the injury risk to the driver in a high-powered car is high. They explained that the higher the power/weight ratio of the car, the greater the risk to the driver of losing control of his car and crashing into a tree or another fixed object.

In rollover crashes, the size of the vehicle is more dominant than its mass because the propensity to rollover is associated with probabilities that are closely related to vehicle size [Filders et al. 1993]. The probability of getting into a situation which makes rollover possible, typically losing directional control is a function of wheelbase. The probability of rolling is a function of track and height of center of gravity. Thus, the SUV and pickups have a high risk of rollover [IIHS 1998].

1.3. CAR-TRUCK COMPATIBILITY

The car-to-truck frontal crash may be the worst example of incompatibility for vehicle-to-vehicle collisions. In the US, from the lightest to heaviest cars, 17 through 26% of occupant death in the car in two vehicle crashes involves medium and heavy trucks [IIHS 1998]. Even the pickup and SUV are lighter in comparison with large trucks. The EEVC WG14 Working Group report of March 1995 indicates that in European countries, 7000 car occupants were fatally injured in traffic accidents and about 4200 of them were killed in car-to-truck accidents [Adalian et al. 1998].

Deloffre et al. (1998) classified the causes of incompatibility between cars and trucks as follows:

- the front-end design of trucks and passenger cars are incompatible due to major difference in ground clearance of the vehicles' stiff zone, causing underride of the cars under the truck;
- the stiffness of a truck front end is larger than that of a passenger car;
- the mass ratio between passenger cars and a truck ranges from 3:1 to 50: 1.

The mass difference between trucks and cars cannot be changed, but front underrun protection devices have been proposed to prevent truck front ends from overriding passenger vehicles. One prototype design is a truck bumper which is an energy absorbing element mounted on a strong support frame [Yamanaka et al. 1978, Mendis 1996]. This structure would prevent a car from underriding a truck and transfer some of the energy of impact to the truck chassis. Such design proved effective, and this indicates that, despite large weight mismatches, changes to front-end geometry and stiffness can improve compatibility.

The ECE/EU Regulation No. 93 that consists of a rigid beam in front of the truck has been created to avoid car underriding. For this purpose, the compatibility between cars and trucks with the front underrun device was examined [Adalian et al. 1998, Deloffre et al. 1998]. This device was called the Front Underrun Prevention System (FUPS), which was a special device added laterally in front of the truck, behind the bumper and underneath the actual chassis. The FUPS consisted of a U-shaped beam, made of high strength steel. The FUPS was optimized using FE analysis in terms of deformation mode and energy absorption on the truck side. The medium car to truck collision test was conducted for a truck with the FUPS at 65 km/h with 2/3 car overlap. The car did not run under the truck and kept its cabin intact. The injury parameters of the occupants in the car were less than injury thresholds. They concluded that 30% of lives could be saved in head-on collisions between cars and truck fitted with FUPS.

In Japan, there have been little research projects on car-to-truck collisions and their countermeasures. The trucks are prescribed by the regulation of Japan to install a rear under-bumper to prevent underride of the car in rear-end collision. The regulation also requires the truck to have a side guard to prevent the involvement of cyclists and pedestrians in turning. However, there are no regulations which require the truck to install the front underrun guard for frontal crashes, and no trucks have this guard.

1.4. PEDESTRIAN ACCIDENTS

1.4.1. Problem Scope

In a larger sense, the compatibility can be extended to the impact of vehicles with unprotected road users such as pedestrians because the injury risk of the crash partners in these cases are too different

[Appel 1995, Schimmelpfenning 1996, Tarrière 1997]. This type of compatibility is accomplished only by partner-protection of the vehicle.

In Japan, there are approximately 2,700 pedestrian fatalities each year. These pedestrian fatalities occupy about 28% of all fatalities in traffic accidents. This ratio is higher than that of other motorized countries. Moreover, Japan takes a leading part in responsibility at the IHRA of ESV and it is required to take the lead for pedestrian protection. Since the pedestrian accident analysis and the proposition of countermeasures are expected, one of the purposes of this thesis is to clarify the injury risks of pedestrians in pedestrian-vehicle accidents.

In a vehicle-pedestrian impact, the pedestrian injury risks depend on the vehicle shape because the impact locations and velocities of body regions for pedestrian vary with vehicle shape. There are some publications which discussed the effects of the shape of the bonnet-type car such as bumper height, bumper lead and hood edge height on the injury risk to the pedestrian [Cavallero et al 1983, Ishikawa et al. 1991, Higuchi et al. 1991]. Although, the registrations of various shapes of vehicles such as the van, mini van and the SUV are increasing, the pedestrian behavior and injury risks have not been compared for these different types of vehicles.

1.4.2. Impact Test Method

In order to evaluate the injury risks of pedestrians in impact by vehicles, the impact tests using anthropometric test devices are effective. The pedestrian dummies based on the Hybrid II and III types were developed for full scale dummy tests. However, the repeatability of impact test of pedestrians using the pedestrian dummy is insufficient because the dummy behavior and injury parameters in impact is strongly affected by small differences of initial posture and its configuration. Furthermore, when the stiff shoulder of the dummy contacts the car body, the behavior of the dummy changes, as a result the contact position and impact severity of the head can be different from those of human. It is also indicated that the joint stiffness of the dummy is higher than that of a human. The pedestrian dummy with a higher biofidelity was developed by Akiyama et al. (1999), and kinematics of the dummy was validated with that of postmortem human subjects.

Although the head impacts onto the various car body regions in real-world accidents, the impact locations of the head are limited when using a pedestrian dummy [Harris 1989]. Thus, the sub-system tests using impactors as a headform, upper legform and a legform are often adopted and impacted onto the various locations of the car body to evaluate the injury risk to each body region. The European Experimental Vehicle Committee (EEVC) proposed a test method for assessing the protection of a pedestrian in an accident, and three sub-system tests are proposed: headform to bonnet top, legform to bumper and upper legform to bonnet leading edge [EEVC 1998] (see Figure 1.8). The International Standard Organization (ISO) also presents a similar sub-system of tests.

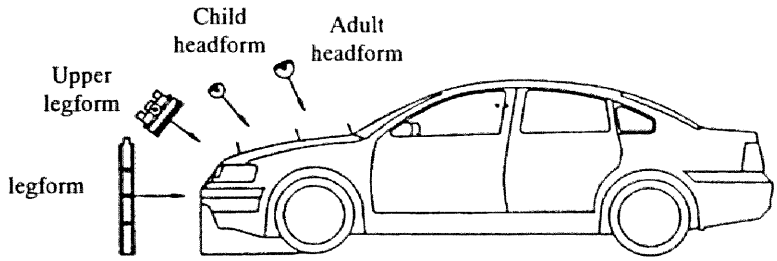

Figure 1.8. Pedestrian impact test method [EEVC 1998].

Head injuries cause a serious threat to life and the recovery is often incomplete. Therefore, it is most important to evaluate the injury risk to the head. The EEVC test method describes that the head impact test shall be made with the bonnet top within the boundaries prescribes by the wrap around distance (WAD) of 1500 mm and 2100 mm at a velocity of 40 km/h [EEVC 1998]. In this test method, the windscreen and A pillars are excluded from the test area. The headform impactor should not contact the windscreen glass before impacting the vehicle structure, even though the tested area is the windscreen frame. A rear-end reference line (see Figure 1.9) has been defined as the most rearward points of contact between a sphere and the bonnet top, and the adult headform impacts should be conducted 82.5 mm (i.e. half diameter adult headform) forward of this line [EEVC 1998]. In the Euro NCAP, as the pedestrian impact tests are carried out by following this test procedure, only head injury risks from the bonnet-top area are evaluated.

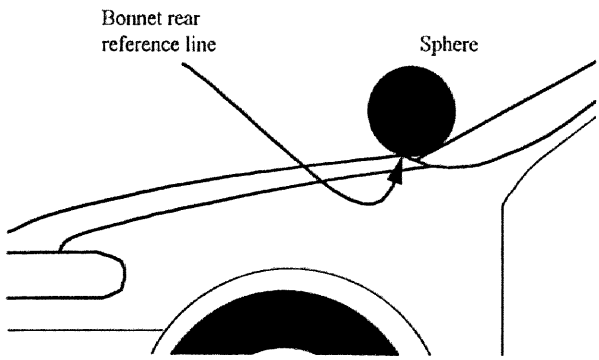

Figure 1.9. Determination of bonnet rear reference line [EEVC 1998].

The EEVC presented the test methods in a first report of EEVC WG10 [Harris 1989]. In that time when the pedestrian test methods were discussed, cars had upright frontal areas and a long hood. Since the modern car has become smaller with a short and steep bonnet, the head impact locations has changed from the hood to cowl or windscreen in real-word accidents. According to the ITARDA report (1996), among the 26 accidents where the pedestrian head contacted the car body, 57.7% of head contact was against the windscreen, 19.2% against hood, 11.5% against the A pillar and 11.5% against roof edge.

Because of the changes of the head contact locations caused by modern car shapes, it was pointed out that the injury risks to the head by contact around the windscreen should be investigated [NHTSA 1993, EEVC 1998]. Especially, for the mini car the pedestrian may have a high possibility that the head makes contact around the windscreen.

1.5. AIMS OF THE PRESENT STUDY

Each country has various traffic environments. In the US, the number of LTV and SUV is large and vehicles travel at high velocity. There are a number of small cars in the EU, however, they are not so small as mini cars in Japan. Japan has special traffic condition of mixed traffic with many mini cars and trucks, and the roads are narrow with many poles at the roadsides. The number of accidents involving pedestrian is the largest among motorized countries. Since the compatibility strongly depends on vehicle size and population, the compatibility should be investigated in each country. Since no research has been carried out on vehicle compatibility in Japan, in this thesis various aspects of compatibility in Japanese traffic situation will be investigated.

Previous studies have dealt with one element of compatibility such as car-to-car, car-to-truck and car-to-pedestrian. In this thesis, a new methodology of combination of accident analysis and simulations is introduced to analyze the *total compatibility* including car, truck and pedestrian. The interaction between each compatibility will be discussed. A new analysis of accident data from Japan will be performed to describe the total compatibility. A mathematical simulation can describe the cause of high injury risk. Based on the accident analysis and simulation, a test method of the compatibility will be proposed. The main goal of this thesis is also to propose countermeasures to obtain a better level of total compatibility through this methodology.

This thesis discusses the following subjects.

In Chapter 2, the compatibility of the car will be discussed based on accident analysis and mathematical simulations. Although the vehicle mass has the largest effect on the vehicle compatibility, an absolute injury rate of the occupant according to vehicle mass has not been obtained. Therefore, the relation between injury rate and vehicle mass will be formulated based on delta-V. The stiffness, geometry compatibility and effectiveness of the seatbelt will be discussed from the accident data in Japan.

The effects of mass, stiffness and geometry are combined when the compatibility is analyzed by car classes. In the US, injuries related to SUVs were found to be the most serious problems for compatibility [Gabler and Hollowell 1998, IIHS 1998]. The most compatible and incompatible car class in Japan will be investigated in this thesis.

There are not sufficient research projects which investigate the compatibility in side impact and single-car crashes. By using accident data, the compatibility in side impact and single-car crash will be also discussed from the point of view of vehicle mass and impacted objects.

Many previous studies on the compatibility of car-to-car crashes focused only on vehicle acceleration and deformation of a car without examining an occupant injury risk [Ragland 1998, Tarrière 1997, Sugimoto et al. 1998, Wykes 1998]. Although, some studies evaluated the injury risk to the driver, they used a one-dimensional simple mass-spring model [Ventre 1972, Tarrière et al. 1994]. On the other hand, though the injury risk to the driver in full rigid barrier crashes have been discussed in may studies from simulations and tests, only acceleration-related injury was examined [Sakurai 1989, Suzuki 1992]. However, in order to investigate the compatibility of the mini car in car-to-car crashes, the effect of intrusion on the injury risk should be considered. Therefore, in this study, a mathematical model of a mini car with driver that can estimate both effects of acceleration and compartment intrusion will be developed. Using this model, the injury mechanism of the driver due to acceleration and intrusion will be clarified.

For countermeasures to improve vehicle compatibility, improvement of the mini car will be proposed by using the mathematical model. Since there are no research projects which investigated the effect of the other car in car-to-car crashes, the partner-protection of the other car will be also examined.

In Chapter 3, the crash test procedures to evaluate the compatibility will be discussed. Currently a full rigid barrier crash and an offset deformable barrier crash test are carried out in the regulations [NHTSA 1997, Lowne 1994]. There have been little research that discuss the full rigid barrier crash and the offset deformable barrier crash tests to evaluate the vehicle compatibility. From mathematical simulations by changing the crash velocity based on car mass and stiffness, these crash test procedures will be examined in order to reproduce the car-to-car collisions.

A MDB crash test has been proposed by the NHTSA in order to evaluate the compatibility [Ragland et al. 1991, NHTSA 1997, Ragland 1998]. Since the MDB crash tests have been carried out mainly in the US, the medium and large cars were evaluated and the compartment intrusions were not large. Therefore, in this study by considering the Japanese traffic conditions, the MDB crash test will be performed using a small car. The results will be compared with those of large cars in the MDB crash test as well as with those of the same type of the small car in a full rigid barrier crash and an offset deformable barrier crash tests. The importance and problems of the MDB crash test for the mini and the small car will be pointed out.

In Chapter 4, the compatibility between truck and car will be discussed. Since the accident situation of car-to-truck collision has not been clarified in Japan, the compatibility of vehicles including car, trucks and buses will be examined by using micro and macro accident data. There have been some research projects on a front underrun guard of the trucks in the EU [Adalian et al. 1998, Deloffre et al. 1998]. These studies focused on the compatibility between a truck and a medium car. Since there are a number of collisions between a truck and a mini car in Japan, the optimum stiffness of the front underrun guard on the injury risk to the driver in the mini car will be discussed based on mathematical simulations.

In Chapter 5, the compatibility between a vehicle and a pedestrian will be investigated. The number of vehicles with various shapes such as minivans and vans is increasing [ITARDA 1996]. A bonnet-type car has also changed to having a short and steep bonnet. However, there has been little research on the influence of the current vehicle shape on the pedestrian injuries.

The analysis of pedestrian impact will be carried out by using the current accident data. The injury risk, injured body regions and head contact locations will be examined for various type of vehicle. In order to clarify the influence of vehicle shape on the pedestrian injury, a mathematical model will be developed based on the characteristics of a human body. Pedestrian kinematics and injury parameters will be compared for two different vehicle shapes such as a bonnet-type car and a van.

Since the head impact test procedures of a pedestrian proposed by EEVC and ISO are based on the shape of a car that is 10 years old, only the bonnet area is tested [EEVC 1998, ISO 1999]. However, the current accident data have shown that the head makes contact frequently with the windscreen and its surrounds [ITARDA 1996]. Therefore, in this study the head impact tests will be carried out onto a windscreen, windscreen frame and A pillar, and the injury risk will be clarified. Based on the accident analysis, mathematical simulations and head impact tests, recommendations concerning the design of the vehicle that is compatible with pedestrians will be proposed.

2. CAR COMPATIBILITY

2.1. INTRODUCTION

Since the number of the passenger car accidents is the largest, the compatibility of passenger cars is most important. In the compatibility subject of the IHRA, the passenger car compatibility is discussed as a matter of first priority [NHTSA 1998]. The car mass has the largest effect on the compatibility. The stiffness and geometry incompatibility can have potential to cause serious results.

Mini cars occupy 14% of the total passenger cars in Japan, and the registrations of this type of car are increasing [ITARDA 1995]. Though the compatibility of this car type has not been investigated, the injury risk to the occupants in the mini car is likely to be severe due to its light mass and small size. Therefore, from the traffic conditions in Japan it is necessary to clarify the current situations and to propose countermeasures for improving the compatibility of mini cars.

The purpose of this chapter is to clarify the characteristics of the car compatibility in Japan and to propose countermeasures for incompatible cars. In Section 2.2, the compatibility of the car in car-to-car frontal collisions will be discussed. The crashes of the mini car are simulated and the countermeasures for the compatibility of the mini car are proposed (Section 2.3). The compatibility in side and single-car crash is also discussed in Sections 2.4 and 2.5, respectively.

2.2. ACCIDENT ANALYSIS

The compatibility of vehicles in vehicle-to-vehicle frontal collision is classified as the mass, stiffness and geometry compatibility [Ventre 1972]. We examined the mass compatibility by using the relations based on delta-V from macro accident data. Then the geometry compatibility is discussed by using the in-depth micro accident data. Since various kinds of cars are involved in the real accidents, the phenomena of the mass, stiffness and geometry incompatibility occur at the same time. Therefore, the compatibility according to car class are analyzed because each vehicle class has a different distribution of these three parameters.

The macro accident data were obtained from the integrated database of ITARDA from 1992 to 1995 which consists of accident, vehicle and road data. This database includes the data of accidents reported to the police throughout Japan. The police collect the data only on accidents where at least one occupant suffered injury or death. Accordingly, in this paper the probability of injury means the fraction of injuries to occupants involved in such accidents. Micro data were obtained from the database of the in-depth accident investigation of the Japanese Ministry of Transport dated 1987 to 1992. Only injuries to drivers were examined to simplify the analysis.

2.2.1 Mass Compatibility

Mass distribution

The compatibility problems that are caused by vehicle mass depend on the vehicle mass distribution in the car fleet. We examined the distribution of passenger vehicles in Japan according to mass and the results are shown in Figure 2.1. The data were collected from the vehicle registration database in the Japanese Ministry of Transport. The car masses range from 500 kg to 2000 kg. The average mass of passenger cars is 1131 kg, which is smaller than that of cars in the United States. One reason that the average mass is so small in Japan, is the existence of the mini car, whose mass average is only 639 kg and the size of which is defined by Japanese law.

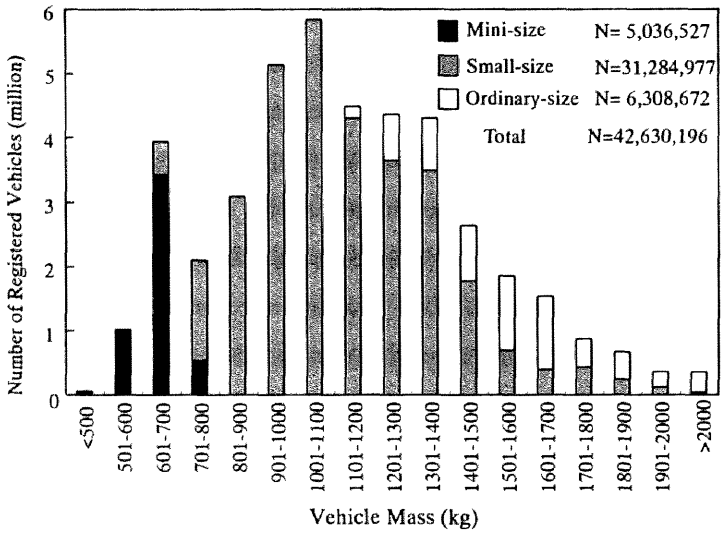

Figure 2.1. Registered passenger vehicles versus vehicle mass in Japan (Dec. 1994)

Vehicle mass and injury rate

Vehicle mass has a greater effect on the severity of occupant injuries in car-to-car frontal collisions than in other accident configurations. In order to examine the relation between vehicle mass and injury rate, the macro database of ITARDA from 1992 to 1995 was used. For a car-to-car frontal collision, accidents were collected in which the impact location on both vehicles is on the front end.

Figure 2.2 shows the probability of serious and fatal injury to the driver of car 1 in a car-to-car frontal collision between car 1 and car 2. The probability of serious and fatal injuries increases as the mass of car 1, m_1, decreases and that of car 2, m_2, increases. When m_1 is less than 700 kg and m_2 is greater than 1401 kg, the probability of serious and fatal injury to the driver of car 1 is 9.5%. In contrast, when m_1 is greater than 1401 kg and m_2 is less than 700 kg, the probability of serious and fatal injury to the driver of car 1 is 0.95%. Therefore, when a 700 kg car collides with a 1401 kg car, the driver in the 700 kg car is 10 times as likely to be seriously and fatally injured as in the 1401 kg car.

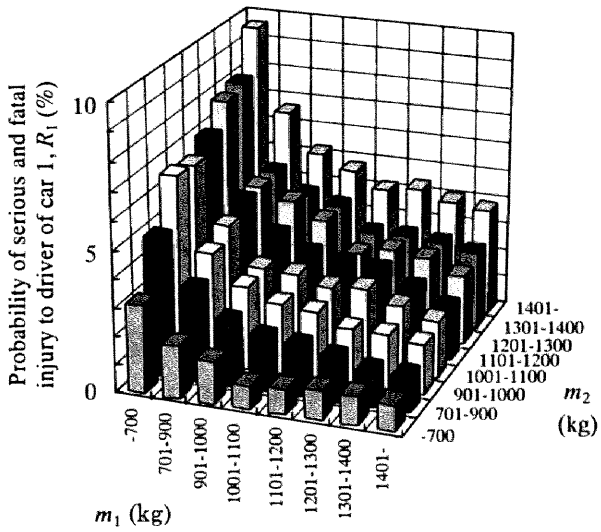

Figure 2.2. Probability of serious and fatal injury to driver of car 1 in car-to-car frontal collision.

Evans (1993) found that the ratio of the injury rate in a lighter car to that in a heavier car may be expressed by the power ratio of the car mass of the heavier car to that of the lighter car. In the current study, the individual injury rate is expressed by the average car mass ratio. According to Joksch (1993), the injury rate R can be expressed by delta-V (Δv) as:

$$R = \left| \Delta v / \alpha \right|^k \tag{2.1}$$

where α and k are parameters obtained by curve fitting. For many car-to-car frontal collisions, delta-V is approximated for a central collision. Assuming that the restitution coefficient is zero, the delta-V can be expressed by using the average mass ratio as:

$$\Delta v_1 = \frac{m_2}{m_1 + m_2} v_c \tag{2.2}$$

where Δv_1 is the delta-V of car 1, v_c is the closing speed, and m_1 and m_2 is the mass of car 1 and 2, respectively.

Substituting Eq. (2.2) in Eq. (2.1), the injury rate of driver 1, R_1, can be obtained as follows:

$$R_1 = \left| \frac{m_2}{m_1 + m_2} \frac{v_c}{\alpha} \right|^k = a \left(\frac{m_2}{m_1 + m_2} \right)^k \tag{2.3}$$

where $a = \left| v_c / \alpha \right|^k$.

Before discussing the applicability of Eq. (2.3), the relationship between the coefficient a, closing speed and vehicle mass must be examined. The average travelling velocity versus vehicle mass in car-to-car frontal and single-car collisions were examined (Figure 2.3). The travelling velocity is one of

the items included in the accident data, which is defined as the velocity at the moment when the driver perceives the danger of accident. Therefore, the velocity implied is that of the car before the driver brakes or steers to avoid the accident, and is usually compiled mainly from drivers' testimony. In car-to-car frontal collisions, the travelling velocity does not change significantly with vehicle mass (32.5-35.2 km/h) as shown in Figure 2.3. On the other hand, in single-car collisions, this velocity increases from 48.4 to 68.6 km/h as the vehicle mass increases. It has been observed that younger people are involved in single-car crashes more often than car-to-car frontal collisions, and furthermore these single-car crashes frequently occur during the night [ITARDA 1996]. This difference of the occurrences between single-car and car-to-car crashes leads to these different inclinations of travelling velocity.

It has been shown that the travelling velocity is closely related to the crash velocity [IHRA Pedestrian 1997]. Thus, in car-to-car frontal collisions, the coefficient a in Eq. (2.3) is assumed to be independent of vehicle mass.

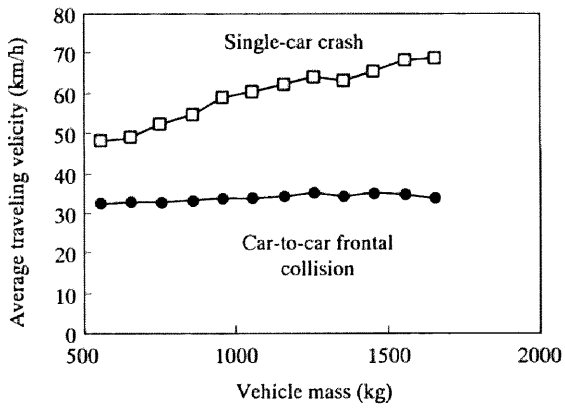

Figure 2.3. Average traveling velocity and vehicle mass.

By applying Eq. (2.3) to a real accident, the probability of serious and fatal injury to the driver (belted and unbelted) of car 1 can be calculated as shown in Figure 2.4. The parameters k and a were calculated to investigate the effect of seatbelts for two levels of injury severity as shown in Table 2.1. Based on this method, the parameter k obtained was 2.64 for the belted drivers sustaining fatal and serious injury. This value is almost the same as the 2.62 shown by Evans [1994]. However, he obtained this value based on Eq. (1.1) by calculating the injury ratio of belted car drivers in the heavier car to those in the lighter car, and considered all directions of impact. Equation (2.3) also indicates that the average mass ratio $m_2/(m_1+m_2)$ affects the probability of injury in the same way as the closing velocity v_c. Therefore, heavier cars as well as cars at a high velocity are aggressive to other cars.

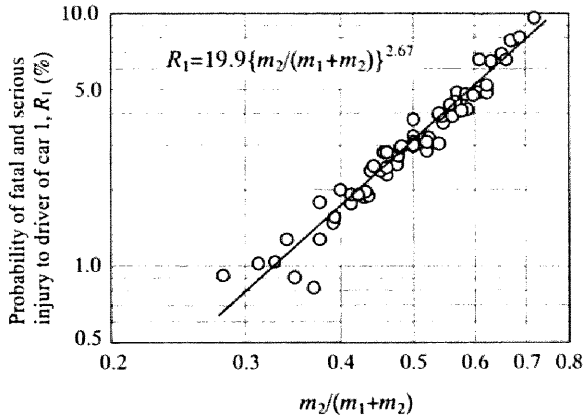

Figure 2.4. Average mass ratio and probability of injury to driver in car 1 (Belted and unbelted driver).

Table 2.1. Parameter k and a

Injury severity	Seatbelt	k	a
Fatal and serious	Belted	2.64	13.9
	Unbelted	2.49	33.4
Fatal, serious and minor	Belted	1.08	107.8
	Unbelted	0.955	123.5

The injury risks to the driver in a two-car crash with identical mass can be discussed from Eq. (2.3). The average mass $m_2/(m_1+m_2)$ takes the same value of 0.5 for light/light cars and heavy/heavy cars if the car mass are identical ($m_1=m_2$). Thus, in a crash of two cars with equal mass, the vehicle mass has no effect on the injury risk of the driver. This is true if it can be assumed that the cars have the same safety levels from the full rigid barrier crash test such as the FMVSS. The injury risks to the drivers in a two-car crash with identical mass are independent of car mass, since the barrier crash is equivalent to a two-car crash between the same cars. The car size is different for a heavy car and a light car. We may say that if similar restraint systems are used, the injury risk of the driver is the same in either case of two heavy cars and two light cars, as far as the intrusion into the compartment does not affect the injury risk. However, as the intrusion is larger for a smaller car due to its size, the risk of intrusion-based injury to the occupant can be higher for two-light car crashes than that for two-heavy car crashes.

Seatbelt effectiveness and car mass

Since the influence of the vehicle mass and the seatbelt on the injury rate is large, we discuss the combined effects of the vehicle mass and seatbelt. The probability of serious and fatal injury versus vehicle mass is shown in Figure 2.5. Wearing a seatbelt reduces the risk of serious and fatal injury over the entire range of vehicle mass. The probability of fatal or serious injury for belted drivers is between 1.5 and 5.1%, whereas that for unbelted drivers is between 4.3 and 11.6%, which shows that the effect of the vehicle mass is large for unbelted drivers. Thus, wearing a seatbelt is more important for the occupants of a lighter car in order to mitigate the severity of injury.

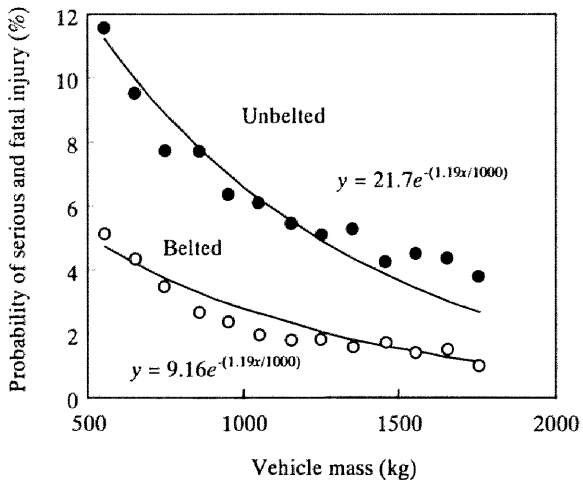

Figure 2.5. Effect of seatbelt on probability of serious and fatal injury to driver in car-to-car frontal collision.

It is well known that an unbelted driver is apt to travel at higher velocity and to be involved in a more severe crash than a belted driver [Evans 1991]. Therefore, in the results of Figure 2.5, the effectiveness of the seatbelt is overestimated because unbelted drivers travel at much higher velocity on average. In order to evaluate the effect of the seatbelt correctly, it is necessary to exclude the influence of the crash severity. For the reduction of this exposure problem, a double pair comparison method [Evans 1991] was used to compare the injury rates between belted and unbelted drivers.

When the relative injury risk to the driver is evaluated by the ratio of the number of fatalities in car 1 to that in car 2, there are no effects of vehicle closing velocity because both car 1 and 2 are involved in the same collisions. The ratio of serious and fatal injury rate of the driver in car 1 to that of the driver in car 2, R_1/R_2, is obtained by the ratio of the number of serious and fatal injuries of the drivers in car 1 to that of the drivers in car 2. By using this method, the injury rate is not affected by the differences in crash velocities between two cars driven by belted and unbelted drivers.

Figure 2.6 shows the ratio of injury rate classified by seatbelt wearing of the driver in car 1 and car 2. To simplify the comparison, the same approximation value for parameter k of 2.67 was used. When both drivers wear seatbelts or do not wear seatbelts, R_1/R_2 is expressed as:

$$R_{1,Belted} / R_{2,Belted} = R_{1,Unbelted} / R_{2,Unbelted} = (m_2 / m_1)^{2.67} \tag{2.4}$$

where $R_{i,\ Belted}$ is the injury rate of the belted driver in car i, and $R_{i,\ Unbelted}$ is that of the unbelted driver in car i. The data obtained by the double pair comparison method for belted/belted and unbelted/unbelted drivers is distributed along the approximate curve in Figure 2.6. In the case where the driver in car 1 does not wear a seatbelt and the driver in car 2 wears a seatbelt, the ratio of serious and fatal injury is approximated as:

$$R_{1,Unbelted} / R_{2,Belted} = 1.89(m_2 / m_1)^{2.67} = (1.27 m_2 / m_1)^{2.67} \tag{2.5}$$

This result shows that, when the combination of striking and struck car mass (m_1, m_2) is equal, the serious and fatal injury rate for unbelted drivers is 1.89 times higher than that for belted drivers. Equation (2.5) also shows that in order to gain the same probability of serious and fatal injury, the unbelted driver requires a vehicle mass 1.27 times that of vehicle mass driven by the belted driver.

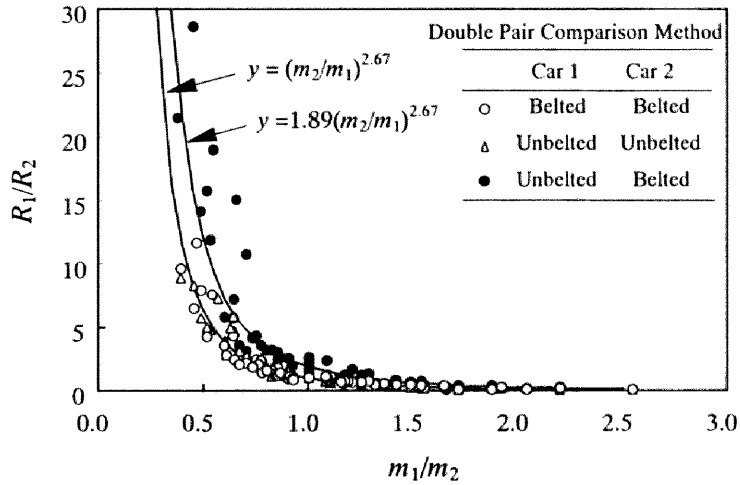

Figure 2.6. Ratio of probability of serious and fatal injury for driver's restraint condition in car 1 and 2.

Compatibility of car mass

The number of driver fatalities per collision is also important in the compatibility. The percentage of driver fatal injuries in the subject car plus that in the other car corresponds to the driver fatalities per accident. From Eq. (2.3), we obtain

$$R_1 + R_2 = \frac{m_1^k + m_2^k}{(m_1 + m_2)^k} a \ . \tag{2.6}$$

R_1+R_2 has a minimum of $2^{1-k}a$ (k>1) when $m_1 = m_2$. Thus, cars with equal masses are the most compatible in a collision since the injuries per accident are minimal and the injury rate is equal for both cars.

The percentage of driver fatalities in the subject and other car is shown in Figure 2.7. As the mass of the subject car increases, the fatality rate of the driver in the subject car decreases; on the other hand, that of the driver in the other car increases. The sum of the percentage of driver fatalities in the subject and the other car indicates the number of driver fatalities per accident where the subject cars are involved. When the car mass is 1150 kg, the number of fatalities per accident takes a minimum value while the fatality rate of the subject car and that of the other car are almost the same. Thus, the car with a mass of 1150 kg is considered most compatible in the current car population in Japan. The compatible car mass of 1150 kg is almost the same as the average mass of cars in Japan, which is 1131 kg (see Figure 2.1). This is because there is a high possibility that the subject car with mass close to the average will crash into another car with a small mass difference from the subject car.

When the mass of the subject car is in the range of 750 kg < m < 1350 kg, the number of fatalities per accident is small. However, when the subject car mass is less than 750 kg or greater than 1350 kg, the number of driver fatalities per accident increases. Thus, in order to decrease the total number of fatalities, it is necessary to design a lighter car by allowing for the safety of the drivers in the subject cars, and to design a heavier car by allowing for the safety of the drivers in the other cars.

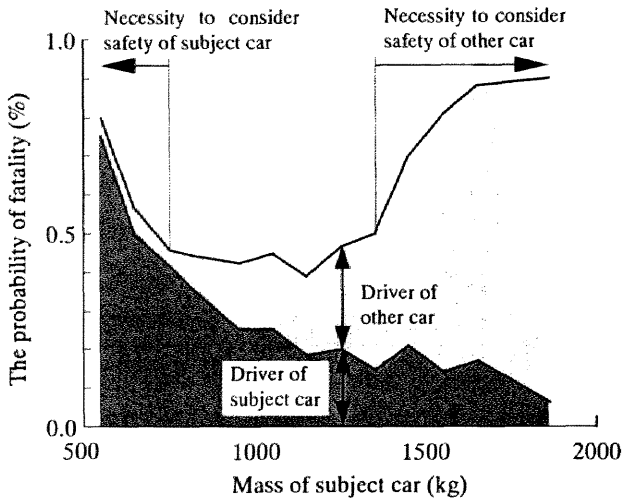

Figure 2.7. Car mass and the driver fatality of subject and other car in car-to-car frontal collisions.

2.2.2. Stiffness Compatibility

The stiffness of a car also affects driver injuries. Low stiffness results in large deformation and in the reduction of survival space for the driver. High stiffness induces in large acceleration of the car. Thus we decided to examine the relation between stiffness and injury risk. Since the stiffness of the car in accidents is difficult to obtain, the crush depth was used.

The data were drawn from the micro accident database of the Ministry of Transport (1987-1992). In real-world accidents, the crush profile of the car varies because the overlap and principal direction of force (PDOF) are different. Thus, there are many ways to evaluate the crush depth of a car in a collision. In order to clarify the effect of the crush depth on the compartment intrusion, we used the average crush depth $\overline{C}$ to represent the crush profile of the car as:

$$\overline{C} = \frac{\int_0^{w_0} C\, dw}{w_0} \tag{2.7}$$

where C is the crush depth and w_0 is the width of the crush profile.

The crush depth of the subject car depends on the stiffness of the other car. Figure 2.8 shows the combination of crush depths of the lighter car $\overline{C}_L$ and heavier cars $\overline{C}_H$ in each collision. Among 71 car-to-car frontal collisions, the number of collisions in which $\overline{C}_L$ is larger than $\overline{C}_H$ is 47 (66.2%). It is believed that this is because lighter cars are inclined to be less stiff.

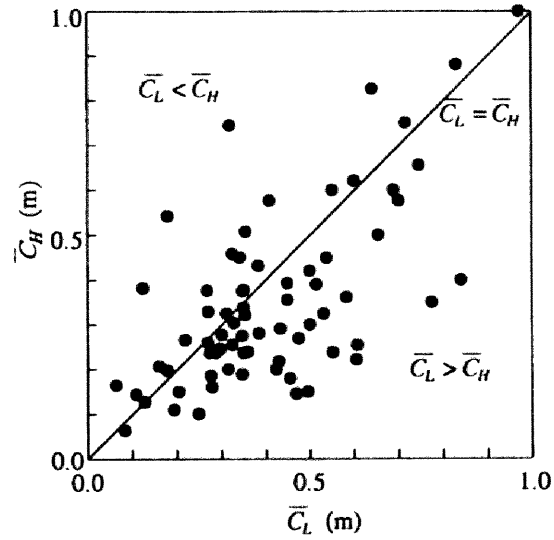

Figure 2.8. Relation between the average crush depth of the lighter car and the heavier car in crash (N=71).

The intrusion into the passenger compartment is larger as $\overline{C}$ increases (Figure 2.9). For light cars with a mass of less than 750 kg, the intrusion into the passenger compartment corresponding to the crush depth seems to be larger compared to that of other cars. A light car is almost always a small-sized car. Due to the large crush depth, a small-sized car results in a large intrusion into the passenger compartment and a high injury risk to the driver such as femur fractures.

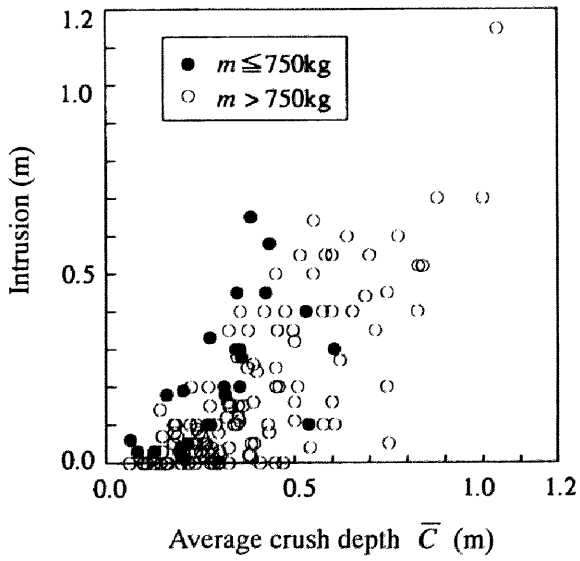

Figure 2.9. Relation between average crush depth and intrusion (N=147).

The combination effect of the mass and the stiffness of the car on the injury risks to drivers was examined here. The injury severity of the driver in the lighter and heavier cars was examined by the crush depth of the lighter car $\overline{C}_L$ and that of the heavier car $\overline{C}_H$ (Figure 2.10). Due to high acceleration, the percentage of the severe injury (MAIS 3+) is higher in the lighter car regardless of

the crush depth of the car. The percentage of serious injuries to the driver in the lighter car is about 75% for $\overline{C}_L < 1.5\overline{C}_H$. However, when the crush depth of the lighter car is much larger than the heavier car ($1.5\overline{C}_H < \overline{C}_L$), the risk of severe injury in the lighter car becomes extremely high: in the lighter cars, 18 drivers were severely injured and only one driver was slightly injured. It can be concluded that cars with small mass and low stiffness have the highest risk to the driver in car-to-car frontal collisions.

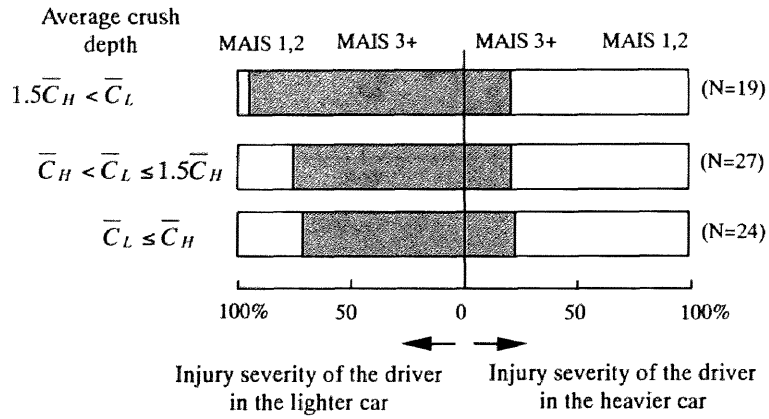

Figure 2.10. The injury severity of the driver classified by the crush depth of the car.

When the crash configurations, such as the velocity, the angular velocity and the position of each car, are the same, the maximum crush energy absorbed by the deformation of both cars E_1, E_2 is given by [Ishikawa 1993a]:

$$E_1 + E_2 = \frac{1}{1 - m_n m_t m_0^2}\left(\frac{1}{2} m_n RDS_0^2 + \frac{1}{2} m_t RSS_0^2 + m_n m_t m_0 RDS_0 RSS_0\right) \tag{2.8}$$

where, $RDS_0 = v_{20n} - a_2\omega_{20} - v_{10n} - a_1\omega_{10}$,

$RSS_0 = v_{20t} + b_2\omega_{20} - v_{10t} - b_1\omega_{10}$,

$$m_n = \frac{\gamma_{1n} m_1 \gamma_{2n} m_2}{\gamma_{1n} m_1 + \gamma_{2n} m_2}, \quad m_t = \frac{\gamma_{1t} m_1 \gamma_{2t} m_2}{\gamma_{1t} m_1 + \gamma_{2t} m_2},$$

$$\gamma_{1n} = \frac{k_1^2}{k_1^2 + a_1^2}, \quad \gamma_{2n} = \frac{k_2^2}{k_2^2 + a_2^2}, \quad \gamma_{1t} = \frac{k_1^2}{k_1^2 + b_1^2}, \quad \gamma_{2t} = \frac{k_2^2}{k_2^2 + b_2^2}.$$

In a central collision, Eq. (2.8) yields:

$$E_1 + E_2 = \frac{1}{2}\frac{m_1 m_2}{m_1 + m_2} v_c^2. \tag{2.9}$$

The total absorbed energy depends only on car mass and closing velocity, but the stiffness of both cars has no effect on this energy. The absorbed energy is shared by the lighter and heavier cars according to its stiffness. It is therefore important that the smaller car does not absorb much crush energy, so that the integrity of the passenger compartment should be maintained. The large car should absorb more energy than the smaller car because it commonly has a larger deformation area.

2.2.3. Geometry Compatibility

Incompatibility between cars occurs not only due to its mass and stiffness but also due to front geometry. We discuss the geometry compatibility through micro accident data from the Ministry of Transport. Figure 2.11 shows the geometry incompatibility between a SUV and a small sedan. The bumper and frame height of SUVs are higher than those of a small sedan. This incompatibility of the frame height can cause differences in the deformation mode between cars.

Figure 2.12 and Figure 2.13 show crushed cars in a head-on collision. Car A (SUV, 1820 kg) went beyond the centerline of the road and collided with car B (Small car, 1160 kg) with a 30% overlap. Car A overrode car B due to the difference in the front frame height. The maximum crush depth of car A was 43 cm and the passenger compartment remained intact. On the other hand, the front frame of car B could not absorb the crush energy as it was designed for a crash against a rigid barrier. The hood deformed in the upward direction. The maximum crush depth of car B was 60 cm, and the compartment deformed so that the bottom of the A-pillar moved backward 10 cm and the intrusion of the dashboard on the driver's side was 10 cm.

Both drivers in the two cars failed to wear a seatbelt. The driver in car B suffered a brain contusion (AIS 5) by contact with the windscreen, fracture of seven ribs (AIS 3) by contact with the steering wheel, and also fracture of the tibia (AIS 2) due to intrusion of the whole front panel. On the other hand, the driver in car A suffered a wrist fracture from the steering wheel (AIS 2). There are reports of many other cases in which those incompatibilities of geometry cause very serious damage.

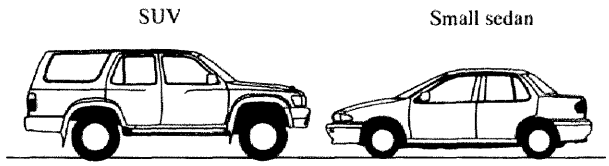

Figure 2.11. Difference in height of front structure between two cars.

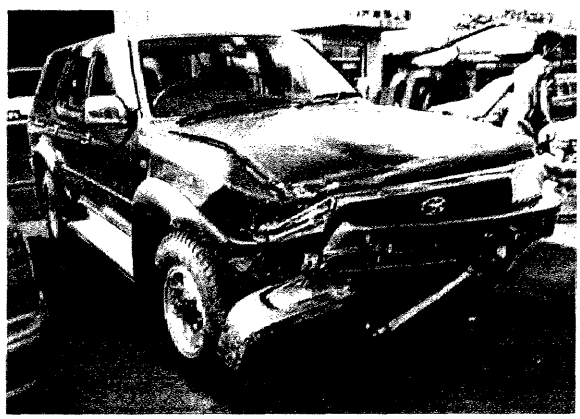

Figure 2.12. Car A.

Figure 2.13. Car B.

2.2.4. Compatibility Analyzed by Car Class

Car class

The effects of mass, stiffness and geometry are combined when the compatibility is analyzed by car classes. We examine the compatibility by the car class using macro accident data of ITARDA for the four years from 1992 to 1995. The analysis is conducted only for cars with a model year of 1988 or later. In the current research, cars are categorized into eight classes; mini, small sedan, medium sedan, large sedan, sports and specialty, wagon, van and Sports Utility Vehicle (SUV). Vehicle examples with their classes are shown in Table 2.2.

The number of cars accounts for about half the total vehicle registrations. Figure 2.14 shows the distribution of registered cars according to their classes in 1992 and 1995 [ITARDA 1996]. The number of cars increased by a factor of 1.4 from 27,772 to 39,657 thousand. Moreover, the distribution of the car classes changed. The proportions of the registered numbers of wagons, vans and SUVs have increased. On the other hand, the proportion of sedans has decreased, especially the medium sedan which reduced from 19.5 to 15.8%. As the variety of cars is increasing, the frequency of collisions between various classes of cars is increasing. Thus, the compatibility for various types of cars is becoming a topic of more important consideration.

Table 2.2. Car classes [ITARDA 1996].

Vehicle class	Vehicle example
Mini car	Alto, Mira, Today, Minica, Vivio, Wagon R
Small sedan	March, Corolla, Sunny, Civic, Familia
Medium sedan	Corona, Bluebird, Accord, Galant
Large sedan	Mark II, Crown, Celsior, Skyline, Cedric
Sports and Specialty	Cappuccino, MR2, 180SX, FTO, RX-7
Wagon	Legacy, Odyssey, RVR, Mark II wagon
Van	Estima, Townace, Serena, Delica
SUV	Land cruiser, Pajero, Jimny, Rav-4

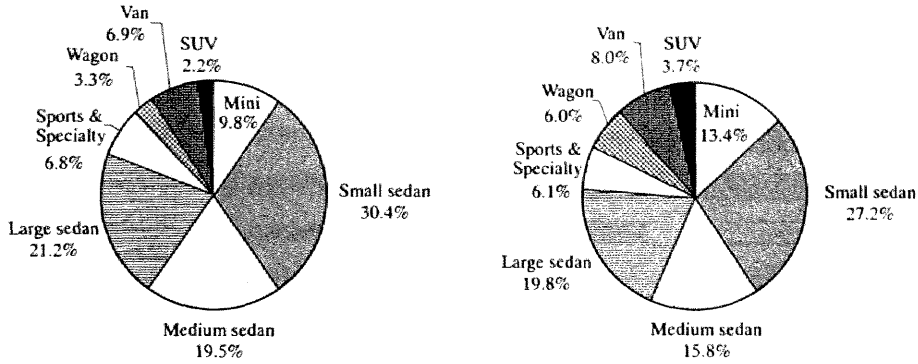

Figure 2.14. Distribution of car registrations in Japan [ITARDA 1996].

Distribution of Fatalities

The distribution of fatalities was calculated from the macro accident data in Japan. This distribution is examined by the number of fatalities internal and external to the subject car in various types of accidents. Figure 2.15 shows the number of fatalities in relation to the subject car per million registrations.

Sports and specialty cars, SUV, van and large sedan types cause more external-type fatalities than any other type of vehicle. SUV and sports and specialty cars, in particular, cause the largest fatalities in the other cars in car-to-car collisions. Cyclists sustain more fatalities when struck by sports and specialty cars and vans, while more pedestrians are killed by accidents involving sports and specialty cars and the SUV.

From the analysis of distributions of fatalities, it is found that the total number of fatalities of mini cars is the lowest, and so this car type could be considered as the most compatible vehicle. However, this conclusion cannot be drawn because it was shown that the mini cars are used for short-distance travel at a relatively low velocity [ITARDA 1996], and also because the frequency of internal driver fatalities in car-to-car collision is high. It is also necessary in the analysis of compatibility to exclude the influence of the factors which are not related to the car itself, such as driver behavior, car velocity and accident rate.

The number of fatalities in single-car accidents involving sports and specialty cars is especially large, which can be accounted for by their higher crash velocity and accident rate compared to any other car classes. As a result, the number of fatalities involving sports and specialty cars is large for all types of accidents.

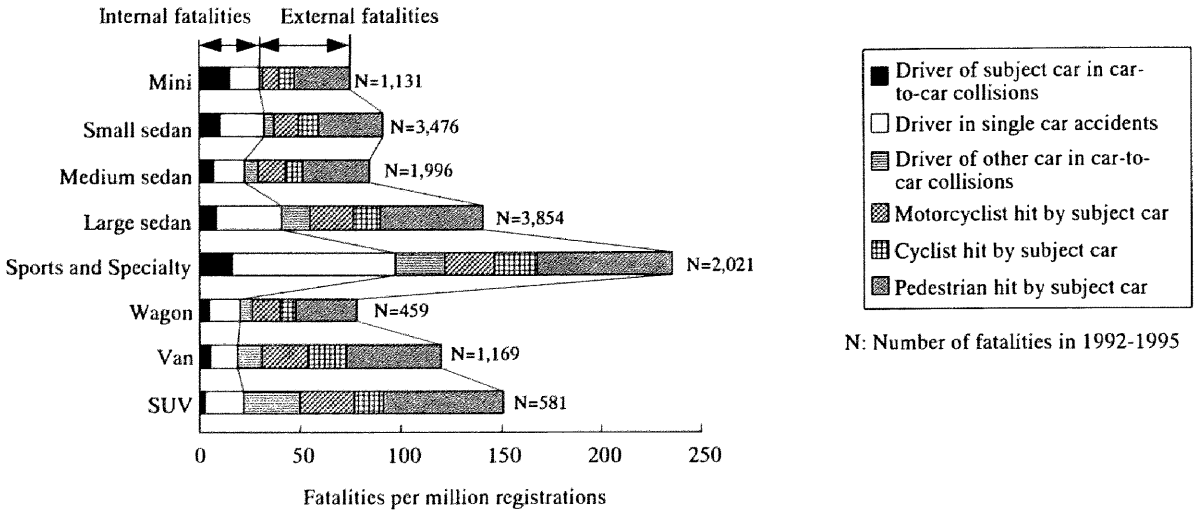

Figure 2.15. Internal and external fatalities of various subject cars for different types of accidents.

Probability of injury

Table 2.3 shows the percentage of serious and fatal injuries to the drivers in cars according to their class. The fatality rate in mini cars is high when they collided with a van or SUV. The total percentage of serious injury to the drivers in the van is high (3.69%) compared to that of fatal injury (0.18%). For example, the total percentage of fatal injury to the drivers in a large sedan (0.18%) is similar to that in a van. However, the total percentage of serious injury (2.41%) is lower than for the van. This is related to the fact that the percentage of serious injury to driver's legs is higher for the van due to the large intrusion compared to other car classes [ITARDA 1996]. It is observed from Table 2.3 that there are no fatalities of the drivers in a SUV in car-to-car frontal collisions, though the percentage of driver fatalities is high when the other car is a SUV.

Table 2.3. Driver fatality (%) in car-to-car frontal collisions (1992-1995).

Subject	Other								
	Mini car	Small sedan	Medium sedan	Large sedan	Sports & Specialty	Wagon	Van	SUV	Total
Mini car	0.03	0.26	0.39	0.72	0.64	0.22	1.31	1.26	0.45
	(2.62)	(4.59)	(5.47)	(6.87)	(5.83)	(6.01)	(7.84)	(8.50)	(5.33)
Small sedan	0.04	0.20	0.20	0.38	0.36	0.34	0.66	0.58	0.27
	(1.42)	(2.98)	(3.34)	(3.91)	(4.39)	(3.38)	(5.09)	(5.14)	(3.36)
Medium sedan	0.05	0.04	0.21	0.35	0.29	0.07	0.50	1.23	0.21
	(0.87)	(2.36)	(2.81)	(3.02)	(3.58)	(3.12)	(4.28)	(4.39)	(2.70)
Large sedan	0.04	0.04	0.09	0.26	0.48	0.06	0.30	0.68	0.18
	(1.05)	(1.92)	(2.35)	(2.83)	(3.10)	(2.61)	(3.08)	(4.90)	(2.41)
Sports and Specialty	0.13	0.05	0.26	0.40	0.30	0.13	0.39	0.32	0.23
	(0.72)	(2.05)	(2.68)	(3.16)	(3.51)	(3.83)	(3.22)	(6.55)	(2.67)
Wagon	0.11	0.04	0.07	0.22	0.38	0.84	0.00	0.38	0.17
	(0.87)	(1.84)	(2.30)	(2.38)	(2.81)	(3.07)	(3.70)	(3.80)	(2.23)
Van	0.09	0.17	0.00	0.17	0.29	0.25	0.29	0.80	0.18
	(1.03)	(2.27)	(4.47)	(4.80)	(3.61)	(3.21)	(6.03)	(8.51)	(3.69)
SUV	0.00	0.00	0.00	0.00	0.00	0.00	0.00	0.00	0.00
	(0.47)	(1.27)	(1.74)	(1.73)	(1.28)	(2.66)	(2.93)	(0.93)	(1.51)
Total	0.05	0.12	0.19	0.36	0.39	0.21	0.52	0.73	0.24
	(1.29)	(2.63)	(3.18)	(3.66)	(3.84)	(3.46)	(4.54)	(5.46)	(3.12)

( ) Serious injury

Compatibility

The goal of vehicle compatibility in vehicle-to-vehicle frontal collisions is to minimize the number of fatalities while maintaining the injury rate of occupants in each vehicle at the same level. Since the aim of this study is to estimate compatibility in a vehicle-to-vehicle frontal collision, a method is employed to determine the total number of fatalities in both vehicles per accident by comparing the ratio of the fatalities occurring in each vehicle.

The number of driver fatalities in the subject and other car per thousand accidents is shown in Figure 2.16. For the SUV and van, the total number of driver fatalities is large and the proportion of the fatalities in other cars is high, and so the SUV and van can be considered to be incompatible cars. On the other hand, for mini cars, the number of fatalities in the subject car is the largest in all car classes. Therefore, mini cars cannot be said to be compatible in car-to-car frontal collisions. The wagons and medium sedans are compatible cars in car-to-car frontal collision because the proportion of the number of fatalities in the subject cars to that in other cars is almost the same, and the total number of fatalities in the subject and the other cars per accident is small. However, the number of incompatible car types such as the SUV and van is increasing in the current traffic environment, while that of the compatible medium sedan car type is decreasing (see Figure 2.14).

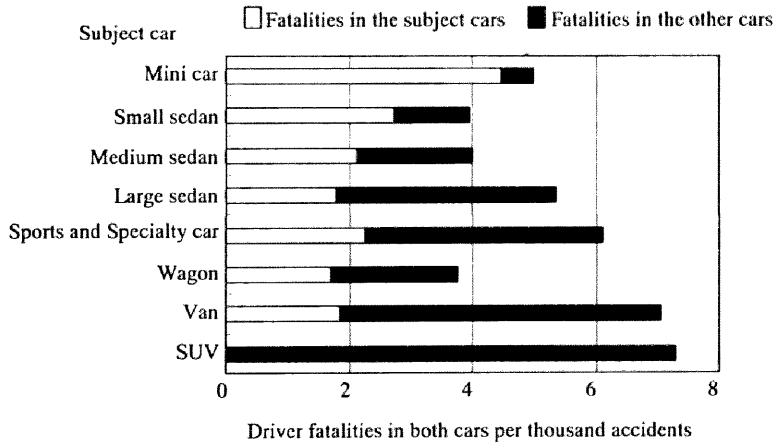

Figure 2.16. Car compatibility.

Car aggressivity

In the present study, the following measures were used to evaluate the aggressivity in vehicle-to-vehicle frontal collisions:

1. (Number of fatalities in the other vehicles)/(Number of fatalities in the subject vehicles);
2. Percentage of fatalities in the other vehicles;
3. Number of fatalities in other vehicles per million of the subject vehicle registrations.

Measures 1 and 3 were suggested by Hollowell [1996]. Using Measure 1, the aggressivity of a vehicle without the influence of human factors can be described. If the crash velocity of the subject vehicle is high, the risk of injury to the occupants in the other vehicles as well as in the subject vehicle is high. Thus, the influence of crash velocity on the aggressivity estimated by Measure 1 will be small. On the other hand, the aggressivity of the vehicle including the influence of crash velocity is estimated when the injury rate of the driver in the other vehicles is used in Measure 2. If the crash velocity of the subject vehicle is high, the aggressivity obtained by Measure 2 will be higher because the number of fatalities in the other vehicles will increase. The aggressivity estimated by Measure 3 includes the influence of travel distances, vehicle velocities and accident rates, reflecting how they are used (Table 2.4).

The measure of examining aggressivity depends on the problem being investigated. For example, vehicle manufacturers can use Measure 1 to estimate aggressivity of vehicles because this measure is related to the vehicle itself. Measure 2, which includes the velocity effect, is usable in studies dealing with road user behaviors. Measure 3 expresses the aggressivity of each registered vehicle, so it can be used when insurance problems are investigated.

Table 2.4. Aggressivity evaluating measure and the effect of crash velocity and accident rate on each measure.

Measure	Definition	Crash velocity	Accident rate
1	(Number of fatalities in other vehicles) /(Number of fatalities in subject vehicles)	X	X
2	Percentage of fatalities in other vehicles	O	X
3	Number of fatalities in other vehicles per subject vehicle registrations	O	O

O= Large effect X = Small effect

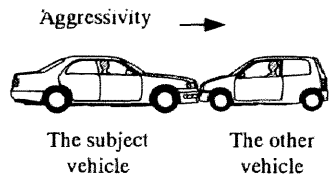

The aggressivity estimated by Measures 1, 2 and 3 is shown in Figure 2.17, Figure 2.18 and Figure 2.19, respectively. In Measure 1, cars can be defined as aggressive when the aggressivity value is greater than one, because the number of fatalities in the other cars is larger than in the subject cars. Therefore based on Figure 2.17, the SUV, van, large sedan and sports and specialty cars can be described as aggressive. According to the analysis of Figure 2.17, the aggressivity ranking of the car itself is shown as:

Mini < Small sedan < Medium sedan < Wagon < Sports and specialty cars < Large sedan < Van < SUV.

The aggressivity of a car according to its class has a similar tendency to the results using Measures 1, 2 and 3 except for the sports and specialty cars. The aggressivity of the sports and specialty cars is large when estimated by Measure 3 using car registrations, although it is not so large when estimated by Measure 1 using the ratio of driver fatality for both cars. This can be explained by the fact that the

accident rate, crash velocity and travel distance of sports and specialty cars are so high that the number of fatalities per car registrations becomes larger. It is possible to consider that the sports and specialty car itself is not aggressive but when it is driven, it has high aggressivity due to human factors.

Hollowell (1996) showed that the aggressivity defined by Measure 3 in the US is 24 for sub-compact, 38 for compact, 39 mid-size, 42 for large, 46 for minivans and 72 for SUV, which are greater than the values shown in Figure 2.19. These rather significant differences cannot be explained even if taking account of the assumptions that only driver fatalities are considered, while in the US study all occupant fatalities in car-to-car collisions were included. This is related to the fact that in the US the cars travel with higher velocity and over longer distances than in Japan. For example, the average travel distance of a car per year is 17,862 km in US against 10,130 km in Japan (1994) [IRF 1995].

According to the results of the accident analyses conducted, in the case of car-to-car frontal collisions, the mini cars and the SUV were found to be the least compatible car types in the traffic situations of Japan. The self-protection of the mini cars is poor, whereas the aggressivity of the SUV is high. Because of the environmental aspects such as its low fuel assumption and emissions and space utility, mini cars are becoming important in the world. This situation contradicts the issue of compatibility.

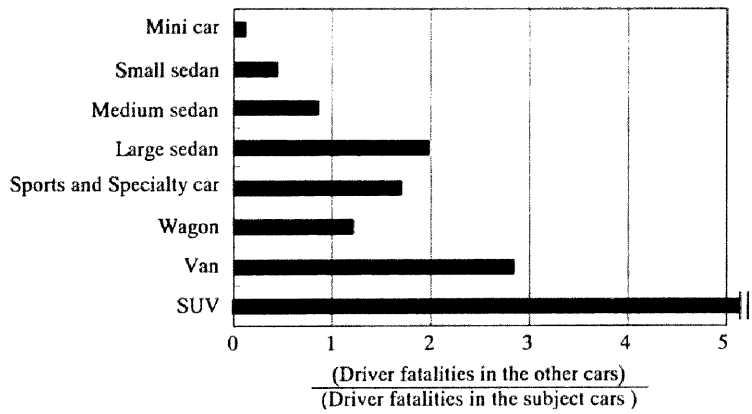

Figure 2.17. Car aggressivity calculated by Measure 1.

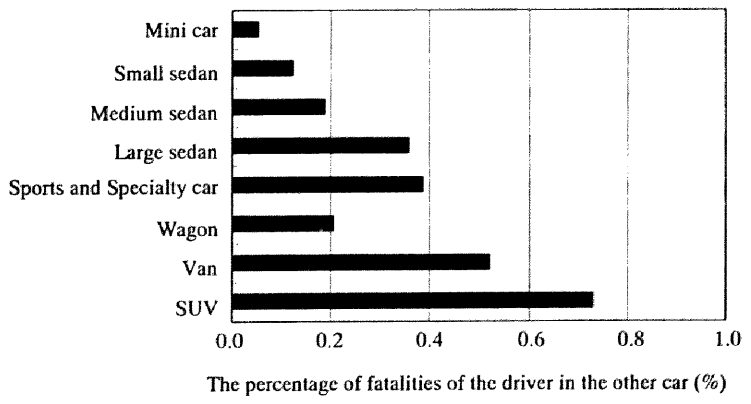

Figure 2.18. Car aggressivity calculated by Measure 2.

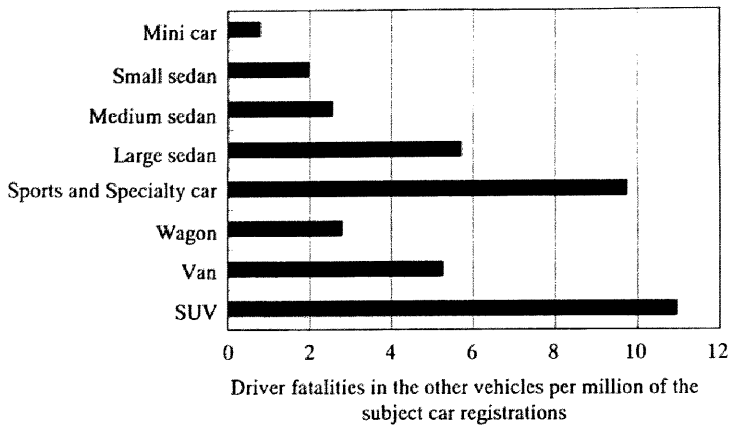

Figure 2.19. Car aggressivity calculated by Measure 3.

2.2.5. Injured Body Regions by Car Size

Because mini cars are expected to increase in number and injury risk to the driver was confirmed to be high, it is necessary to compare the injury pattern of this type of car with small, medium and large cars. We examine the frequency of injuries to different body regions in order to clarify the influences of different accident configurations and vehicle sizes. Figure 2.20 and Figure 2.21 illustrate the number of injuries to major body regions of the drivers in passenger cars per thousand accidents, classified by injury severity, vehicle size, and occupant restraint in car-to-car and single-car frontal collisions.

Some characteristic differences can be found in the frequency with which injuries of a given severity level occur. For fatalities, injury to the head is a major cause of death, followed by the chest. For serious injuries, the frequency of leg injuries is the highest, followed by chest and head. Wearing a seat belt reduces the likelihood and the severity of the impact of the occupant's body against the car interior, and prevents ejection from the car, thereby the severity of injuries become low.

We can also find differences in the pattern of body regions injured in different-sized cars. The frequencies of head, chest and leg injuries are higher for smaller cars in car-to-car frontal collisions, whereas the frequency of the head injury is lower for smaller cars in single-car crashes. In car-to-car frontal collisions, delta-V increases when the car is smaller or lighter, whereas the crash velocity is lower for smaller cars in single-car crashes. Therefore, it seems that the frequency of head injuries strongly depends on delta-V. The chest and leg injuries are also affected by the compartment intrusion, the frequencies of these injuries are higher for smaller cars. In car-to-car frontal collisions, due to the high delta-V and the large intrusion into the compartment, the drivers in mini cars are apt to suffer severe injuries to the head, chest and leg compared with other cars. The optimum restraint systems and stiff compartment can reduce the severity of these injuries to the driver in the mini car. In order to confirm the effect of the restraint system and stiff compartment, a mathematical simulation was performed.

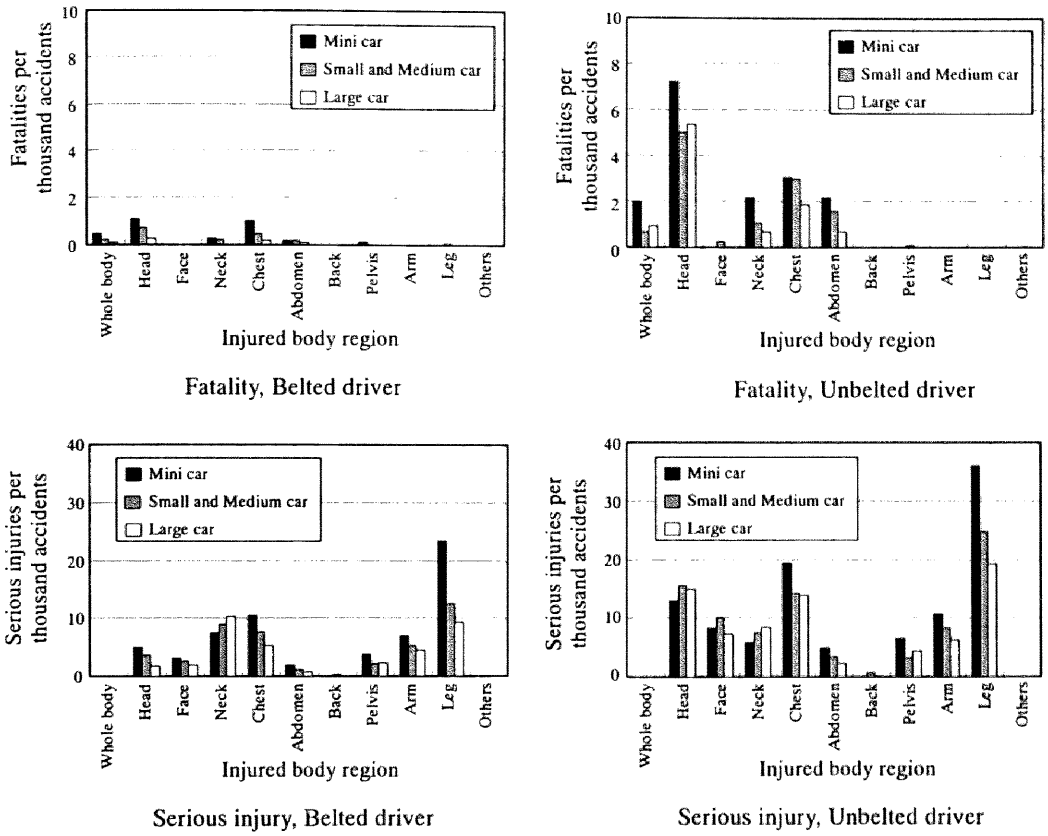

Figure 2.20. Body regions of drivers injured in car-to-car frontal collisions.

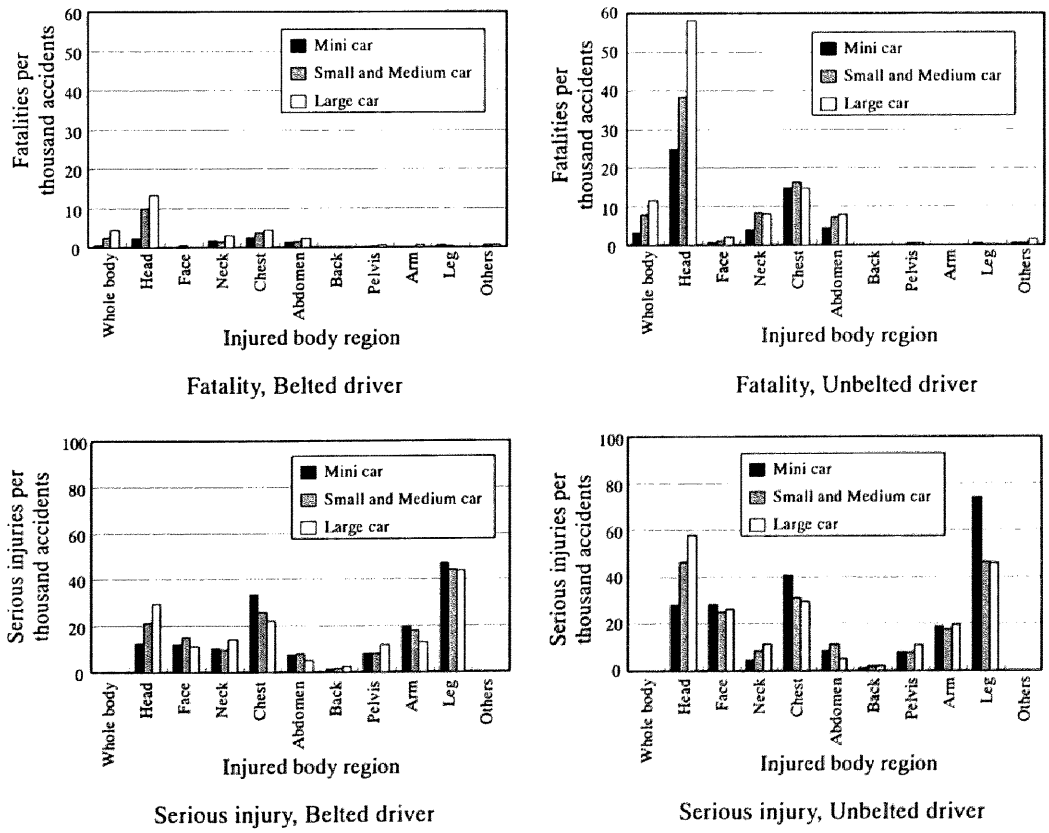

Figure 2.21. Body regions of drivers injured in single-car crashes (Frontal impacts).

2.3. MATHEMATICAL SIMULATION OF MINI CAR COLLISIONS

Accident analyses has indicated that the self-protection of the mini car is a key point to secure the compatibility for passenger cars. Computer simulations of a crash of a mini car were performed in order to clarify the injury risk to the driver of the mini car and to examine a compatible mini car.

The compatibility of a mini car in a collision with a large car has to be achieved without increasing the injury risk to the driver of the mini car in a single-car crash. Therefore, the crash of a mini car into a rigid barrier with full overlap, and the collision with a large car with a 50% overlap was simulated using multi-body analysis program, MADYMO (Mathematical Dynamic Model). MADYMO simulates the gross motion of systems of bodies connected by kinematic joints. The influences of front stiffness and the restraint systems of the mini car on the injury risk to the driver was studied to secure the compatibility of mini cars in frontal collisions.

2.3.1. Car model

The car model used in this thesis is based on a currently produced mini car. We simulated crashes of a mini car into a rigid barrier and large car as shown in Figure 2.22 and Figure 2.23. The mass of the mini car is 700 kg, which is slightly larger than the average mini car (639 kg, see Figure 2.1), and the mass of the large car is 1400 kg.

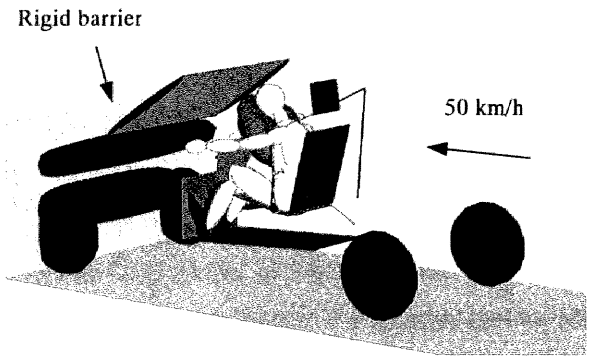

Figure 2.22. Simulation model of a mini car in a frontal crash into a rigid barrier.

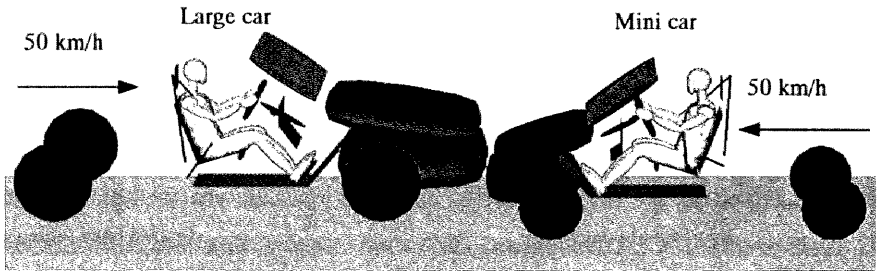

Figure 2.23. Simulation model for a frontal collision between a mini car and a large car with a 50% overlap for mini car.

Car front structures was represented by ellipsoids. In the present model, the force–deformation characteristics of the mini and large cars are approximated by a straight line.

The regression of the stiffness of the car (k) is expressed by using car mass (m) as follows [Ishikawa 1990]:

$$k = 78m^{1/3} \text{ (kN/m)}. \tag{2.10}$$

Using Eq. (2.10), the stiffness of the current mini car (700 kg) is evaluated as 693 kN/m. The stiffness of the mini car is changed from 500 to 1000 kN/m in order to examine the effect of the stiffness in crashes into a rigid barrier and into a large car. The stiffness of the large car (1400 kg) is assumed to be 872 kN/m by Eq. (2.10), which is used in the simulation of a car-to-car collision.

In an offset crash, the damage profile of the car is classified into direct damage and induced damage. Due to the induced damage, the stiffness of the car in the offset crash increases by 30% per width of the car [Ishikawa 1995]. Thus, the front stiffness of the car in an offset collision is estimated as:

$$k_{offset} = 1.3k \times (overlap\ ratio) \tag{2.11}$$

where k_{offset} is the stiffness of the car in the offset crash and k is that in the full overlap crash. In car-to-car collisions, the forces acting on both cars have the same magnitude but a different direction. The deformation of each car is calculated using force–deformation characteristics according to this force.

According to Matsumoto et al. [1990], the intrusion of the firewall (x_{firewall}) can be approximated as:

$$x_{\text{firewall}} = 0.75(x - x_0) \tag{2.12}$$

where x is the deformation of the car and x_0 is the car deformation when the engine contacts the firewall. The deformation x_0 of the mini car is smaller than that of the large car due to its small size. In the current model, x_0 is estimated as 0.175 m for a mini car and 0.350 m for a large car. Based on the experimental results (Figure 2.24), the longitudinal displacement of the steering column (x_{steering}) can be expressed by the intrusion of the firewall (x_{firewall}) as:

$$x_{\text{steering}} = 0.772(x_{\text{firewall}} - 0.0566). \tag{2.13}$$

In the model, the movements of the firewall and the steering column was simulated as the displacement of translational joints based on Eqs (2.12) and (2.13). To express the intrusion of the firewall, the toe pan is designed to rotate first, and upon becoming perpendicular moves in the driver's direction.

The HYBRID III database from MADYMO was used for the driver. The seatbelt (10% webbing) and airbag (35l) are used for the basic restraint system for drivers in mini and large cars. This combination of restraint systems is commonly used in the current cars. This model of mini car was validated using the results of the full rigid barrier crash and ODB crash tests.

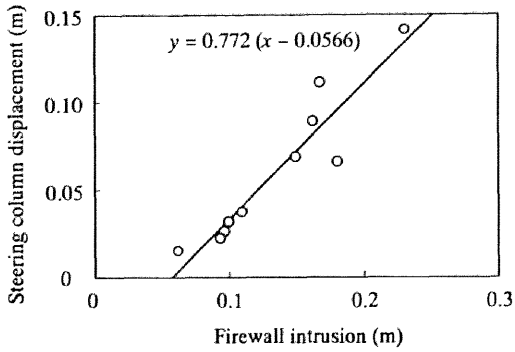

Figure 2.24. Relation between the firewall intrusion and longitudinal displacement of the steering column.

The fatalities of the driver in single-car and head-on collisions account for a large portion of the driver fatalities in mini car accidents. Crashes into a rigid barrier and car-to-car frontal offset collisions are representative of many cases of single-car and head-on collisions. In the present study, the simulations of the crash of the mini car into a rigid barrier and the crash between mini and large cars with 50% overlap for the mini car were carried out.

In this simulation, the crash velocity is taken to be 50 km/h that is prescribed in the crash regulation of the passenger cars. In the present simulation of the car-to-car frontal collision, the crash velocity of each car is 50 km/h. We examined the influences of the stiffness of the mini car on the injury risks to the driver in crashes into a rigid barrier or a large car. The injury parameters of the driver from the simulations were compared with threshold levels (Head Injury Criteria: HIC 1000, chest acceleration 60g, chest deflection 75 mm, femur force 10 kN). HIC is an injury criterion which was introduced by the US government [Versace 1972]:

$$\mathrm{HIC} = \left\{ (t_2 - t_1) \left[\frac{1}{(t_2 - t_1)} \int_0^T a(t)dt \right]^{2.5} \right\}_{\max} \tag{2.14}$$

where $a(t)$ is the resultant head acceleration in g's, and t_1 and t_2 are the initial and final times (in seconds) of the interval during which the HIC attains to a maximum value. HIC value of 1000 is associated with 15% of risk of life-threatening brain injury [Mertz 1984].

2.3.2. Simulation Results

Mini car crash into rigid barrier

The crash of a mini car into a rigid barrier at 50 km/h was analyzed in terms of various stiffness of the mini car (k). Figure 2.25 shows the results of the variation of the acceleration, deformation and the firewall intrusion of the car with the stiffness of the mini car. The acceleration increases with the stiffness, while the deformation and the intrusion decrease. Thus when the stiffness increases, the driver is exposed to a high injury risk due to high acceleration. On the other hand, when the stiffness decreases, the driver is exposed to injury risk due to large intrusions.

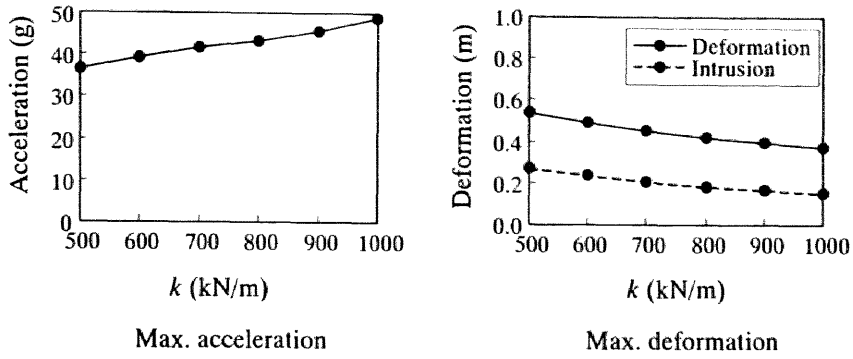

Figure 2.25. Maximum acceleration and deformation of mini car in crash into a rigid barrier with varying stiffness of the mini car (k).

The driver behavior differs according to the differences in the acceleration and the compartment intrusion of the car. Figure 2.26 shows the driver behavior where the stiffness of the mini car (k) is 500 kN/m and 1000 kN/m, respectively. When the stiffness of the mini car is 500 kN/m, the intrusion is large but the acceleration of the car is small. As a result, the head and chest movement of the driver is less, but the foot rotation angle at 500 kN/m is greater than at 1000 kN/m.

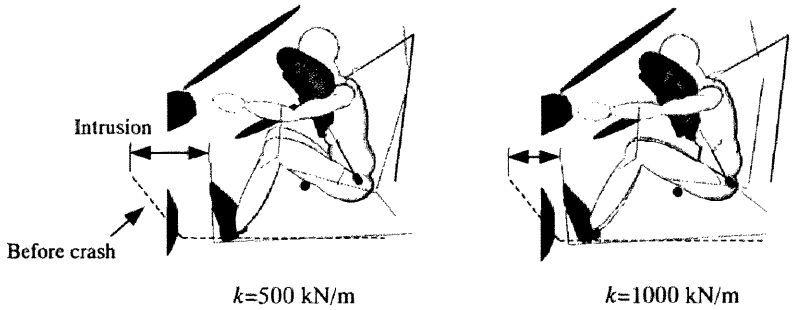

Figure 2.26. Kinematics of the driver in a mini car in a crash into a rigid barrier (50 km/h).

Since the driver behavior differs with the mini car stiffness, the injury risks based on the acceleration and intrusion may be also affected by this stiffness. Figure 2.27 shows the relation between the injury risk to the driver and the stiffness of the mini car (k). When k is the lowest (500 kN/m), the HIC is 706, chest acceleration (3 ms) is 55.9 g and chest deflection is 0.042 m, all of which are less than the injury tolerance levels. The HIC and chest acceleration increase consistently with the stiffness of the mini car. On the other hand, the chest deflection, femur force, tibia axial force and moment do not change so much with the stiffness of the mini car, and its level is less than the injury threshold. These results suggest that in a mini car crash into a rigid barrier, the injury risks to the driver decrease when the front stiffness is low.

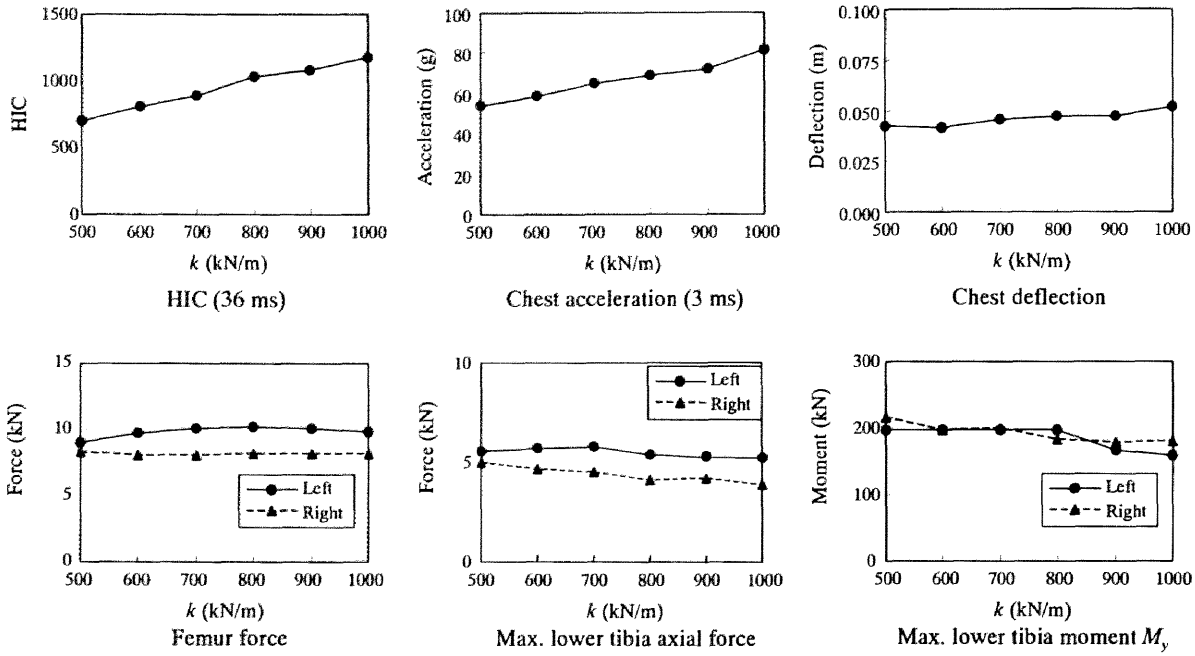

Figure 2.27. Driver injury risks in a crash into a rigid barrier with varying stiffness of the mini car (k) (50 km/h).

The transition to serious injuries of the lower extremities (AIS 3 or more) occurs when the intrusion exceeds 0.25 m [Morris et al. 1997]. As shown in Figure 2.25, the intrusion of the mini car firewall is less than 0.27 m in a crash into a rigid barrier at 50 km/h. Therefore, in this type of crash configuration, the intrusion is a less important factor in determining the injury risk to the driver of a mini car, whereas the acceleration causes the majority of injuries.

Mini car crash into large car

Simulations of an offset frontal collision between mini and large cars were carried out. The overlap ratio of the mini car is 50% and that of the large car is 40%. Figure 2.28 shows the deformation of the car and the intrusion of the firewall by the stiffness of the mini car (k). The acceleration level of the mini car in this type of crash is lower than that in a crash into a rigid barrier, whereas the car deformation and firewall intrusion of the mini car become large, especially when the stiffness of the mini car is small. Thus, in this type of collision, the effects of the acceleration and intrusion are combined, and the risk to the driver of the mini car becomes high.

As can be seen in Figure 2.29, when the mini car is less stiff (k=500 kN/m), the steering column, the instrument panel and the toe pan intrude and hit the chest, knee and foot of the driver, respectively.

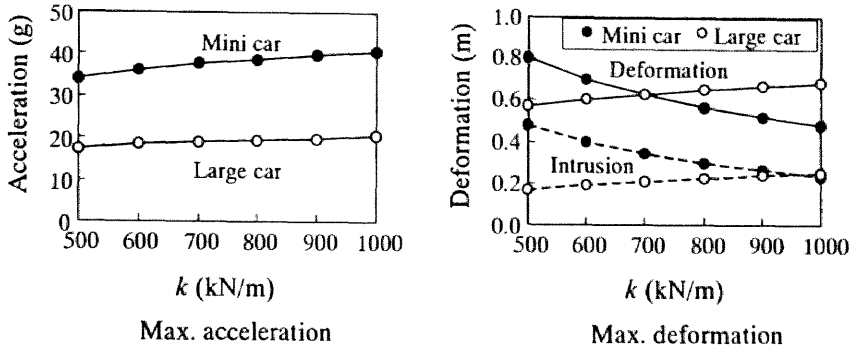

Figure 2.28. Maximum acceleration and deformation of mini and large cars in a car-to-car frontal collision with varying stiffness of the mini car (k).

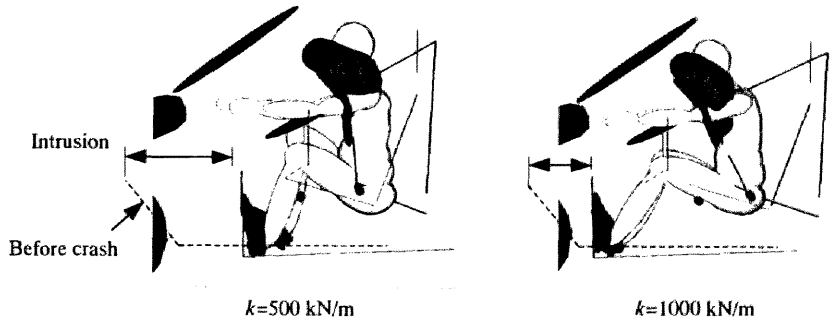

Figure 2.29. Kinematics of the driver in a mini car in a crash into a large car.

Figure 2.30 shows the variation of the injury risks to the drivers in mini and large cars with the stiffness of the mini car (k). When a comparison is made with Figure 2.27 and Figure 2.30, the HIC and chest acceleration of the driver in the mini car are lower in a crash with a large car than into a rigid barrier, whereas the chest deflection, femur force, tibia force and tibia moment are higher. The chest deflection and tibia force are strongly affected by intrusion. Thus, in a crash of the mini car with a large car, the intrusion is an important factor in injuries. In addition, Figure 2.30 indicates that the injury risk of the driver in a mini car is higher than for the driver in a large car, irrespective of the stiffness of the mini car. This result corresponds to the findings from accident analysis that the injury risk to the driver in a mini car is high, while in a large car it is low.

When the stiffness of the mini car increases, there is a decrease in the risk to its driver as estimated on the basis of intrusion criteria such as chest deflection, maximum femur, tibia force and tibia moment. However, the HIC and chest acceleration of the driver in the mini car increase with the stiffness of the mini car because its acceleration becomes high.

As the stiffness of the mini car increases, the risk of injury to the driver in a large car become larger. When the stiffness of the mini car is high, the chest acceleration, chest deflection, femur and tibia forces of the driver in the large car increase because both acceleration and intrusion of the large car

become high. Nevertheless, the risk of injury to the driver of the large car is less than that of the driver of the mini car, and even less than the tolerance level of the relevant injury criteria.

This analysis of collisions between mini and large cars demonstrates that the mini car should be stiff enough to prevent a large intrusion into the passenger compartment in a car-to-car frontal collision because greater intrusion means a higher risk of chest deflection and injury to the driver's lower extremities.

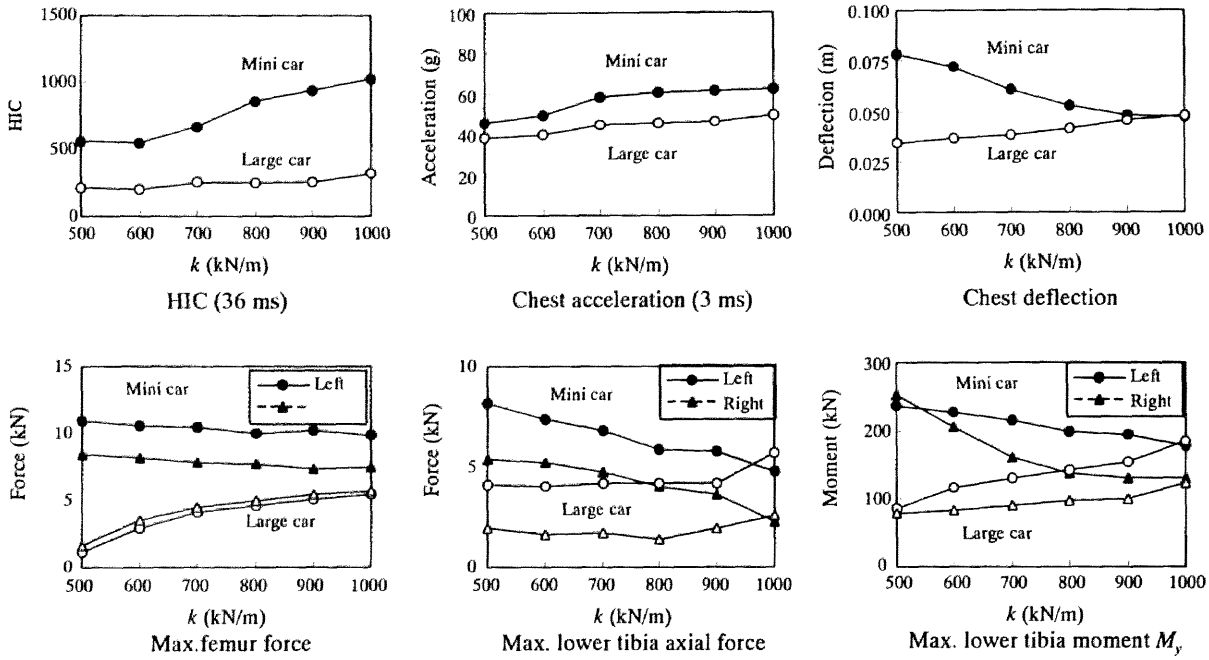

Figure 2.30. Driver injury risks in mini and large cars in a car-to-car frontal collision with varying stiffness of the mini car (k).

Effect of restraint systems

We examined the effects of restraint systems, including a seatbelt force limiter, pretensioner (4 kN, 0.15 m), energy absorbing (EA) steering system (4 kN, 0.15 m), knee bolster and their combination, on the injury risk of the driver in a mini car. The stiffness of the mini car model is 1000 kN/m, which is larger than that of current mini cars to reduce the intrusion into the passenger compartment in a crash. This high stiffness is applied for the mini car because the chest deflection, femur, tibia forces and tibia moment became low at this stiffness level as shown in Figure 2.30. The injury risks to the driver in the mini car in crashes into a rigid barrier or a large car was studied when each restraint system or its combination is used with the basic restraint system (airbag and seatbelt).

Figure 2.31and Figure 2.32 show the effect of restraint systems on the injury criteria of the driver of a mini car in crashes into a rigid barrier and a large car, respectively. The injury-reducing effect of each restraint system for the driver of mini car differs between the two kinds of crashes. In the crash into the rigid barrier, the seatbelt force limiter effectively decreases chest acceleration and HIC by

reduction of force transfer from the seatbelt to the torso of the driver. Nevertheless, the force limiter has a little effect on the injury risks of the driver of the mini car in collision with a large car. In this type of crash, a large force is applied to the driver's chest by the steering wheel, not by the seatbelt. Thus, the seatbelt force limiter has a little effect on reduction of the chest acceleration in a collision with a large car.

The EA steering system is shown effective for both of the above-mentioned crashes. The movement of the steering column can decelerate the driver's head and chest by absorption of energy. The seatbelt pretensioner can reduce the femur force. The knee bolster can also reduce the femur axial force, particularly in a crash with a large car. The restraint systems have little influence on the tibia force of the driver in a crash into a rigid barrier or a collision with a large car. Thus, to reduce the tibia forces, the intrusion of the toe pan must be reduced.

When a mini car with high stiffness is equipped with restraint systems combining airbag, seatbelt force limiter with pretensioner, EA steering system and knee bolster, the injury criteria levels for the driver are below the thresholds in either crashes into a rigid barrier or a large car.

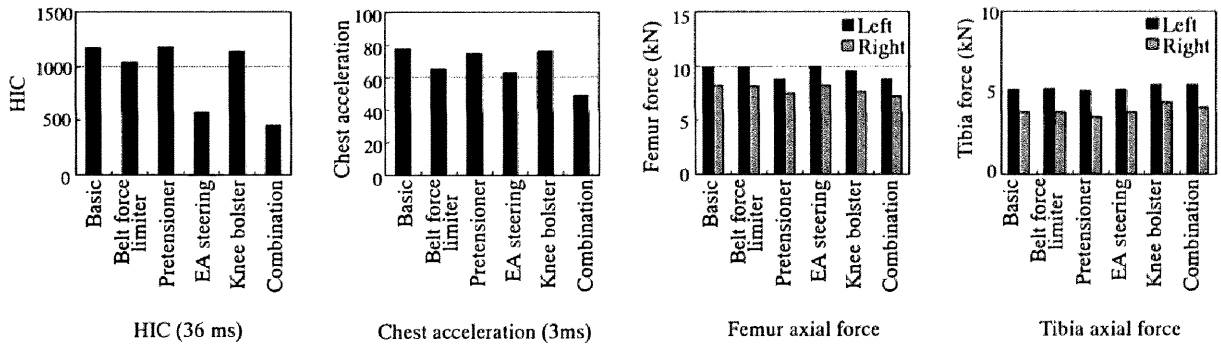

Figure 2.31. Effect of the restraint systems on the injury risks to the driver of the mini car in a crash into a rigid barrier (k=1000 kN/m).

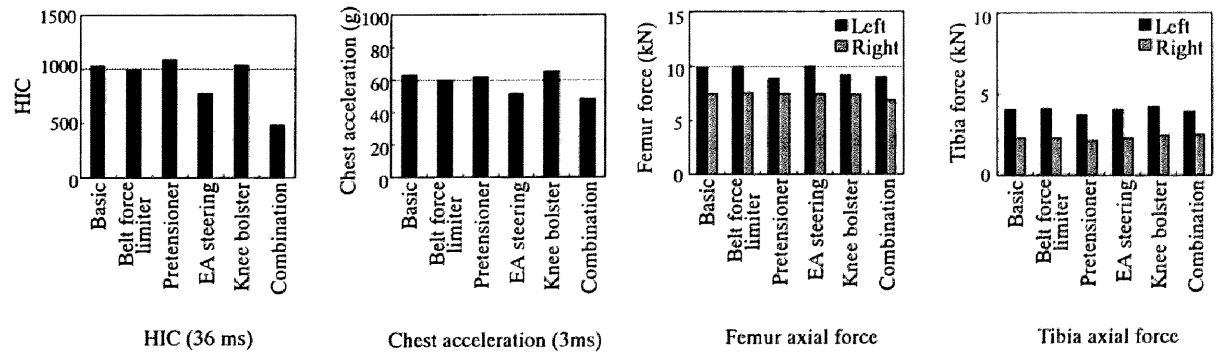

Figure 2.32. Effect of the restraint systems on the injury risks to the driver of the mini car in a collision with a large car (k=1000 kN/m).

Additional crush space of large car

When a large car has been designed to have additional crush space to secure the partner-protection in collisions with a mini car, the injury risk to the driver in the mini car may decrease. Tarrière et al. (1994) proposed a maximum force level 200 kN of a heavy car for compatibility with small car. Thus, in the present study, the additional crush length (c) of 0 to 0.4 m with a force level of 200 kN was simulated (Figure 2.33) without changing the front length of the large car.

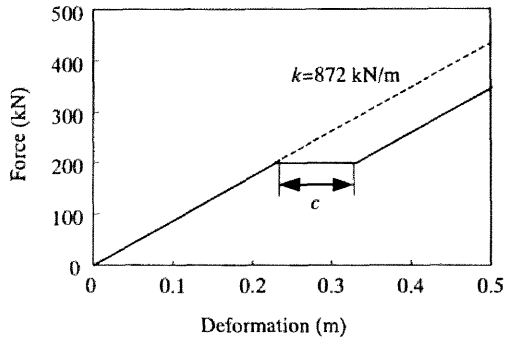

Figure 2.33. Additional crush space of a large car.

It was found that the additional crush space of the large car can reduce the injury risk to the driver in the mini car due to reduction of acceleration and intrusion of the mini car in a collision. Figure 2.34 shows the chest acceleration, chest deflection, femur and tibia forces of drivers in the mini and large cars in terms of the length of additional crush space (c) of a large car (200 kN). The additional crush space reduces the chest acceleration and femur force of the driver in a mini car, when the stiffness of the mini car (k) is high. Particularly when k is small, the chest deflection and tibia force of the driver in the mini car decrease due to the small intrusion into the mini car, as the additional crush space of the large car increases.

The chest acceleration of the driver in a large car decreases when the additional crush space of the large car is large due to the low acceleration of the large car. The chest deflection slightly increases by the additional crush space of the large car. The femur and tibia forces of the driver in the large car increase with the additional crash space of the large car, and have large values when the mini car is stiff. Thus, the analysis indicates that the additional crush space of the large car is effective in reducing injury risk to the driver of the mini car. However, when the mini car is stiff, the risk to the driver in the large car, especially for injuries to lower extremities, becomes high.

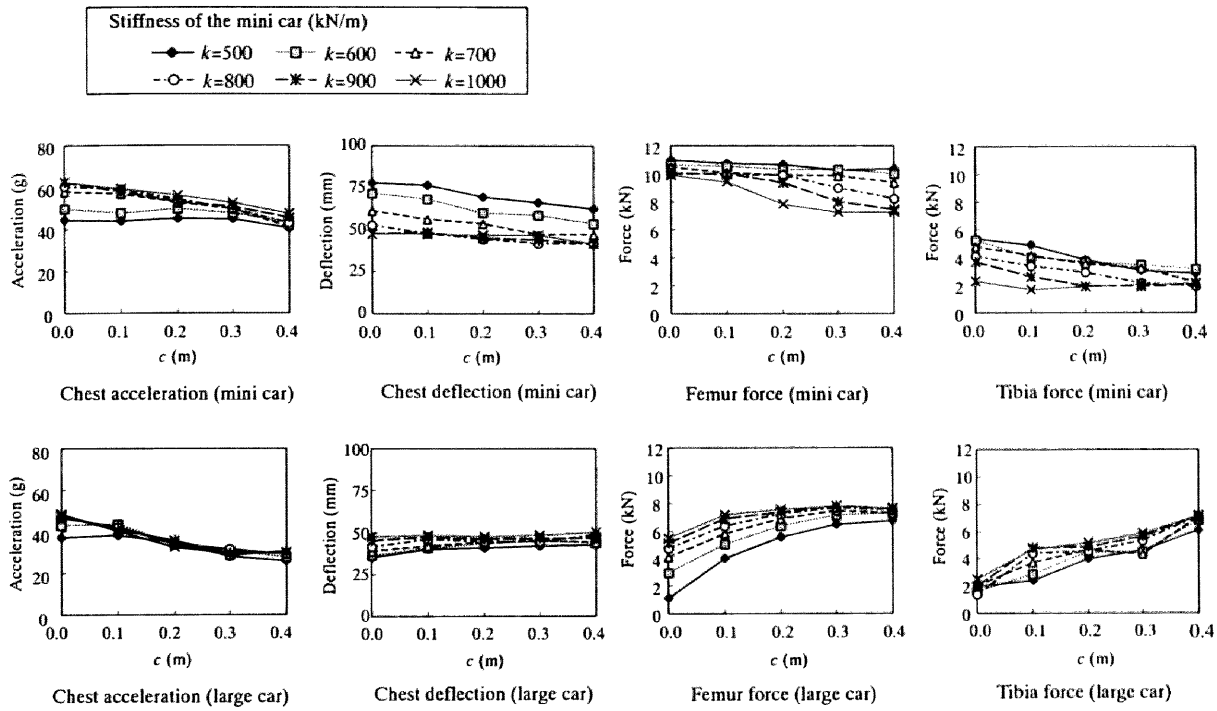

Figure 2.34. Driver injury risks in mini and large cars with the length of additional crush space (c) of the large car

Low velocity crash

Since many mini cars are used in the city, a low velocity crash in the range of 20 km/h is important. In a low-speed crash, the airbag must not deploy because the airbag itself may cause injury to the driver. In such a case, only the seat belt should provide an effective restraint.

We simulated the crash of a mini car into a rigid barrier at 20 km/h. This low-velocity crash was performed under the condition that the seat belt was used for the driver and the airbag did not deploy. The neck shear force and head displacement are used as injury criteria, and the results are compared for different front stiffness of the mini car (k) to estimate the risk of minor injuries.

Figure 2.35 shows the shear force on the lower neck level of the driver with two front stiffness, k=500 kN/m and 1000 kN/m. The maximum force on the lower neck level is larger for k=1000 kN/m than for k=500 kN/m. Thus, the risk of minor injury to the neck is large when the initial force level is high. Figure 2.36 illustrates the head movement of the driver of the mini car in a crash. The forward movement of the driver is larger for k=1000 kN/m than for k=500 kN/m. When the stiffness (k) is large, the mini car has relatively high acceleration, and the risk of the driver neck injury and head contact with the steering wheel become high. Thus, the initial force level of the mini car should preferably be low in order to prevent minor injury.

The maximum force of the shoulder belt of the mini car is 6.1 kN for k=500 kN/m, and 7.21 kN for k=1000 kN/m in this simulation. When the seatbelt force limiter is attached, the force of the seatbelt

may exceed the limit even in a crash at low velocity. In such a case, the seatbelt force limiter allows the driver to move forward, and then the risk of head contact with the steering will increase.

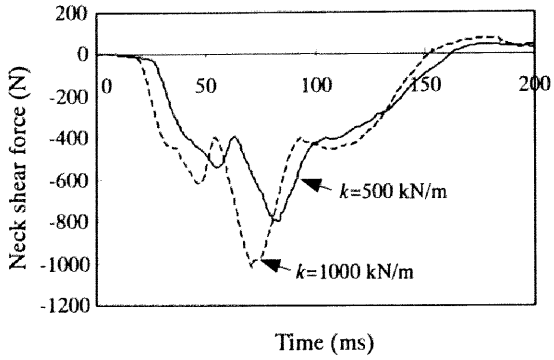

Figure 2.35. Neck shear force of the driver of a mini car in a crash into a rigid barrier at 20 km/h.

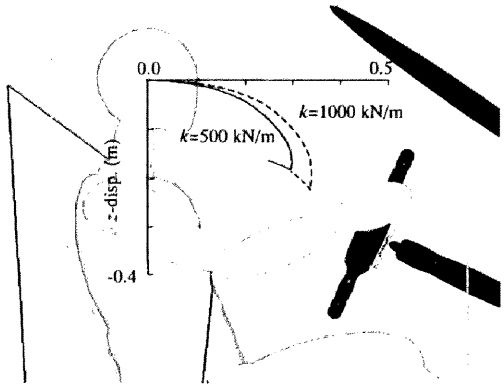

Figure 2.36. Head movement of the driver of a mini car in a crash into a rigid barrier at 20 km/h.

2.4. SIDE IMPACT

2.4.1. Accident Analysis

Mass effect

In side collisions, the factors of mass, stiffness and geometry also induce in vehicle incompatibility, and the occupants in the struck car are at high risk of injuries. However, there has not been considerable number of research on these factors.

We examined the effect of the mass of the struck and the striking vehicle on the probability of driver injury in the struck car. From the macro accident database of ITARDA (1992-1995) the accidents where the front of one vehicle collides with the side of another vehicle was collected. The results are shown in Figure 2.37 and Figure 2.38, respectively. The belted and unbelted drivers were examined together because it is observed in the side impact tests that the seat belt has less effect on the

injury risks to the drivers in side crashes than in frontal crashes [Akiyama and Takahashi 1992]. As the mass of the struck vehicle decreases and the mass of the striking vehicle increases, the probability of injury increases. The probability of driver injury ranges from 3.0 to 6.3% relative to the struck vehicle mass, in contrast to the range from 2.1 to 7.0% for a car-to-car frontal collision. Thus, we can say that the mass of the struck vehicle has more significant influences on injury probability in a car-to-car frontal collision than in a side-impact collision.

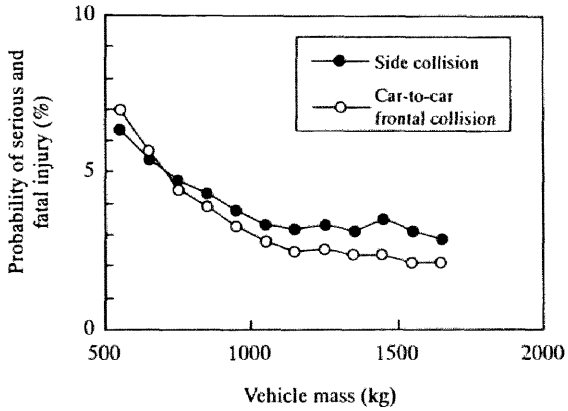

Figure 2.37. Struck vehicle mass and probability of driver injury in side-impact collision. Location of impact is driver side of car (belted and unbelted).

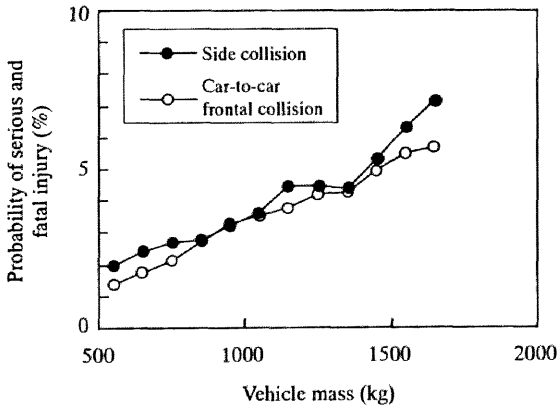

Figure 2.38. Striking vehicle mass and probability of driver injury in side-impact collision. Location of impact is driver side of car (belted and unbelted).

Car class

The combination effects of mass, stiffness and geometry in side collisions can be examined by using car class. The probability of the fatal and serious injuries to the driver in the struck car in a side collision was examined according to the striking and struck car class. Table 5 shows the percentage of the driver fatalities in a struck car in side collisions. The overall average fatal injury rate is 0.32%, which is higher than in a car-to-car frontal collision (0.24%). However, the total driver fatal injury rate

when a mini car is struck is 0.34% in a side collision, which is lower than in a car-to-car frontal collision (0.45%).

Table 2.5. Driver fatality (%) in the struck car in side collisions (1992-1995).

Subject	Other								
	Mini car	Small sedan	Medium sedan	Large sedan	Sports and Specialty	Wagon	Van	SUV	Total
Mini car	0.06	0.11	0.24	0.53	0.48	0.87	1.09	0.78	0.34
	(2.63)	(3.14)	(3.62)	(5.04)	(5.49)	(5.46)	(7.17)	(6.72)	(4.17)
Small sedan	0.10	0.25	0.19	0.55	0.48	0.09	0.71	0.70	0.35
	(1.78)	(2.44)	(2.85)	(3.55)	(4.47)	(3.72)	(4.36)	(6.07)	(3.14)
Medium sedan	0.00	0.13	0.25	0.41	0.29	0.17	0.48	0.78	0.25
	(1.69)	(2.69)	(2.60)	(3.44)	(2.73)	(3.27)	(4.10)	(4.11)	(2.88)
Large sedan	0.00	0.15	0.29	0.36	0.62	0.23	0.43	1.34	0.32
	(1.09)	(2.03)	(2.30)	(2.42)	(3.49)	(1.95)	(3.73)	(5.21)	(2.42)
Sports and Specialty	0.21	0.39	0.21	0.45	0.94	0.65	0.61	2.42	0.50
	(1.07)	(2.16)	(2.59)	(3.17)	(2.81)	(2.61)	(4.28)	(5.19)	(2.65)
Wagon	0.00	0.00	0.34	0.00	0.26	0.00	0.00	0.73	0.11
	(1.30)	(1.45)	(2.35)	(1.80)	(3.34)	(0.70)	(3.24)	(8.76)	(2.18)
Van	0.00	0.00	0.26	0.33	0.43	0.00	0.35	0.61	0.20
	(1.07)	(1.77)	(1.67)	(2.50)	(3.43)	(2.56)	(1.77)	(3.05)	(2.10)
SUV	0.00	0.00	0.24	0.32	0.00	0.00	0.62	0.00	0.15
	(2.36)	(1.52)	(1.91)	(2.24)	(2.77)	(0.00)	(1.23)	(0.00)	(1.85)
Total	0.06	0.18	0.24	0.43	0.51	0.27	0.60	1.01	0.32
	(1.65)	(2.36)	(2.66)	(3.23)	(3.77)	(3.09)	(4.24)	(5.39)	(2.90)

( ) Serious injury

In side collisions, the vehicles are classified as striking and struck. The aggressivity of the striking vehicle in side collisions is estimated by the fatalities in the struck vehicles. The aggressivity can be defined for a side collision by changing 'subject' to 'struck' and 'other' to 'striking' in Measures 2 and 3 of car-to-car frontal collisions as follows (see page 39):

2′ Percentage of fatalities in struck vehicles;

3′ Number of fatalities in struck vehicles per million striking vehicle registrations.

If the aggressivity by Measures 2′ and 3′ is high, the striking vehicle is aggressive in side collisions.

Figure 2.39 and Figure 2.40 show the aggressivity of the striking car on the fatal injury rate of the driver in the struck car using Measures 2′ and 3′. The order of aggressivity of each class has almost the same tendency as for a car-to-car frontal collision. The aggressivity of the SUV is the largest when estimated by Measures 2′ and 3′. It is thought that this is due to the incompatibility of the SUV owing to its large mass and stiffness in conjunction with geometry. The front side members of the SUV are higher than the side sill of a mid-sized car [Shearlaw and Thomas 1996]. The sports & specialty cars also have a large aggressivity for drivers in the struck car, although this is due to its high velocity and accident rate.

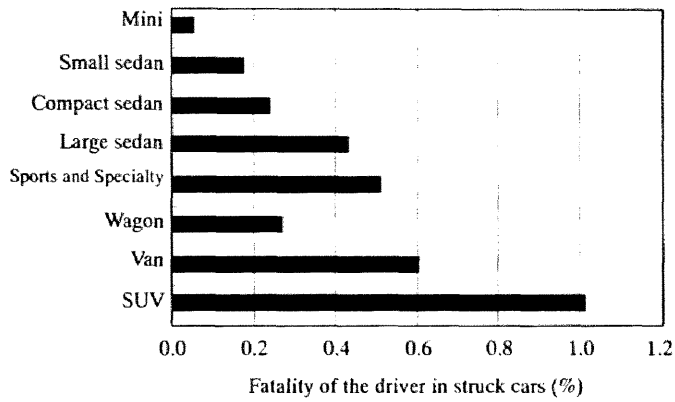

Figure 2.39. Car aggressivity in side collision by Measure 2'.

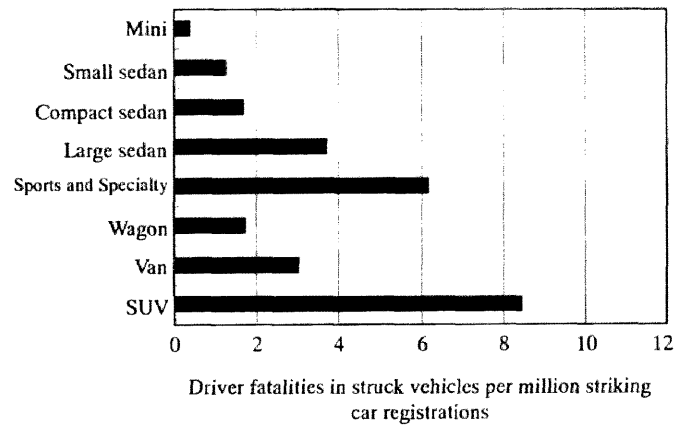

Figure 2.40. Car aggressivity in side collision by Measure 3'

As shown in Table 2.5, when the struck car is a mini car, the driver fatality rate in the struck car reaches a large value of 0.34%, although the aggressivity of the mini car is small (Figure 2.39 and Figure 2.40). On the contrary, the aggressivity of the SUV is the largest among all car types. Accordingly, in side collisions as in car-to-car frontal collisions, the mini car and the SUV are also considered incompatible car types.

When a medium sedan is struck from the side, the driver fatality rate is 0.25%, which is less than the overall average fatal injury rate of 0.32%. When the striking car is a medium sedan, the fatality rate in the struck car is 0.24%, which is also less than the overall average fatal injury rate of 0.32%. Thus, it is considered that a medium sedan is a compatible car type in a side collision because when a medium sedan strikes or is struck, the driver fatality rate in the struck car is less than the overall average fatality rate. For the same reason, a wagon is also regarded as a compatible car type in side collisions.

2.4.2. Computer Simulations

In order to evaluate the effects of the mass of the striking and struck cars, we used the side impact computer simulation model of the Component Test Procedure (CTP) [Yamaguchi et al. 1991]. This CTP model is illustrated in Figure 2.41. It consists of springs and masses to represent the vehicle side structures and side impact dummy (SID). By the use of this model, the influences of the car mass on the SID response were examined. The mass of the struck car is varied from a baseline car, with a mass of 875 kg. The mass and force/deformation characteristics of the car model are not modified.

The effects of the struck and striking car mass on Thoracic Trauma Index (TTI) and maximum pelvis acceleration of the dummy are shown in Figure 2.42. While the TTI and pelvis acceleration of the dummy decrease slightly as the mass of the struck car increases, they become higher as the mass of the striking car increases. In this simple model, the dummy is accelerated by the door immediately after impact, thus the effect of the struck car is small on the dummy response. This small effect of struck car mass and the large effect of striking car mass on the dummy injury parameters has been also confirmed experimentaly [Watanabe et al. 1989].

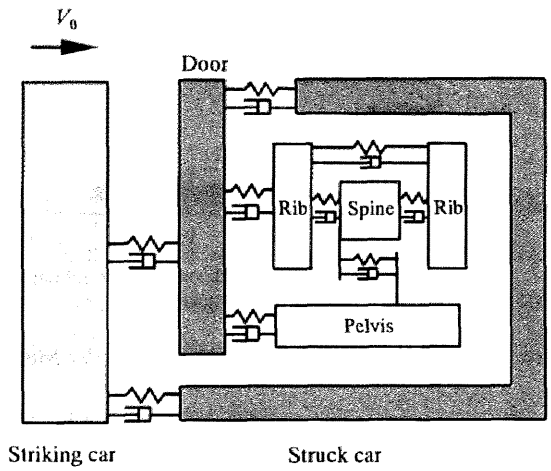

Figure 2.41. Side impact model (CTP).

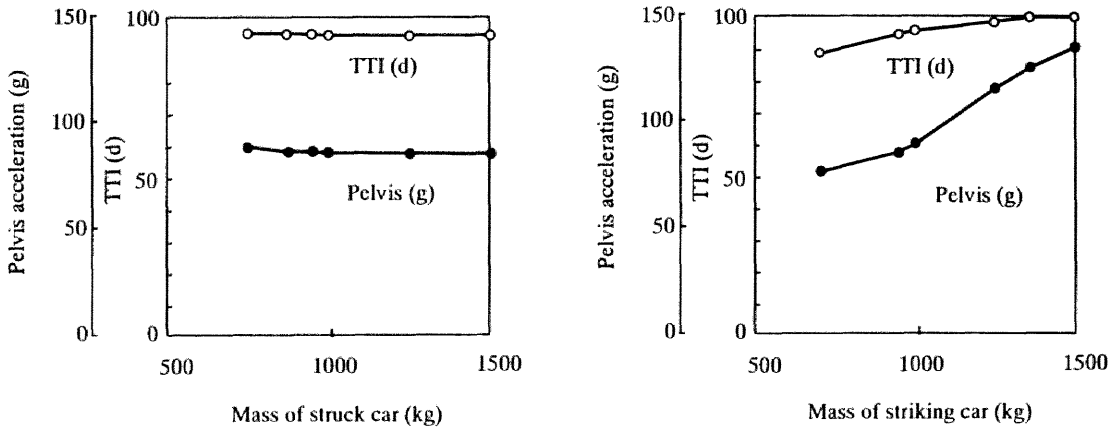

Figure 2.42. The effect of the struck and striking car mass on the dummy response.

In real world accidents as shown in Figure 2.37, the injury rate of the driver decreases with increasing struck car mass. This accident data for side collisions include oblique collisions, and the impact locations include the front and rear fenders, whereas the simulation model in Figure 2.41 is a 90-degree side impact on the passenger compartment. Furthermore, the dummy head was not included in the model because the head does not contact the interior in 90-degree side impact tests. In the real world accidents, however, the head is also a major injured body region in side impacts. An accident analysis was carried out by using the micro data to examine the vehicle mass effects in which side collisions are defined such that the fronts of the striking cars impact the passenger compartments of the struck cars [Mizuno et al. 1996]. The results showed that the injury severity of the impact side occupants does not depend on the struck car mass except for the mini car.

In the case of macro data, on the other hand, injury risk showed significant dependent on the mass of cars. Whereas the injury risk simulated by CTP was not affected by the car mass just as in the case of the micro data. This difference between the results of the simulation model and accident data may be accounted for by the fact that macro data are comprised of accidents with various impact angles and locations of the striking and struck cars.

2.5. CAR FLEET ANALYSIS

The total number of injuries in collisions will be influenced by the number of cars involved and the distribution of their respective masses. We discuss the relation between the distributions of car masses and the total number of fatalities. We used the macro accident data of the ITARDA (1992-1995) and the vehicle registration data of the Ministry of Transport (see Figure 2.1).

The total number of injuries N is calculated as [Evans and Frick 1991a]

$$N = \sum_{i,j} p n_i n_j R_i(m_i, m_j), \tag{2.15}$$

where i, j: vehicle category classified by mass, m_i, m_j,
n_i : number of vehicles in category i,
$R_i(m_i, m_j)$: probability of injury to occupant of vehicle i struck by vehicle j,
p : probability of accident.

Sensitivity analysis was conducted to clarify the effect of the number of vehicles of similar mass on the total number of seriously and fatally injured occupants. The sensitivity γ_i of the number of vehicles n_i to the total number of injuries N is calculated as:

$$\gamma_i = \lim_{\Delta n_i \to 0} \frac{\Delta N}{\Delta n_i} \tag{2.16}$$

To simplify the analysis, we assumed that the probability of accident p is the same for all vehicles, though this is not true, strictly speaking, for the actual vehicle population. In the present analysis, the probability of occupant injury in a bonnet-type car is used for $R_i(m_i,m_j)$ and the numerical distribution of passenger cars is used for n_i. The total number of cars is assumed to be constant ($\sum n_i = const.$). The probability of the injury to the driver in a side-impact collision, in particular, has been defined by taking account of strikes from both sides.

Figure 2.43 shows the results of the analysis for car-to-car frontal and side-impact collisions. When the sensitivity is positive, the number of serious and fatal injuries increases. In both car-to-car frontal and side-impact collisions, the number of serious and fatal injuries decreases when the number of cars with mass from 700 kg to 1400 kg increases. Again it is found that the influence of the number of lighter cars is larger in car-to-car frontal collisions, while that of the number of heavier cars is larger in side-impact collisions.

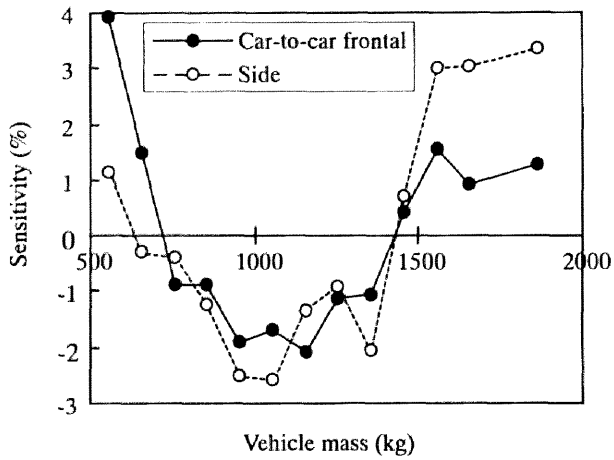

Figure 2.43. Sensitivity analysis of the effect of the numerical distribution of vehicles of given mass on the total number of seriously and fatally injured drivers.

The total number of serious and fatal injuries per year was calculated by Eq. (2.15) using the actual numerical distribution of passenger cars as a baseline, and was found to be 2,645 in car-to-car frontal collisions and 1,234 in side-impact collisions. The numerical distributions of cars which minimize or maximize the number of injuries in car-to-car frontal and side collisions are given in Figure 2.44 and Figure 2.45, respectively. The number of serious injuries and fatalities in car-to-car frontal collisions has a minimum value when the cars are concentrated in the mass region of 901-1100 kg and decreases injuries by 16% compared to the baseline distribution. On the other hand, the numerical distribution of cars with large variation in car mass maximizes the serious injuries and fatalities.

In side collisions, the number of serious injuries and fatalities has a minimum value when the cars are concentrated in the mass region of 801-1000 kg. However, when all cars have an identical and large mass of 1601-1700kg, the number of serious injuries and fatalities has a maximum value. The numerical distribution of cars which gives the minimum or maximum number of injuries is different in

car-to-car frontal and in side collisions because the effect of vehicle mass on the injury severity is different from each other.

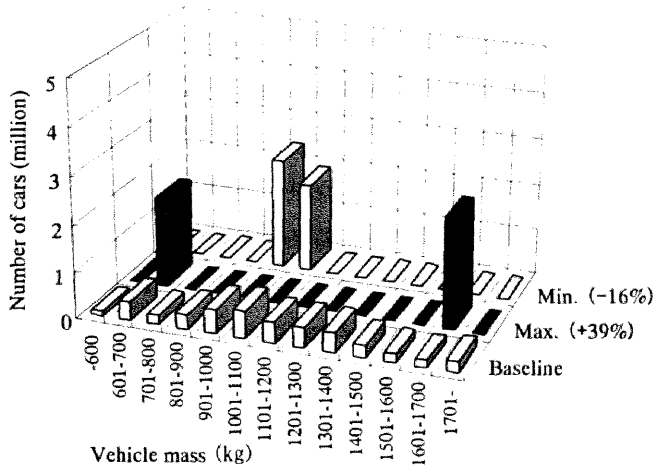

Figure 2.44. The number of car distributions that gives the minimum or maximum number of serious and fatal injuries in car-to-car frontal collisions.

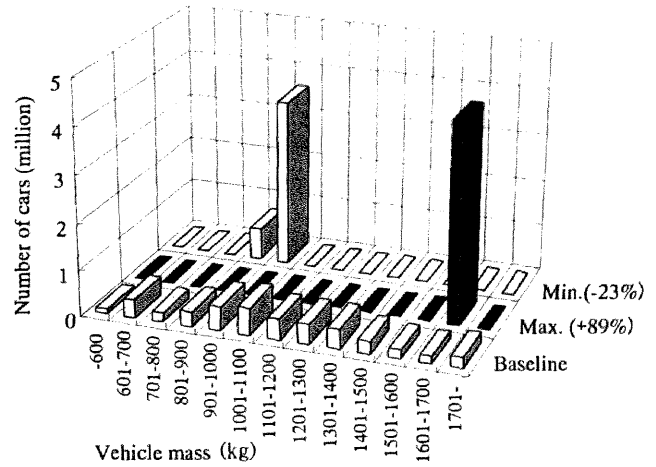

Figure 2.45. The number of car distributions that gives the minimum or maximum number of serious and fatal injuries in side collisions.

2.6. SINGLE-CAR CRASH

The fatalities of the drivers in single-car crashes occupy the largest portion of car accidents [ITARDA 1998]. In a rigid barrier crash, theoretically the car mass has no effect on the driver injury risk. However, in the real world collisions, the stiffness and geometry of the object that the car crashes into will affect the deformation and acceleration of the car. Moreover, the object that the car collides with brakes and absorbs some of the deformation energy. These characteristics of the objects can be considered as the compatibility of the fixed object with the car.

In order to clarify the compatibility of the fixed object with the car, we examined the fatality rate in a single-car crash by car mass, class and the type of fixed object. The macro accident data of the ITARDA (1992-1995) were used. The fatality rate of the driver was calculated from the number of injuries divided by that of drivers involved in the accidents reported to the police.

The relationship between the fatality rate and the mass of a bonnet-type car with travelling velocity was examined. This analysis was carried out for accidents in which the front ends of cars collided against fixed objects. The results are shown in Figure 2.46. When analyzing the total fatality rate involved in single-car collisions without considering car velocity, the fatality rate increases as the car mass increases. However, if the fatality rate is calculated under the condition that the travelling velocity is less than 50 km/h, the fatality rate decreases with car mass. The accident conditions are different between light and heavy cars; the heavy car is more likely to crash at a high velocity. Thus, when normalized by crash velocity, the fatality rate decreases with car mass. The same phenomenon was also shown by Evans (1984) using the ratio of driver fatalities to pedestrian fatalities. As shown in Figure 2.46, the analysis using vehicle velocity can clearly shows the effect of car mass.

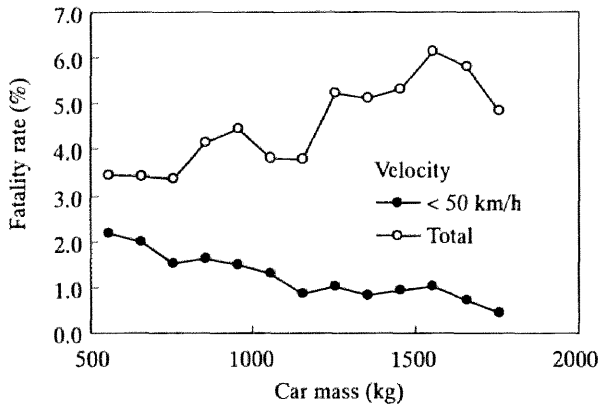

Figure 2.46. Relationship between fatality rate of the driver and car mass classified by travelling velocity in single-car crash.

In a single-car collision, the fixed object with which the car collides has large effects on the fatality rate of the driver. Figure 2.47 shows the fatality rate of the driver in single-car collisions, classified by the fixed object and the location of the impact. Accidents on expressways were excluded because the crash velocity and the fixed object are much different from those of general roads.

In a single-car collision with a fixed object, the fatality rate is high when a side of the vehicle collides with the fixed object. This means that the side of a car has little compatibility with fixed objects. In particular, when the car is impacted on the driver side into rather slender objects, such as a light pole, road sign, or central reserve/median strip, the fatality rate is high at more than 25%. As regards the impact by these slender objects, the fatality rate in a driver-side impact is about twice as large as that in a passenger-side impact. When the impact location is on the driver side of the car, it is considered that these objects cause a direct intrusion into a small area of the door, leading to the high

fatality rate for the driver. The fatality rate in a collision with a guardrail is 19.0% on the driver side, 14.0% on the passenger side, and 3.8% in front, which is the lowest for all impacted locations examined. Thus, the guardrail have the highest compatibility of the fixed objects. The compatibility of the bridge, light pole, road sign and the central strip is lower. By putting up guardrails along roads, the driver fatality rate can be reduced by about 60% and the road environment will be more compatible for cars.

For each type of road, the velocity distribution of the cars and probability of a crash with certain fixed objects is different. Figure 2.48 indicates that the fatality rate depends on the road types. In this analysis, the accidents where impact locations of cars were front, side and left were examined. The fatality rate decreases as the road width is smaller, irrespective of kind of road; national, prefecture or municipal. These results are related to the velocity distribution of the cars. For all types of roads, a guardrail is effective in reducing the fatality rate of the driver. The fatality rate due to the guardrail is low: national highway (5.36%), municipal roads (4.26%). This demonstrates that the guardrail has a high compatibility even at different velocities.

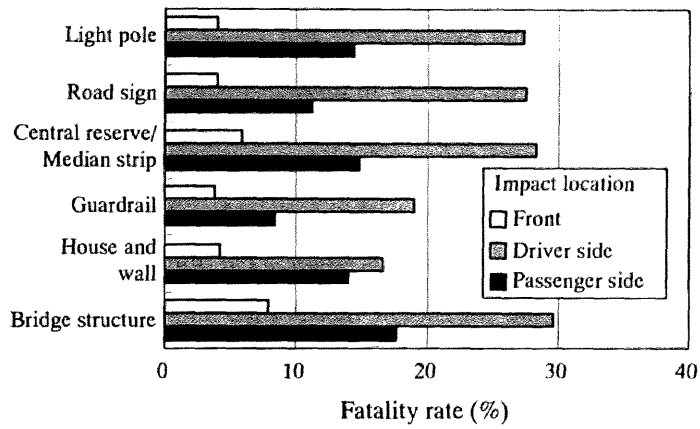

Figure 2.47. Fatality rate of the driver in single-car collision with fixed object classified by location of impact (excluding expressway)

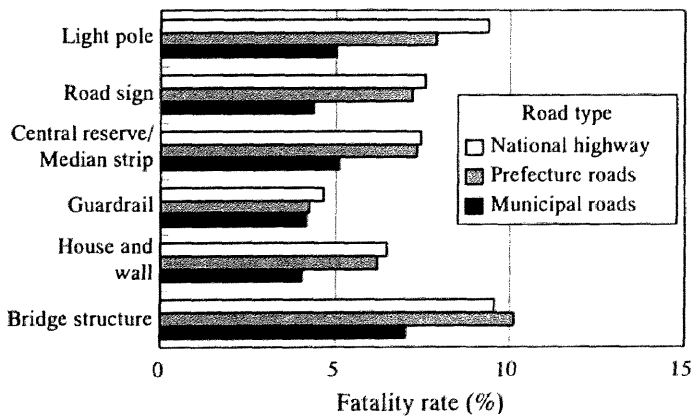

Figure 2.48. Fatality rate of the driver in single-car collision with fixed object classified by road type (excluding expressway).

2.7. DISCUSSION

The compatibility of the cars was discussed by taking account of three factors: mass, stiffness and geometry. In car-to-car frontal collisions, the injury rate of the driver can be expressed by the average mass of the car. The combination of low mass and low stiffness induces high injury risk to the driver. The geometry incompatibility can cause the outcome that the car front structures cannot absorb energy as it was intended to in the design of the car.

The number of fatalities per registered mini car in real accidents is small, and so the mini car may be considered compatible. However, in the method used in such a study, the injury risk to the driver in the mini car can be underestimated because the accident rate and crash velocity of this type of car are usually low. When the injury risk to the driver is estimated using the probability of fatal injury in a certain range of velocity, it is clear that the mini car is an incompatible car type. Based on the accident analyses of Section 2.2.4, it can be concluded that in car-to-car frontal collisions, the mini car as well as the SUV are the least compatible car types with low self-protection and high aggressivity, respectively.

On the other hand, the medium sedan and the wagon are considered compatible cars in car-to-car frontal collisions. The proportion of the number of fatalities in the subject cars to that in other cars is almost the same and the total fatalities in the subject and other cars are few.

Two cars with identical mass are most compatible, because the injury rate is the same and the total number of injuries is the smallest. Therefore, the cars with average mass in the car fleet are most compatible. Among the current car population in Japan, a car with a mass of 1150 kg is considered the most compatible. The effect of the numerical distribution of cars on the number of injuries was discussed in Section 2.5. However, when the compatibility could be accomplished and smaller cars would become safer, the numerical distribution of cars will not affect the results so significantly as the analysis using the actual accident data of existing cars shows.

To estimate the safety of the driver in a mini car, simulations were performed using MADYMO for crashes into a rigid barrier and into a large car. A high injury risk to the driver of the mini car in a collision with a large car cannot be evaluated by the crash test into a rigid barrier that is currently required by the law. In a crash into a rigid barrier, there is no influence of car mass on the injury risk to the driver and the influence of intrusion is small. However, in a collision with a large car, the driver of the mini car is at high risk of injury due to the high acceleration and large intrusion based on its small mass and size.

In Section 2.3, countermeasures for the safety of the mini car in car-to-car frontal collisions were also suggested based on the MADYMO simulations. Two methods are considered to reduce the injury risk to the driver of a mini car. The first is to stiffen the mini car. Since the acceleration of this car tends to be high, optimized restraint systems combining airbag, seatbelt force limiter, pretensioner, EA steering system and knee bolster are necessary. The stiff front structure and special restraint systems of the mini car can directly reduce the injury risk of the driver. In this method, no modifications of the

large car are necessary to reduce the injury risk to the driver in the mini car. However, if the mini car is stiff, the driver of the large car is at high risks of injuries to chest and leg due to the intrusion into the large car. The aggressivity of a stiff mini car should be considered not only in car-to-car frontal collision but also in other types of collisions, such as side and rear-end collisions. In a low-velocity crash in which the airbag must not deploy, the risk of minor injury to the driver in the stiff mini car may increase due to high acceleration.

The second method to reduce the injury risk for mini cars is to provide a large car with additional crush space designed for a crash with a mini car. It is possible that by reducing the acceleration and the intrusion of the mini car, the injury risk to the driver in the mini car would be reduced. Thus, in both cases of whether the mini car is less stiff or stiff, this additional crush space in a large car is effective in reducing the injury risk to the driver of the mini car. On the contrary, this additional crush space of the large car causes intrusion into the compartment of the large car, and so the injury risk to the driver of the large car, particularly to the lower extremities, increases when the mini car is stiff.

When optimum restraint systems such as an airbag and a seatbelt are installed to the mini car, further improvement of self-protection of this car will be difficult. However, partner-protection of a large car has a potential to reduce the injury risk to the driver in the mini car and to accomplish total compatibility. The side effect of partner-protection of a large car such as increasing the compartment intrusion can be managed more easily than modifying a mini car because it has a large front space. In side collisions, the aggressivity of the large car is a serious problem. The partner-protection of the large car for a frontal collision will be also effective for the protection of the occupants in the struck car in a side collision. Further research will be necessary for a large car to provide partner-protection without reducing self-protection.

3. CRASH TEST PROCEDURES

3.1. INTRODUCTION

There are many crash test procedures for evaluating the injury risk to the driver of a car. At present, mainly two kinds of the frontal crash test procedures are carried out in the regulations – full rigid barrier crash and offset deformable barrier (ODB) crash tests [Lowne 1994, NHTSA 1997].

The studies on the crash test procedures have examined the validity of the individual crash test procedure, but the single car crash test and the car-to-car crash test procedure were not directly compared. The possibility that the single car crash test procedure can serve as an alternative to the car-to-car crash test has not been investigated yet. The relationship between the full rigid barrier crash, ODB crash and MDB crash test procedures has not been examined.

In this chapter, the crash test procedures for evaluating the compatibility will be examined. In Section 3.2, the accident analyses will be carried out for car-to-car frontal crashes, and the most frequent crash configurations will be clarified. In Section 3.3, we will compare the injury parameters observed in the full barrier crash tests and ODB crash tests prescribed in the relevant regulations. In Section 3.4, based on theoretical analyses and computer simulations, we will discuss the crash test procedures which can evaluate the compatibility of car-to-car offset frontal collisions. The validity of the MDB crash test procedures will be discussed in 3.5 from the view of computer simulation and experiment. Finally, Section 3.6 discusses the relations between full barrier crash, ODB crash and MDB crash test procedures for evaluating the compatibility of the car.

3.2. ACCIDENT ANALYSIS

In order to develop the crash test procedure for the compatibility, it is necessary to investigate the accident configurations. However, in Japan there has been little investigation into the crash configurations for car-to-car frontal collisions. Therefore, we examined the car-to-car frontal collisions based on the micro accident data of ITARDA (1993-1997) [ITARDA 1999b] from the viewpoint of the impact angle and overlap ratio defined in Figure 3.1.

The number of all accidents and that of severe accidents were examined by the impact angle and overlap ratio (Figure 3.2). In all accidents, the impact angle varies from –40 to 40 degrees. 67.1% impacted on the right side, and 20.7% on the left side. Full overlap (100%) yields only 4%. In regard to severe accidents for the driver (MAIS 3-6), the frequency of the collisions where the impact angle is zero and overlap ratio is from 1/3 to 2/3, is the largest, and occupy 53.8% of all severe collisions.

Tarriere (1994b) and Kahane et al. (1994) also found that the most severe injuries were observed in accidents at low angles such as 0-15°.

In order to examine the overlap ratio more closely, the relation between overlap ratio and frequency of the accidents was examined based on the micro data. The results are shown in Figure 3.3. For all accidents, the frequency varies slowly and has a maximum at the overlap ratio of 21-30%. On the other hand, the accidents with severe injury risk to the driver (MAIS 3-6) are caused by the overlap ratio of 31-40%. This is consistent with the results of Thomas (1994) and O'Neill et al. (1994) and Buzeman et al. (1998b), who found that for frontal crashes the highest injury risk is in 1/3 overlap impacts. Therefore, this fact suggests that this overlap ratio at the highest injury risk may be the same for all countries, irrespective of different car populations and road environments.

From the accident analysis for car-to-car frontal collisions in Japan, the frequency of the overlap ratio of about 40% on the right side of the car with impact angle of 0 degree is the largest among the severe collisions. This configuration should be reflected in the car-to-car frontal crash tests for evaluating compatibility.

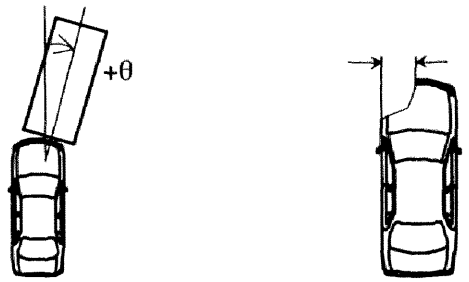

Figure 3.1. The definition of impact angle and overlap ratio.

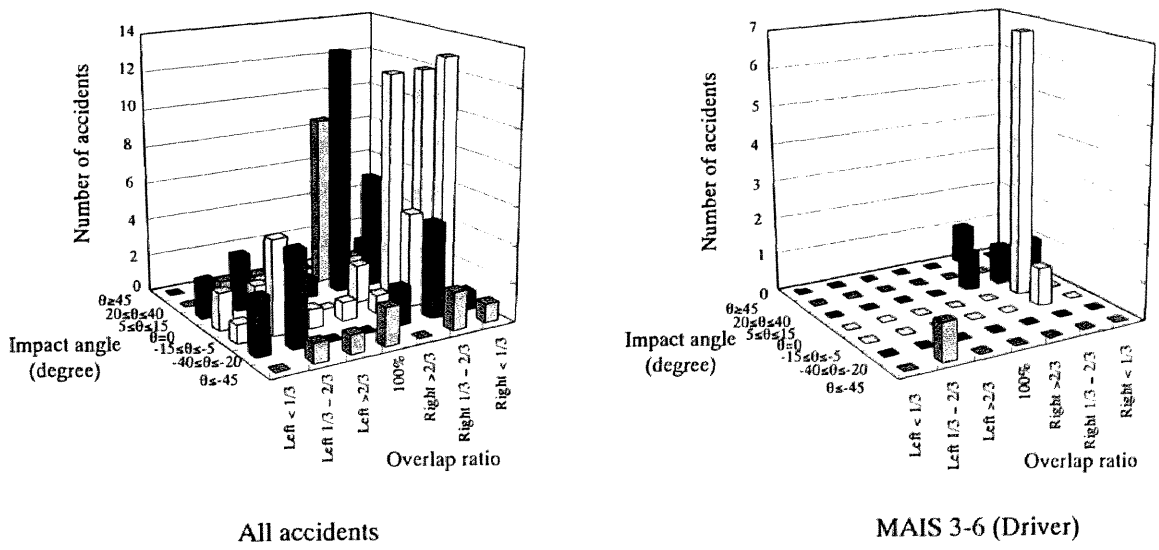

Figure 3.2. Distributions of impact angles and overlap ratios of the car in car-to-car frontal collisions.

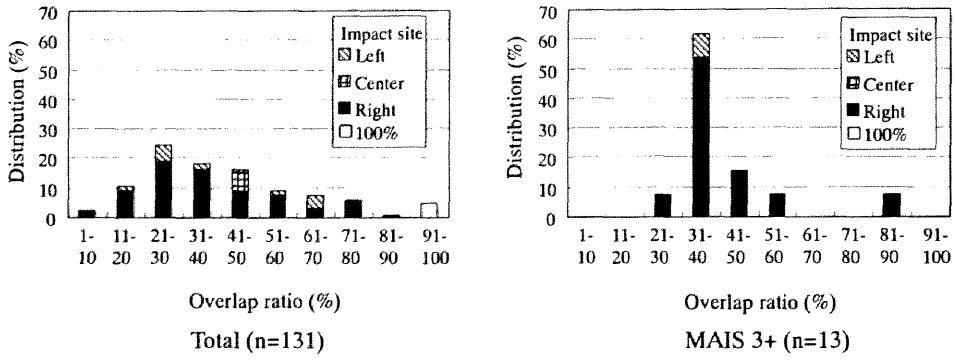

Figure 3.3. Distributions of overlap ratios of the cars and injury severity to the driver in car-to-car frontal collisions.

3.3. CRASH TESTS AND INJURY PARAMETERS

Currently, two crash tests for evaluating the occupant protection in cars are prescribed in the regulations of the motorized countries. Generally in full frontal crash tests, the acceleration levels become high, whereas in the ODB crash test, the intrusion into the passenger compartment becomes large [NHTSA 1997].

The New Car Assessment Program (NCAP) have been carried out in the US, EU, Australia and Japan for the consumers to select and buy safe cars. In the NCAP tests, the crash velocity is usually higher than the regulations in order to reveal the differences of the crashworthiness of the cars. The US and Japan NCAP perform the full rigid barrier crash tests, whereas the Euro-NCAP performs the ODB crash tests. The Australia NCAP performs both full frontal crash test and ODB crash test for the same types of cars. In the Australia NCAP, the full frontal crash test are conducted at a speed of 56 km/h, and the ODB crash tests are at 64 km/h. Using the data from the Australian NCAP, the injury parameters of the driver dummy for the full frontal and ODB crash tests can be compared.

We compared the injury parameters for full rigid barrier crashes and ODB crashes based on the data of the Australia NCAP, and the results are shown in Figure 3.4. As observed in the figure, the acceleration-related injury parameters such as the HIC and the chest acceleration in a full rigid barrier crash are proportional to those in an ODB crash. The levels of the HIC and chest acceleration are higher in the full rigid barrier crash than those in the ODB crash because the car accelerations are higher in the full rigid barrier crash tests. On the other hand for the intrusion-related injury parameters such as the chest deflection and femur force, the values of these parameters in full rigid barrier crashes seems to be in inverse proportion to those in ODB crashes.

Each crash test procedure evaluates different features of the crashworthiness. It can also be considered that a safe car in the full frontal crash test is not necessarily safe in the ODB crash test. Furthermore, whether the occupant safety in the car-to-car crash can be evaluated by these crash tests using single car is not clear, and will be discussed in the following section.

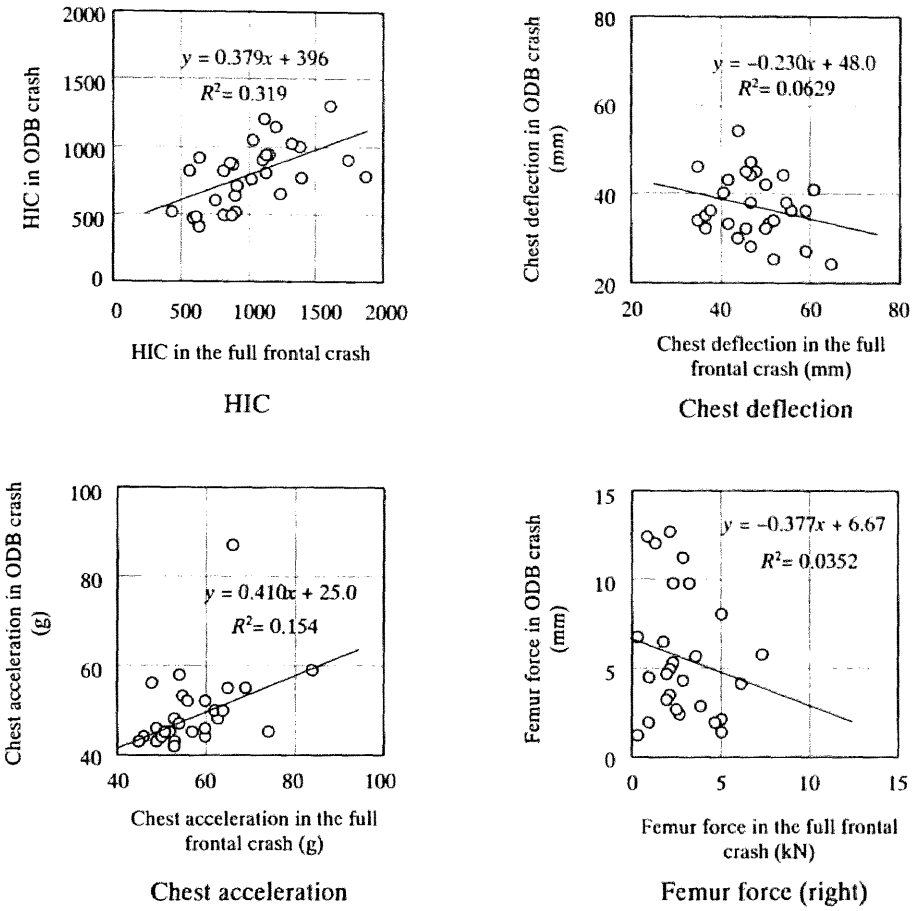

Figure 3.4. Comparison of the injury parameters of the driver in full frontal crash tests (56 km/h) and ODB crash tests (64 km/h).

3.4. SIMULATIONS OF CRASH TESTS

The crash test procedures which evaluate the compatibility in car-to-car offset frontal collisions can be discussed using theoretical analyses and computer simulations. We compared the crash test procedures such as full rigid barrier, offset rigid barrier, ODB and MDB crash tests to evaluate the car-to-car crash compatibility (see Table 1-1). The crash velocity of an offset-rigid barrier crash to reproduce a car-to-car offset frontal crash was examined in terms of the acceleration and the deformation of the car using a simple-mass spring model. To compare the risk of injury to the driver when using different crash test procedures, the injury parameters of the driver were also examined by the multi-body simulation program MADYMO.

3.4.1. Theoretical Analysis Using Simple Mass-Spring Model

By using a simple mass-spring model, we examined the crash velocity of a car in a rigid barrier crash to reproduce the car-to-car collision. A one-dimensional car behavior in a rigid barrier and a car-to-car crash can be approximated by a simple mass-spring model shown in Figure 3.5 and Figure 3.6.

For the rigid barrier crash, as shown in Figure 3.5, assuming the restitution coefficient is zero, the maximum car acceleration (α_1) and deformation (d_1) of car 1 are calculated as follows:

$$\alpha_1 = \sqrt{\frac{k_1}{m_1}}\, V_B, \quad d_1 = \sqrt{\frac{m_1}{k_1}}\, V_B \tag{3.1}$$

where m_1 is the mass of car 1, k_1 is the linear stiffness of the front structure of car 1 and V_B is the crash velocity.

For the car-to-car frontal crash model shown in Figure 3.6, the maximum acceleration (α_1, α_2) and deformation (d_1, d_2) of car 1 and 2 are obtained as:

$$\alpha_1 = \frac{\sqrt{KM}}{m_1} V_C, \quad d_1 = \frac{\sqrt{KM}}{k_1} V_C \tag{3.2}$$

where $V_C = v_{20} + v_{10}$ (closing speed),

$$M = \frac{m_1 m_2}{m_1 + m_2}, K = \frac{k_1 k_2}{k_1 + k_2}.$$

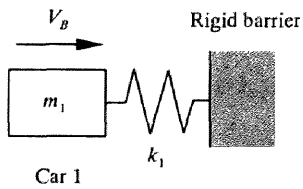

Figure 3.5. Simple mass-spring model for rigid barrier crash.

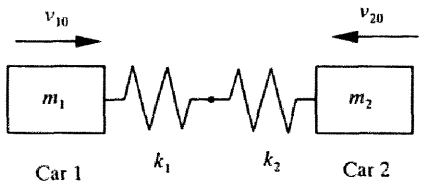

Figure 3.6. Simple mass-spring model for car-to-car frontal collision.

We consider the condition that either the acceleration or deformation of the car in a car-to-car collision can be reproduced by the rigid barrier crash. Firstly, we assume that the maximum

deformation is the same in a rigid barrier crash and in a car-to-car collision. Thus, from Eqs (3.1) and (3.2), we obtain the crash velocity as follows:

$$V_B = \sqrt{\frac{KM}{k_1 m_1}}\, V_c = \sqrt{\frac{k_2 m_2}{(k_1 + k_2)(m_1 + m_2)}}\, V_c = \text{EBS}. \tag{3.3}$$

As is well known, this velocity is exactly the Equivalent Barrier Speed (EBS). By substituting the EBS ($=V_B$) of Eq. (3.3) into Eq. (3.1), the maximum acceleration of the car α_1 in a rigid barrier crash leads to that in a car-to-car collision as shown in Eq. (3.2). This result shows that the rigid barrier crash at the EBS may reproduce not only the maximum deformation but also the maximum acceleration of the car in the car-to-car collision.

Note that even if the maximum acceleration and deformation in an offset rigid barrier crash at the EBS are the same as those in a car-to-car collision, the duration of impact is different. Thus, the curves of the acceleration-time and deformation-time histories are different for both types of crash.

When the stiffness of the car 1 and 2 are the same, k_1=k_2, the EBS (we call this velocity the Mass-related Equivalent Barrier Speed; MEBS) is calculated from Eq. (3.3) as:

$$V_B = \sqrt{\frac{m_2}{2(m_1 + m_2)}}\, V_c \ (= \text{MEBS}). \tag{3.4}$$

In the rigid barrier crash at the MEBS, the mass difference in a car-to-car collision can be corrected. Moreover, by the use of the MEBS it is not necessary to change the crash velocity with the stiffness of the car contrary to the EBS.

A deformable fixed-barrier crash can also be examined using the model shown in Figure 3.5, by replacing the stiffness of the car by the combined stiffness of the car and deformable barrier in series. Assuming the linear stiffness of the deformable barrier k_d, the maximum acceleration and deformation are obtained when substituting $k_1 k_d /(k_1 + k_d)$ instead of k_1 in Eq. (3.1). However, if both the acceleration and deformation of the car in crashing into a deformable barrier are the same as in a car-to-car collision, the stiffness of the deformable barrier should be infinity. This condition coincides with the fixed-rigid barrier. Therefore the deformable fixed-barrier crash cannot reproduce car-to-car collision in terms of the maximum acceleration and deformation in the same test.

Though simple spring-mass models are usually used for a one-dimensional crash, we applied the model to frontal offset crashes for approximation. Since the maximum acceleration and deformation in a car-to-car offset crash are reproduced by the offset rigid barrier crash at the EBS, the injury parameters of the driver may also be reproduced. On the other hand, is it possible to reproduce the injury parameters of the driver in car-to-car crash from an offset rigid barrier crash at the MEBS? To answer these questions, computer simulations was conducted and the injury parameters of the driver was compared for the car-to-car collision, the rigid barrier crash at the velocity of the EBS and the MEBS.

3.4.2. Mathematical Simulation of Mini Car Crash

In order to compare the injury parameters in crash tests, the mathematical simulation using MADYMO was carried out. The car model used in the mathematical simulations is based on a currently produced mini car. The model of the mini car and large car is the same one as used in Section 2.3. Figure 3.7 presents a model of a mini car used to simulate the offset frontal crash into a rigid barrier. The overlap ratio of the mini car is 50%, and that of the large car is 40%. The closing speed for the crash between the mini and the large car, V_C, is 100 km/h. A seatbelt (10% webbing) and airbag (35 l) were used for the restraint system of the drivers in the mini car.

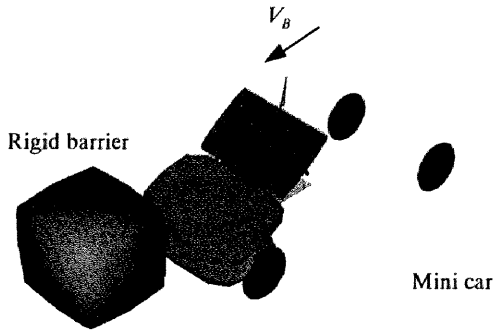

Figure 3.7. Simulation model of a mini car in an offset rigid barrier crash (overlap ratio is 50%).

From Eqs (3.3) and (3.4), the velocities of the offset rigid barrier crash, EBS and MEBS, used to reproduce the maximum acceleration and deformation in car-to-car offset frontal crashes was calculated (see Table 3.1). The mass of the dummy (75 kg) is included in the mass of the cars m_1 and m_2, because an inertial load of dummy in impact is transferred to the car by the seatbelt and the airbag. The crash velocity EBS varies with the stiffness of the mini car, while the MEBS is constant. The injury parameters of the driver in the mini car are compared for the offset rigid barrier crash at the MEBS and EBS, and also for the car-to-car offset frontal crash.

Table 3.1. EBS and MEBS for offset rigid barrier crash. Let m_1 775 kg, m_2 1475 kg (including dummy mass) and V_C 100 km/h.

Car 1		Car 2		EBS (km/h)	MEBS (km/h)
k_1 (kN/m)	$k_{1,offset}$ (kN/m)	k_2 (kN/m)	$k_{2,offset}$ (kN/m)		
500	325	872	453.4	61.8	57.3
600	390			59.3	
700	455			57.2	
800	520			55.3	
900	585			53.5	
1000	650			51.9	

By using Eq. (3.1), the maximum acceleration and deformation of the mini car in the offset rigid barrier crash were calculated at the EBS and MEBS for the various stiffness, k. The results are shown in Figure 3.8 and Figure 3.9. Note that the maximum acceleration and deformation of the offset rigid barrier crash at the EBS coincide with those of the car-to-car offset frontal crashes.

At the MEBS, the maximum acceleration of the car in the offset rigid barrier crash is smaller for lower stiffness and larger for higher stiffness than that at the EBS (see Figure 3.8). The same tendency can be observed for the maximum deformation (Figure 3.9). Thus for the crash at the MEBS, the injury risk of the driver specified by the maximum acceleration and deformation in the less-stiff car is underestimated, whereas that in the stiff car is overestimated compared with the crash at the EBS.

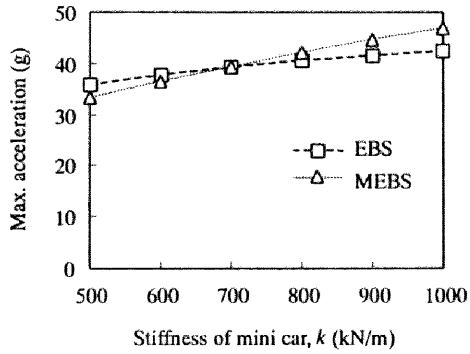

Figure 3.8. Maximum acceleration of the mini car in the offset rigid barrier crashes at EBS and MEBS.

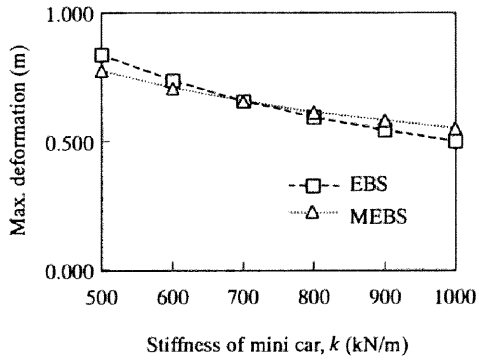

Figure 3.9. Maximum deformation of the mini car in the offset rigid barrier crashes at EBS and MEBS.

The injury parameters of the driver in the mini car are compared from the results of the MADYMO simulation. The injury parameters of chest acceleration, chest deformation and tibia axial force of the driver are shown in Figures 3.10, 3.11 and 3.12, respectively. As shown in Figure 3.10, the chest acceleration of the driver increases with the stiffness of the mini car. The three plots of the different crash test procedures almost agree with one another. However, the chest deflections and the tibia axial forces of the driver in an offset rigid barrier crash at the MEBS have different trends to those in the car-to-car offset frontal crash and offset rigid barrier crash at the EBS. The variations of the chest deflection and lower tibia axial force of the driver are smaller at the MEBS than those at the EBS and in the car-to-car collision.

These results suggest that the acceleration-related injury parameters of the driver in the car-to-car offset frontal crashes can be reproduced by the offset rigid barrier crash at both the EBS and the MEBS. However, the intrusion-related injury parameters cannot be reproduced by the offset frontal barrier crash at the MEBS because the stiffness of the car is not a factor in determining the MEBS. Thus, the variation of the maximum deformation of the simulated stiffness of the mini car is smaller in the offset rigid barrier crash at the MEBS than in the car-to-car offset crash.

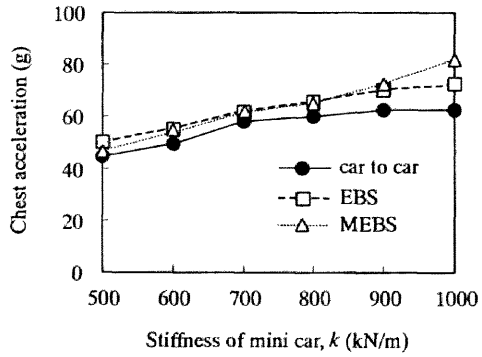

Figure 3.10. Chest acceleration of the driver in mini cars for offset rigid barrier and offset car-to-car crashes.

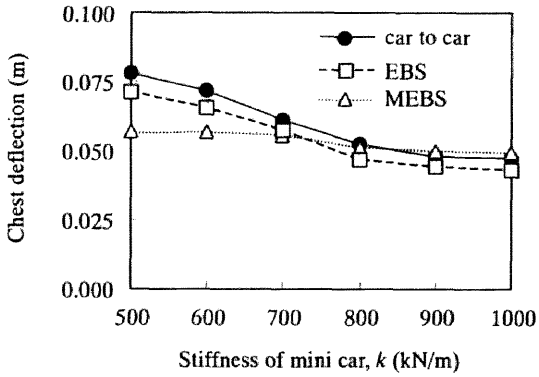

Figure 3.11. Chest deflections of the driver in the mini car for offset rigid barrier and offset car-to-car crashes.

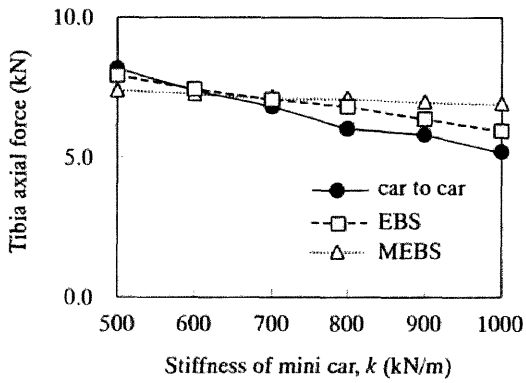

Figure 3.12. Lower tibia axial forces of the driver in the mini car for offset rigid barrier and offset car-to-car crashes.

3.5. MDB CRASH TEST

3.5.1. Simulation

A MDB crash test may be one of the procedures able to reproduce car-to-car collisions. A simulation of the MDB crash test was carried out for a mini and a large car. The MDB is the same as that used in the EU side impact tests, whose mass is 950 kg. The mini and large car models are the same as those used in Section 2.3. The crash configuration is shown in Figure 3.13. The initial velocity of the MDB and car is 50 km/h in opposite directions. The overlap of the car is 40%.

The simulation results are shown in Table 3.3. The maximum deceleration and intrusion of the mini car is larger than those of a large car due to its small mass and size. The intrusion-related injury parameters of chest deflection and femur forces become high because the compartment intrusion is large due to the small overlap ratio. The injury parameters of the driver in the mini car are higher than those in the large car. This MDB crash test can evaluate the vehicle mass effect, whereas it is well known there are no mass effects in a full rigid barrier crash test and the ODB crash test.

The aggressivity of the car can be evaluated based on the maximum force or maximum acceleration of the MDB. In the simulation, the maximum force level of the MDB is 295 kN in a mini car crash, and 371 kN in a large car crash (see Figure 3.14). If the maximum force level of the MDB is prescribed as 295 kN in this simulation, the large car should be less stiff. In collision between a mini car and this less-stiff large car, the maximum force level will be less than 295 kN. This is because based on Eq. (2.9), the total crush energy in a collision between the mini car and the large car is smaller than that in collision between a MDB and large car since the MDB is heavier than the mini car. Thus, if this maximum force level is taken as the collapse force level of the mini car compartment, the crash force will not exceed this level and the intrusion into the mini car can be small.

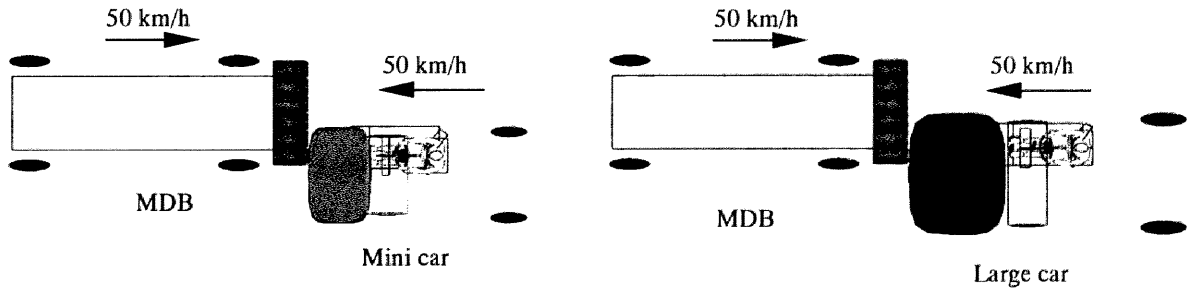

Figure 3.13. Simulation model of MDB crash test (overlap ratio is 40%, EU barrier).

Table 3.2 Simulation results

(a) Car parameters

	Mini car	Large car
Max. car deceleration (g)	41.8	26.0
Max. car deformation (m)	0.809	0.820
Firewall intrusion (m)	0.480	0.315
Max. MDB deceleration (g)	32.3	40.1
Max. MDB deformation (m)	0.5	0.5

(b) Injury parameters

	Mini car	Large car
HIC	638	419
Chest 3ms-G	52.0	51.8
Chest deflection (mm)	89.8	58.9
Femur force right (kN)	12.2	7.2
left (kN)	13.7	6.9

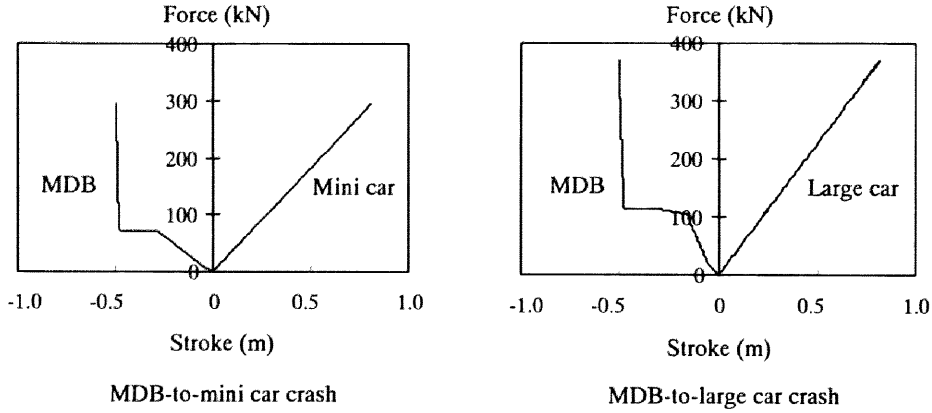

Figure 3.14. The force-stroke characteristics in simulations.

3.5.2. Crash test

The MDB crash tests have been investigated [Ragland 1998, Sugimoto et al. 1998] in order to evaluate the compatibility of the cars. However, since they used medium and large cars in the tests, the effects of acceleration and intrusion are not as significant as in the case of the mini and small cars.

By focusing on the traffic in Japan, we then carried out the MDB crash test using a small car (curb weight 1096 kg) at the closing velocity of 112 km/h and 40 percent overlap on the driver side. The impact angle of the MDB is 0 degree. A Hybrid III dummy was positioned in the driver seat with a seatbelt. A driver airbag was fitted to the car. The MDB (1368 kg) was the same type that is used for FMVSS 214.

The test results are compared with those in full rigid barrier crash and in the ODB crash tests where the same car type was tested. To compare the results with an ODB crash test (64 km/h), the aluminum honeycomb element adopted in the ODB crash test was mounted on the MDB. For a large car, the deformation of the car in the MDB crash test at 112 km/h was the same level as that in the ODB crash test at 64 km/h [Sugimoto et al. 1998]. The results were also compared with those of the full rigid barrier crash (55 km/h). The injury parameters in a full rigid crash test at this velocity can be comparable with those in a ODB crash test at 64 km/h (See Figure 3.4). The data of the full rigid barrier crash was taken from Japan NCAP and that of the ODB test was from Australia NCAP and IIHS crash test report [IIHS 1997].

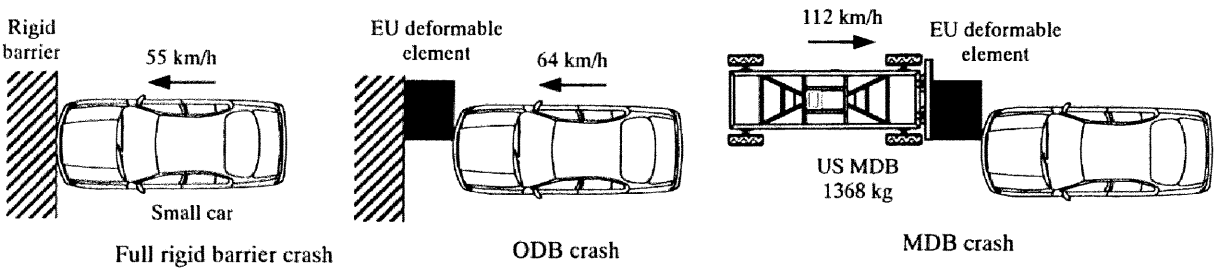

Figure 3.15. Crash tests.

The deceleration-time histories of the car and MDB are shown in Figure 3.17. The bottoming-up of the aluminum honeycomb element of the MDB occured at 30 ms, and the deceleration became high (35g) at 40 ms. Due to the collapse of the compartment, the deceleration of the car became high (65g) at 58 ms. The deceleration of the car in the MDB crash test was compared with the full rigid barrier crash and ODB crash test (see Figure 3.17). The MDB crash test showed the highest deceleration peak of the three crash tests. In the ODB test, the peak deceleration was lowest and the peak value was late. The deformation and intrusion of the car in the MDB crash test were larger than those in other types of crashes (see Figure 3.18). The three crash tests evaluate different crashworthiness and in the MDB crash test both deceleration and deformation of the car is large.

The ratio of injury parameters in the ODB and the MDB crash to the full rigid barrier crash test are shown in Figure 3.19. In the MDB crash test, both the acceleration and intrusion-related injury parameters of the dummy were high. The chest acceleration, chest deflection, femur forces (right) and tibia index (right) were above the injury thresholds, whereas in other crash tests all the injury parameters were less than the injury thresholds except the tibia index (right) in the ODB crash. The injury parameters of the dummy in this test were higher than those using large cars [NHTSA 1997]. Thus from experiment it is confirmed that the MDB crash test is more severe for small cars.

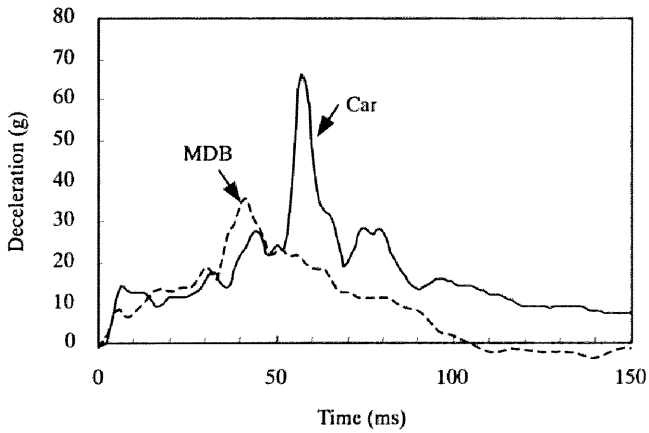

Figure 3.16. Longitudinal deceleration of car and MDB in the MDB crash test.

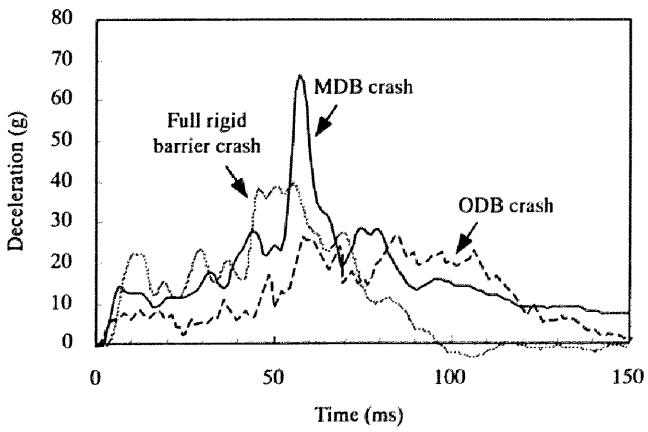

Figure 3.17 Longitudinal deceleration of the car from full rigid barrier, ODB [IIHS 1997] and MDB crash test.

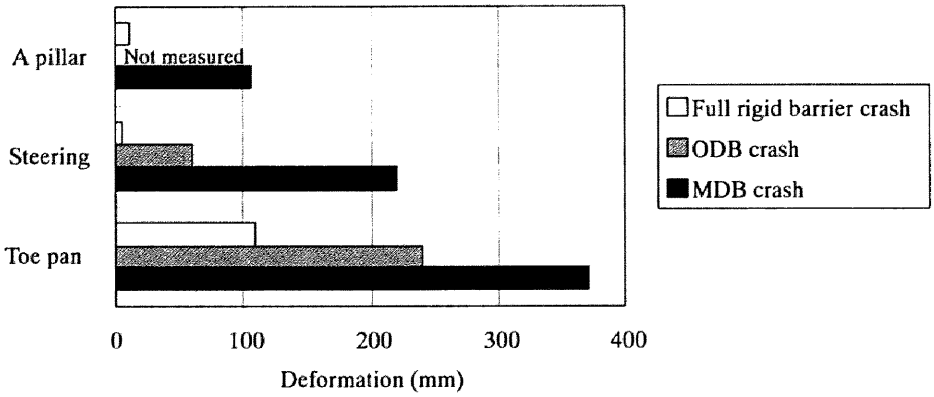

Figure 3.18. Deformation of the car for full rigid barrier, ODB [IIHS 1997] and MDB crash test..

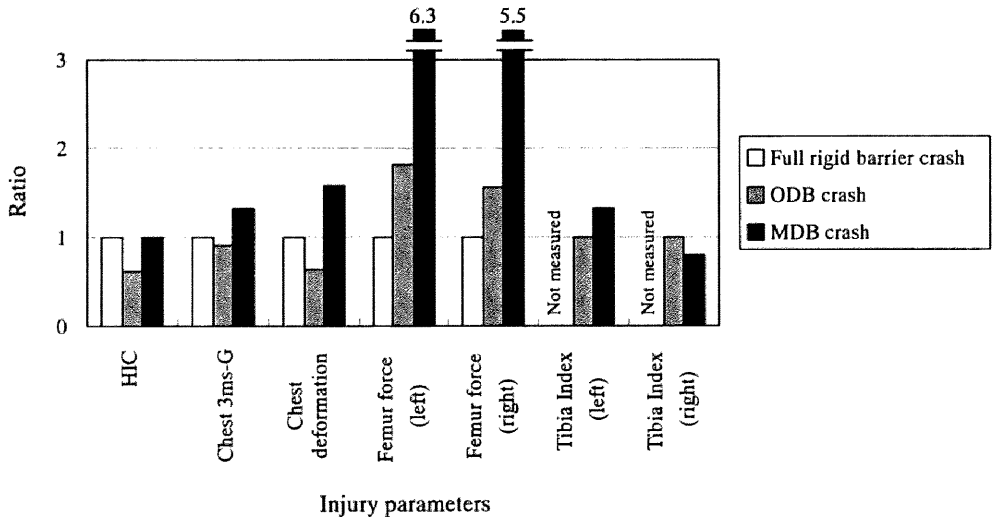

Figure 3.19. Injury parameters in various crash tests relative to the full rigid barrier crash. For tibia index, the ratio is obtained based on ODB crash test. The data of full rigid barrier crash are from Japan NCAP and those of ODB crash test are from the Australia NCAP.

3.6. DISCUSSION

Crash test procedures to evaluate the compatibility of the car in car-to-car frontal crashes were examined. Based on the accident data from Japan, the configuration of car-to-car frontal crashes is proposed. The collinear collision with an overlap ratio of 40% is recommended to evaluate the risk of serious injuries to the driver in car-to-car frontal collisions in Japan.

Based on the results of the mathematical simulation, the injury parameters of the driver in a car-to-car offset frontal collision can be predicted by the offset rigid barrier crash if the crash velocity is the EBS, that is, the speed based on the mass and stiffness of the car. However, when we apply the crash

velocity of the car in an offset rigid barrier crash by the MEBS (i.e., according to the mass of the car), though the acceleration-related injury parameters can be estimated, the intrusion-related injury parameters can not be estimated by this velocity. Thus, in estimating the intrusion related-injury parameters of the driver in a car-to-car offset frontal collision, the stiffness of the car should be taken to determine the crash velocity in the offset rigid barrier crash test. For the mini car whose compartment intrusion can be large, EBS should be employed. The offset rigid barrier crash test with a constant velocity of 50, 56 or 64 km/h specified in the regulations and NCAP, cannot be used to estimate the risk of injury to the driver in a car-to-car offset frontal collision because these velocities are independent of the mass and the stiffness of the car. This is true particularly when the subject car deviate from the average car on which the developed crash test procedures are based.

Moreover in the actual conditions, it is difficult to estimate the EBS before the crash test. Thus, it is difficult to evaluate the injury risk of the driver in a car-to-car offset frontal collision from an offset rigid barrier crash. Especially for the mini car in which both the effects of acceleration and compartment intrusion should be evaluated, the offset crash test into a rigid barrier can not be the alternative to the car-to-car offset collision test.

Based on the analysis in this study, it was found that in order to evaluate the self-protection of the mini car correctly, an actual car-to-car collision should be reproduced in some way. The setup to simulate a car-to-car offset collision is the MDB crash test procedure. Only the MDB crash test can evaluate the injury risk to the driver on the basis of the acceleration and intrusion, and can examine the mass, stiffness and geometry factors of the compatibility. For the evaluation of the injury risk to the driver in the mini car, where acceleration and the intrusion are apt to be large, the MDB crash test should be conducted.

In the currently proposed MDB crash test procedure by NHTSA [Ragland 1998], only the self-protection of the occupant was estimated. Since the compatibility consists of self-protection as well as partner-protection, in the MDB crash test procedure, the aggressivity of the large car also has to be estimated by measuring the maximum force level of the MDB. In order to protect the partner car, this force level should be less than the collapse force level of the compartment of the partner car. It may be also possible to evaluate also the geometry compatibility if the geometry and the stiffness of the MDB are designed properly. In addition, the detailed specification of the MDB should be chosen carefully to represent the average car in each country since each has a different car population and traffic situation. The potential to evaluate the compatibility from full rigid barrier crash, ODB crash and MDB crash tests was compared, and the results are summarized in Table 3.3.

In the real world, cars are involved in various types of crash configurations. Thus, in order to evaluate the crashworthiness of the car correctly, the MDB crash tests should be carried out in addition to the full rigid barrier crash and ODB crash test.

Table 3.3. Crash test procedures to evaluate the compatibility performances of the car.

Crash test	Compatibility			Injury risk	
	Mass	Stiffness	Geometry	Acceleration	Intrusion
Full rigid barrier crash test 	×	×	×	○	×
ODB crash test 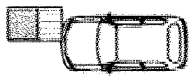	×	△	×	×	○
MDB crash test 	○	○	△	○	○

Note: ○ possible to evaluate, × impossible to evaluate, △ there is a potential to evaluate

4 CAR-TRUCK COMPATIBILITY

4.1. INTRODUCTION

In a car-to-truck collision, the injury risk of the occupants in the car is extremely high due to the differences in mass, stiffness and geometry of both vehicles. This high aggressivity of the truck is a crucial problem for cars, for which effective countermeasures have not been sufficiently investigated. There has been little research on the compatibility for all vehicles, including trucks, in Japan, thus the accident analyses should be carried out by using both macro and micro data.

In order to reduce the injury risk in truck-to-car accidents, many studies have proposed the effectiveness of the truck underrun guards [Mendis 1996, Adalian et al. 1998, Deloffre et al. 1998]. This guard is attached under the bumper of the truck and consists of a deformable material such as aluminium honeycomb that can absorb the crash energy by deformation. However, most studies focused on the compact car. Though the mini car is common in Japan, in Chapter 2 this car type was confirmed to be incompatible in collisions. Therefore it is necessary to simulate mini car-to-truck crashes and examine the effectiveness of the underrun guard is examined.

The compatibility between trucks and cars in frontal crashes will be analyzed by using accident data and computer simulations. The accident analyses will be performed in Section 4.2 by using macro data (Section 4.2.1) and micro data (Section 4.2.2). From the macro data, the aggressivity of the truck will be examined by different measures including the effects of the vehicle mass, vehicle registrations and traveling velocity. The current aggressivity of trucks will be also compared with that of 10 years ago. Finally, the collision between the mini car and truck with an underrun guard will be examined based on the MADYMO simulation.

4.2. ACCIDENT ANALYSIS

4.2.1. Macro Data Analysis

The compatibility between cars and trucks are examined by using the macro accident database of ITARDA (1993-1997). In order to compare the compatibility between those vehicles with that in 10 years ago, the police data of 1989 were also used.

In Japan, 639 car occupants were fatally injured in head-on collisions in 1997 [ITARDA 1998]. We examined the occupant fatalities in the cars by the types of the other vehicles. The results are shown in Figure 4.1. The fatalities in car-to-car collisions occupy 31%, 23% in car-to-truck, and 8% in car-to-dump truck collisions. Thus, for the fatalities of the occupants in the cars, the compatibility between a car and a truck, as well as the one between cars, is an important problem.

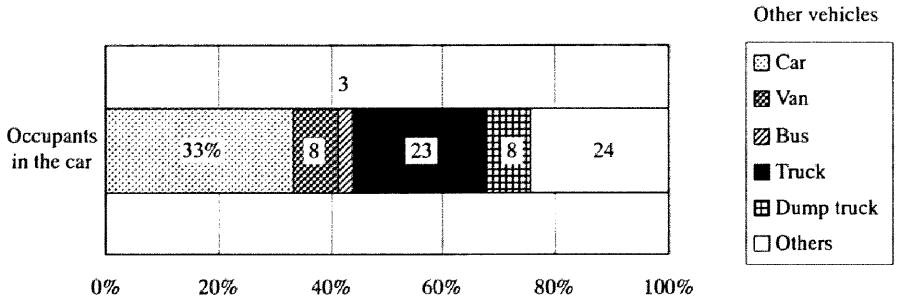

Figure 4.1. The distributions of occupant fatalities in the car classified by the other vehicles in head-on collisions of Japan (1997, N=639)

Mass effect

Though it is well known that the vehicle mass has a large effect on the occupant injury in vehicle-to-vehicle collisions [Evans 1991b], the effect of vehicle mass in a car-to-truck crash has not been discussed sufficiently. Therefore, we examine the injury rate of the driver in the car by using the mass of the trucks and passenger cars.

The probabilities of fatal and serious injury to the drivers of passenger cars in car-to-truck and car-to-car frontal crashes were examined with reference to the subject passenger car mass (Figure 4.2). The probability of the fatal and serious injury to the driver tends to decrease with car mass. However, in the case of a car-to-truck crash involving an unbelted driver, this probability does not decrease very much and the injury risk is extremely high. The effect of the subject car mass on the decrease of probability of death and serious injury is smaller in a car-to-truck crash than in a car-to-car crash. The probability of the fatal and serious injury to a belted driver in a car in car-to-truck crash is almost the same level as for the unbelted driver in a car in a car-to-car crash.

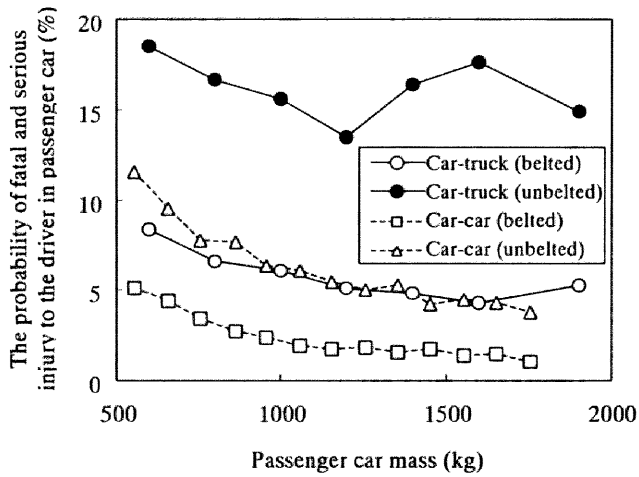

Figure 4.2. Effect of subject car mass (passenger car) in car-to-truck and car-to-car frontal crashes.

The variation of the probability of fatal and serious injury to the driver in a passenger car (subject car) with respect to the other vehicle mass is shown in Figure 4.3. This risk increases largely with increase of the truck mass up to 5 tons. If the other vehicle mass is less than 2 tons, the probability of fatal and serious injury to the driver in the subject car in a car-to-truck crash coincides with that in a car-to-car crash. This result indicates that the aggressivity of a small truck is on the same level as for cars, if the vehicle masses are identical. On the other hand, when the truck mass exceeds 5 tons, the probability of fatal and serious injury to the driver in the subject car does not increase much.

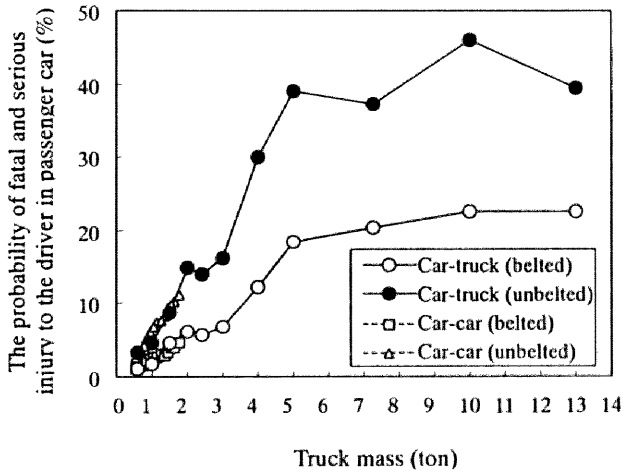

Figure 4.3. Effect of other vehicle mass in car-to-truck crashes.

The compatibility and aggressivity of the truck

The truck compatibility and aggressivity is examined in vehicle-to-vehicle frontal collisions including whole 4-wheel vehicles. The vehicles are classified into 7 groups (based on the police accident data in 1997 and 1989); bus, trailer, large truck, ordinary truck, passenger car, mini truck and mini car. Trucks are classified using Gross Vehicle Weight (GVW) as the ordinary truck (GVW < 8 ton), and the large truck (GVW ≥ 8 ton).

The compatibility of vehicles including trucks was examined by vehicle classes and year transitions. Figure 4.4 shows the number of fatalities in the subject and the other vehicle per thousand accidents in 1989, 1995, 1996 and 1999. The trailer, the large truck and the bus are incompatible because the total number of driver fatalities is very large and the proportion of fatalities in the other vehicle is high. On the other hand, the mini car and the mini truck are also incompatible due to poor self-protection because the number of fatalities in the subject vehicle is larger than in the other vehicles.

With respect to the passenger car, the total number of fatalities in the subject and the other vehicles per accident is the smallest, and the proportion of the number of the fatalities in the subject vehicles to that in the other vehicles is almost the same. This means that the passenger car is the most compatible vehicle. However, the large number of collisions between passenger cars can influence this calculation.

The truck compatibility has not changed much between 1989 and 1997. The self-protection of the passenger car has been improved because the fatalities in this type of car are becoming fewer in number. The crash regulation for passenger cars introduced in 1994 could be one of the causes for this improvement of self-protection. However, there have not been very much change on the aggressiveness of the passenger cars since 1989. Thus in order to secure the compatibility of the passenger car, the aggressivity of the passenger car has to be reduced.

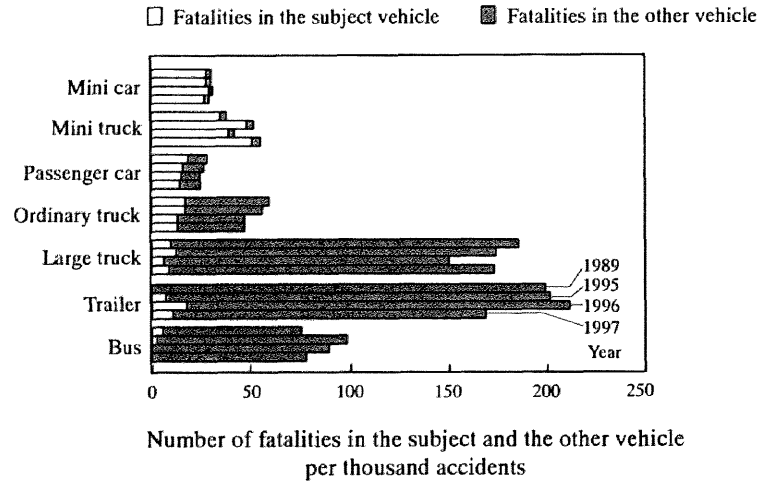

Figure 4.4. Vehicle compatibility.

Truck aggressivity can be affected not only by the vehicle itself but also by human factors such as the crash velocity and accident rate. Vehicle aggressivity was examined by the same Measures 1, 2 and 3 as described in Section 2.2.4. By Measure 1, vehicles such as ordinary trucks, large trucks, trailers and buses are found to be considerably aggressive because the number of fatalities in the other vehicle is far larger than that in the subject vehicle (Figure 4.5). The aggressivity of ordinary trucks and the large trucks by Measure 1 is 2.5 and 13, respectively. Comparing this ratio between 1997 and 1989, the situation has not been improved.

The aggressivity of vehicles of different vehicle types has a similar tendency when Measures 1, 2 and 3 are used. If we compare the large truck with the passenger car in Figure 4.5 and Figure 4.6, the aggressivity of trucks based on Measure 2 is smaller. Therefore, it is found that the influence of the crash velocity of the large truck is negative. From this result, it is supposed that large truck may travel more slowly than the passenger car.

The aggressivity of the large truck according to Measure 2 in Figure 4.6 is about 18 times higher than that of the passenger car, whereas, the aggressivity of the large truck based on Measure 3 in Figure 4.7 is about 86 times higher than that of the passenger car. Since the effect of the accident rate is included in Measure 3, the aggressivity of the large truck due to human factors such as accident rate is higher than the passenger car. Therefore, it is concluded that the reason of high aggressivity of large trucks is not due to the crash velocity but rather the vehicle itself together with the human factors such as the accident rate.

The aggressivity of buses by Measure 1 is the same as for large trucks and trailers. However, in Measure 2, the aggressivity of the bus is less than half of that of the large trucks. This result indicates that the crash velocity of buses is lower than that of large trucks. Similarly, the aggressivity of the bus estimated by Measure 3 is less than a quarter that of large trucks. This low aggressivity of buses estimated by Measure 3 is due to human factors such as accident rate, which is much lower than for the large truck. These results imply again that the aggressivity of large trucks becomes high due to human factors, and it can be reduced by changing the working environment of truck drivers.

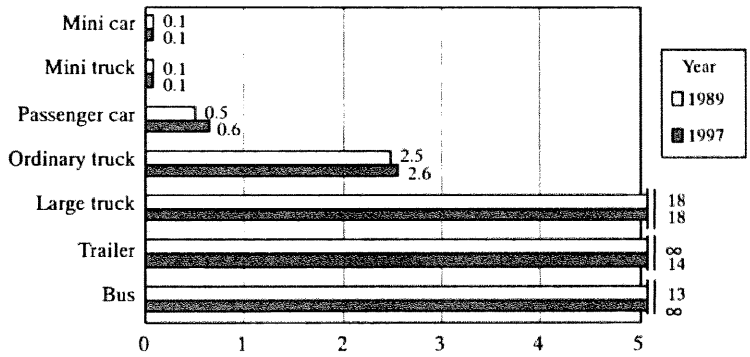

(Driver fatalities in the other cars)/(Driver fatalities in the subject cars)

Figure 4.5. Vehicle aggressivity by Measure 1.

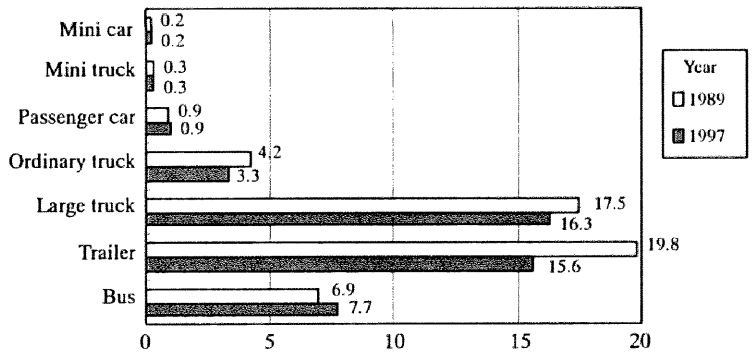

The percentage of fatalities of the driver in the other car (%)

Figure 4.6. Vehicle aggressivity by Measure 2.

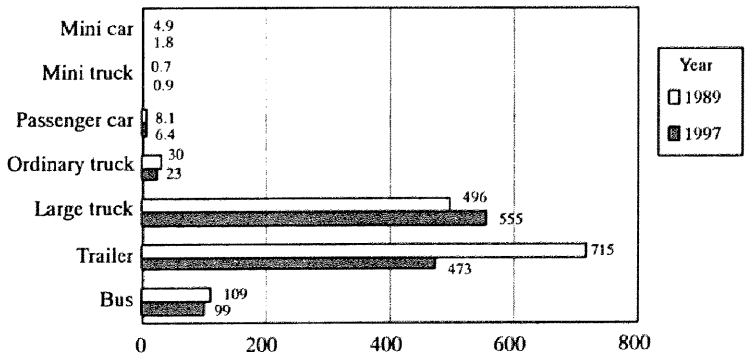

Driver fatalities in the other vehicles per million subject car registrations

Figure 4.7. Vehicle aggressivity by Measure 3.

Compatibility between trucks and passenger cars

Since the number of passenger cars account for a large proportion of vehicle registrations, the compatibility of vehicles with such cars is important. Therefore, the vehicle aggressivity against a passenger car is evaluated by using Measure 1. Vehicles are classified as classical car (sedan, sports and specialty, and wagon) mini car, van, SUV and light/medium/heavy trucks (based on the ITARDA data in 1993-1997). Only driver injury is discussed to simplify the analyses.

As the number of the classical cars is the largest in the vehicle registration, the compatibility between classical cars and trucks are important. We estimated the driver fatality ratios in both vehicles in collisions of the passenger cars by vehicle class using the macro data in Japan (Table 4.1). When passenger cars collide with a large-sized vehicle, the fatality ratio is larger. Particularly in a crash with a heavy truck the fatality ratio reaches infinity (124:0). In a crash with the SUV and van, the fatality ratio is also high due to high aggressivity. The number of classical car fatalities is the largest in car-to-car crashes (215); and in crashes with large-sized vehicles such as medium or heavy trucks, the number of fatalities in classical cars is also large (95 and 124, respectively). However, the number of fatalities of classical cars in crashes with a SUV and van is smaller than that in crashes with trucks.

The fatality ratio of the drivers in mini cars based on the macro data is shown in Table 4.2. In collisions between mini car and the other vehicle, the fatality ratio is so large (more than 10) that the compatibility of mini cars seems very poor. Therefore, the drivers in mini cars have a higher risk of death than in other vehicles. These results indicate that the compatibility of the mini car and the truck is an important problem in Japan. In Japan the problem of the truck is more serious than that of the SUV.

Table 4.1. Fatality ratio of the driver in frontal crash with passenger cars (1993-1997).

Crash partner	Fatality ratio (Number of fatalities)
Classical car vs. Mini car	0.1:1.0 (5: 61)
Classical car vs. Classical car	1.0:1.0 (215:215)
Classical car vs. Van	3.8:1.0 (31: 8)
Classical car vs. SUV	13.5:1.0 (27: 2)
Classical car vs. Light truck (3<GVW≤7 ton)	11.7:1.0 (35: 3)
Classical car vs. Medium truck (7<GVW≤8 ton)	31.7:1.0 (95: 3)
Classical car vs. Heavy truck (GVW>8 ton)	∞ :1.0 (124: 0)

Note: Classical car = sedan, sports and specialty, and wagon

Table 4.2. Fatality ratio of the driver in frontal crash with mini cars (1993-1997).

Crash partner	Fatality ratio (Number of fatalities)
Mini car vs. Mini car	1.0:1.0 (0: 0)
Mini car vs. Classical car	12.2:1.0 (61: 5)
Mini car vs. Van	10.0:1.0 (10: 1)
Mini car vs. SUV	∞ :1.0 (5: 0)
Mini car vs. Light truck (3<GVW≤7 ton)	∞ :1.0 (15: 0)
Mini car vs. Medium truck (7<GVW≤8 ton)	∞ :1.0 (14: 0)
Mini car vs. Heavy truck (GVW>8 ton)	∞ :1.0 (36: 0)

Note: Classical car = sedan, sports and specialty, and wagon

4.2.2. Micro Data Analysis

Method

A countermeasure for the compatibility problem can be clarified by analyzing the crash configurations. However, the configurations of the car-to-truck collision have not been discussed sufficiently, especially in relation to the traffic conditions in Japan. Therefore, the distributions of velocity and overlap ratio in crashes are examined. By using the micro accident data of ITARDA (1993-1997) [ITRADA 1999b], in-depth studies of car-to-truck frontal collisions are carried out. In the database, the number of car-to-car collisions was 70 and that of car-to-truck collisions was 27. The driver injuries in cars that collided with the trucks are examined based on the crash configurations such as crash velocity, impact angle and overlap ratio. The injuries to the drivers are examined by the injury severity (AIS), injured body regions and their causes, and these results are compared with those of the car-to-car collisions.

Crash configuration

The cumulative frequencies of a crash velocity of the car by the injury severity of the driver are shown in Figure 4.8. For driver in the cars in car-to-car and car-to-truck collisions, the cumulative frequency of 50% of sever injury (MAIS 3-6) is associated with a crash velocity of about 50 km/h. However, the shapes of curves of the cumulative frequencies are dissimilar for both types of collisions. The frequency of the injury severity increases gradually in the car-to-car collision, whereas in car-to-truck collision it rises rapidly at the 40 km/h. Over this velocity, the injury risk to the driver is supposed to increase due to large intrusion into the passenger compartment of the car.

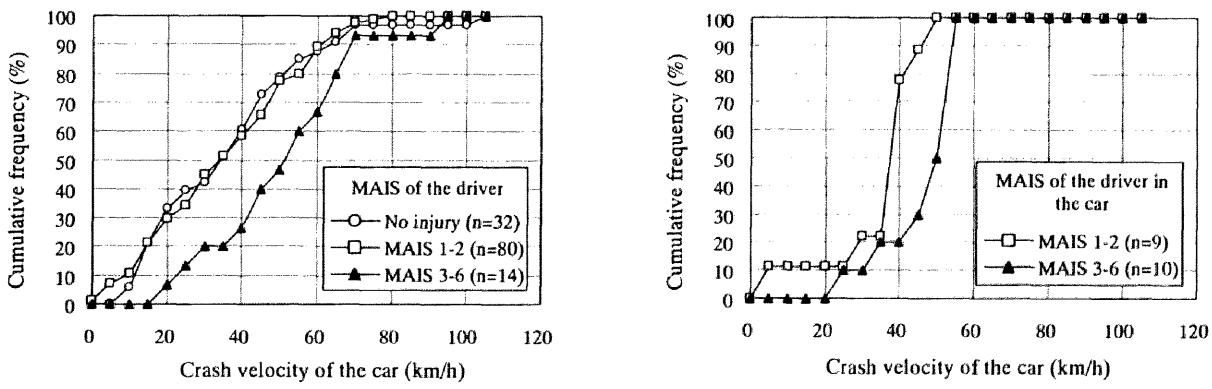

Car-to-car collision　　Truck-to-car collision

Figure 4.8. The crash velocity and the MAIS of the driver in the car for car-to-car frontal collisions and car-to-truck collisions.

The overlap ratios of cars and trucks are shown in Figure 4.9. For severe injuries (MAIS 3-6), the overlap ratios of cars are more widely distributed than those in car-to-car crashes. Therefore, in car-to-truck collisions, the injury severity of the driver in the car may be by the intrusion due to underride of

the car rather than that due offset impact. As the width of the truck is large, the overlap ratios of the truck are likely to be small, and the number of accidents has a maximum at the overlap ratio of 11-30%. With such a small overlap of trucks, cars do not contact the frame of the trucks and the risk of underride of the cars increases.

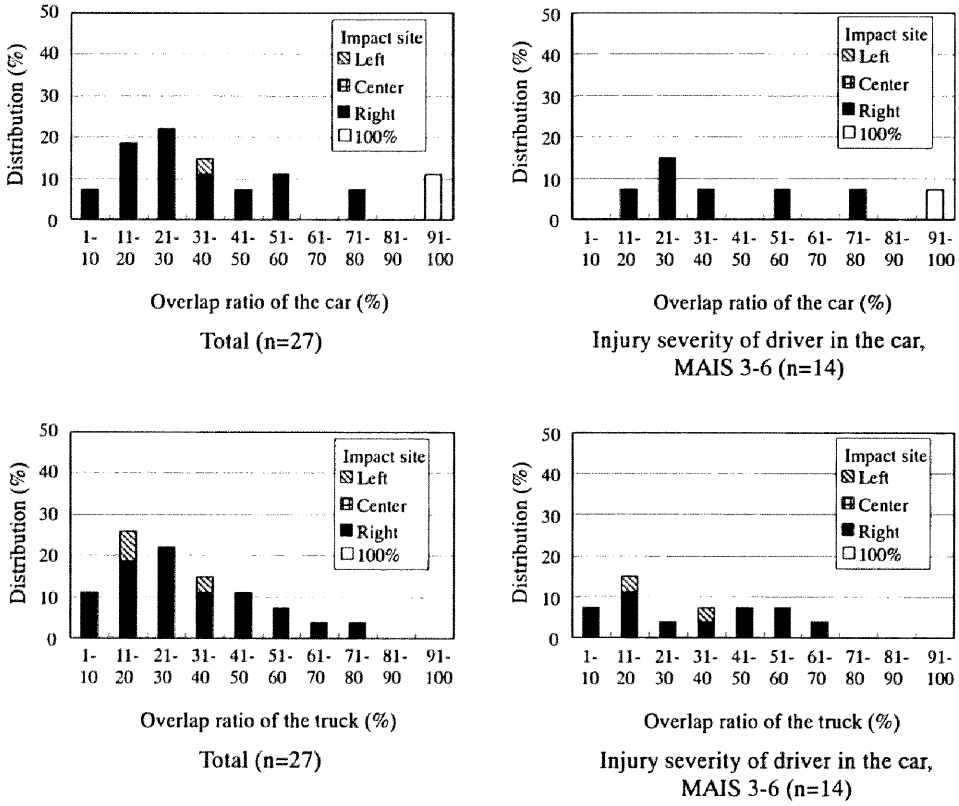

Figure 4.9. Overlap ratio of the cars and trucks in car-to-truck frontal collisions.

Injury risk

The driver injury risks of cars were compared for car-to-car and car-to-truck collisions by the use of micro data. Figure 4.10 shows the distributions of the injury severity of the drivers for car-to-car and car-to-truck collisions. In car-to-car collisions, 11.4% of car drivers are severely injured (MAIS 3-6), and in car-to-truck collisions this ratio is 53.8%, which reflects the high injury risks to the drivers in the cars when they have collided with the trucks.

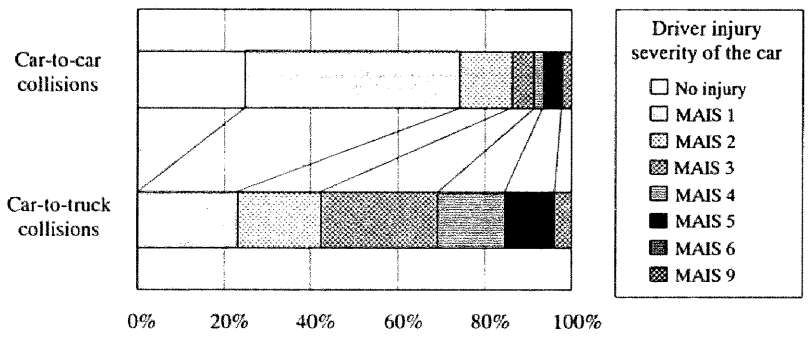

Figure 4.10. Injury severity of the driver in the bonnet-type car.

Injured body regions and injury sources of the drivers in cars were also compared for car-to-car collisions with car-to-truck collisions. Number of injuries to the driver body regions was counted. The results are shown in Table 4.3 and Table 4.4. The windscreens cause the largest number of injuries in car-to-car collisions, whereas the steering assemblies are the largest in car-to-truck collisions. In car-to-truck collisions, the intrusions into the passenger compartments of the car as well as the penetration of the front bumpers and front panels of the truck are the causes of injuries. Belted drivers are frequently injured on the head in car-to-car collisions, and on the chest in car-to-truck collisions. These results indicate that in car-to-truck collisions the deformation and the compartment intrusion of a car strongly affect the injury risk to the driver in the car.

Table 4.3. Car driver injured body regions and injury sources in car-to-car frontal collisions.

	Belted drivers (No injuries=30)										Unbelted drivers (No injuries=0)									
Injury source	Head	Face	Neck	Chest	Abdo men	Spine	Arm	Leg	Un-known	Total	Head	Face	Neck	Chest	Abdo men	Spine	Arm	Leg	Un-known	Total
Steering assembly	2(1)	4		1	1		1	2		11(2)		1		5(1)				3(1)		9(2)
Windscreen	1					2				3	10(2)	9								19(2)
A pillar										0	1	2								3
Floor								1		1										0
Seatbelt				4	1(1)		1			6(1)										0
Instrument panel							1	2		3	1(1)	1						3		5(1)
Console box								1		1										0
Pedal								1		1								2(1)		2(1)
Door panel										0	1	1								1
No contact						12				12						2				2
Indirect						3				3						3(1)		1(1)		4(2)
Glass		1								1										0
Intrusion	1(1)				1(1)					2(2)	1(1)	1						1(1)		2(2)
Ejection										0	1(1)	1								1(1)
Unknown						1	1		1	3									2	2
Total	4(2)	5	0	5	3(2)	18	4	7	1	47(5)	15(5)	13	0	5(1)	0	5(1)	0	10(4)	2	50(11)

Notes: ( ) shows the injuries of MAIS 3-6

Table 4.4. Car driver injured body regions and injury sources in car-to-truck frontal collisions.

	Belted driver (No injury =1)										Unbelted driver (No injury =1)									
Injury source	Head	Face	Neck	Chest	Abdo men	Spine	Arm	Leg	Un-known	Total	Head	Face	Neck	Chest	Abdo men	Spine	Arm	Leg	Un-known	Total
Steering assembly		1(1)								1(1)				5(2)						5(2)
Windscreen	1									1	2(1)	1								3(1)
A pillar										0							1(1)			1(1)
Floor								1		1										0
Instrument panel								1		1								1(1)		1(1)
Front bumper										0	1(1)									1(1)
Front panel	1(1)									1(1)										0
No contact										0										0
Indirect						1(1)				1(1)						1				1
Glass		1								0		1								1
Intrusion										0	1(1)			2(2)				1(1)		4(4)
Unknown							1			0				1				1		2
Total	2(1)	1	0	0	0	1(1)	4	2	0	6(3)	4(3)	2	0	8(4)	0	1	1(1)	3(2)	0	19(10)

Notes: ( ) shows the injuries of MAIS 3-6

Case study

Typical accident of a large truck and a car is investigated as a case study of underride of the car. The truck (10 840 kg) collided with a stationary car (1460 kg) at the velocity of 105 km/h. The overlap ratio of the truck was so small (12%) that the truck frame did not contact the car and overrode the car. Though the direct damage of the truck was apparent, the induced damage could not be observed because the stiffness of the truck in the lateral direction is small (direct damage is the deformation area by contact with the crashed objects and induced damage is that caused by direct damage). The maximum intrusion of the car was 35 cm at the instrument panel. In order to prevent underride of the car, the stiffness in the lateral direction of the truck should be increased to enhance the energy absorption into the truck frame.

Due to this large intrusion into the compartment, the driver in the car sustained lung injuries (AIS 4), femur fracture (AIS 3), face laceration (AIS 1) and upper extremity abrasion (AIS 1). On the other hand, the driver in the truck sustained no injury.

Figure 4.11. Vehicle damages from car-to-truck collision.

4.3. MATHEMATICAL SIMULATION

In order to examine the effect of the underrun guard on the injury risks to the driver of a mini car, collision of a mini car with the truck was simulated by using MADYMO. The mini car model is the same one as used in Section 2.3. The truck model is developed in a similar way to the mini car model. The total mass of the truck is put at 8 tons because the greatest number of truck registrations are in this class. The crash configuration in the simulation is a full frontal collision as shown in Figure 4.12. The mini car collides at 50 or 60 km/h with a stationary truck.

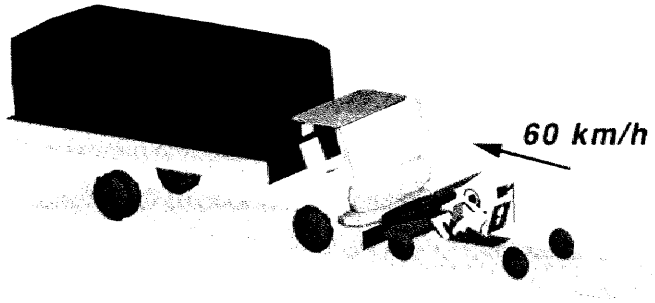

Figure 4.12. MADYMO simulation model of truck and car collision

The force-deformation characteristics used in the simulation are shown in Figure 4.13. The front underrun guard stiffness of the truck is defined to have a constant collapse force level (F). This force was simulated at various levels ranging from 30 to 250 kN. The maximum deformation of the underrun guard is 400 mm due to the structural limitations of the truck. The mini car stiffness is approximated to be linear (500 kN/m) for simplification of the simulation.

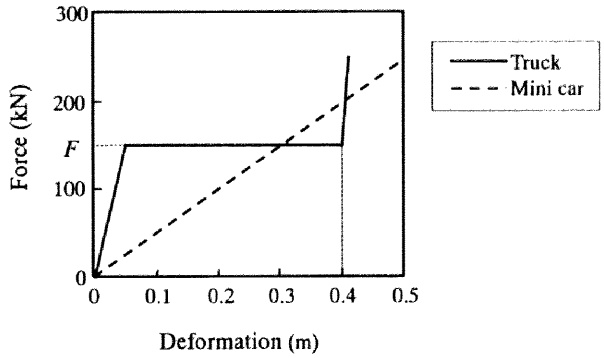

Figure 4.13. Force-deformation characteristics used in the simulation.

The maximum deformation of the underrun guard of the truck and the front structure of the mini car are shown in Figure 4.14. The total deformation of both vehicles generally decrease with increase in collapse force level (F). At 50 km/h, when the collapse force level (F) is less than 130 kN, the underrun guard deforms entirely (400 mm); at more than 130 kN, it does not deform entirely. The deformation of the mini car leads to a minimum at a collapse force level of 130 kN. This result shows that when all of the deformation zone of the underrun guard is crushed, the deformation of the mini car can be the lowest. At 60 km/h, this optimal force level increases to 170 kN.

Figure 4.15 shows the relationship between the collapse force level and the peak deceleration of the mini car at the center of gravity. At 50 km/h, when the collapse force level is more than 130 kN, the peak deceleration of the mini car increases. When the collapse force level is less than 130 kN, the deceleration of the mini car is also higher than that at 130 kN. This is due to contact with the stiff structure after entire deformation of the underrun guard. This phenomenon can be explained from the time history of the deceleration as shown in Figure 4.16. With a collapse force level of 100 kN, there

are two peaks on the deceleration curve. The latter peak is higher than the former due to contact with the stiff structure of the truck. When the collapse force level is 160 kN, the whole deceleration level becomes high. From the results of Figure 4.14 and Figure 4.15, it can be concluded that the collapse force level that minimizes the deformation of the mini car can also minimize the deceleration. This can be the optimal force level for the deformation and deceleration of the mini car. The optimal force level is higher for 60 km/h than for 50 km/h.

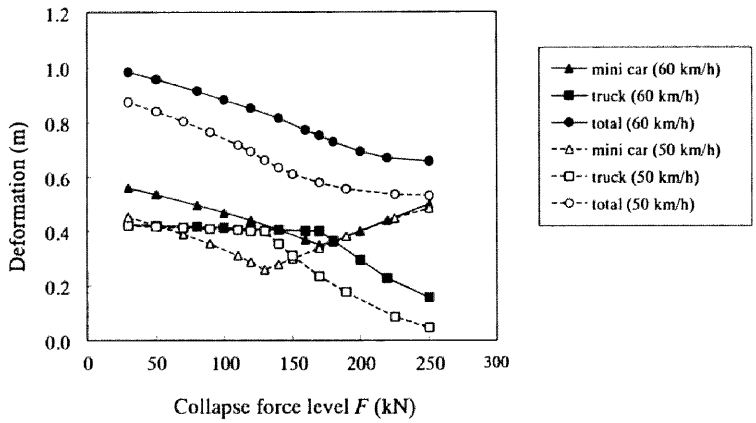

Figure 4.14. Maximum deformation as function of collapse force level.

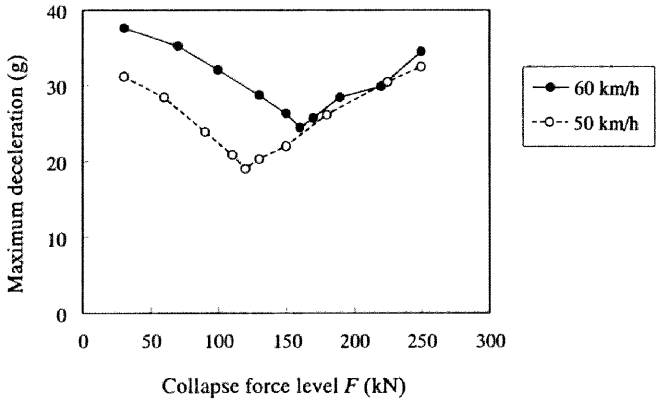

Figure 4.15. Maximum deceleration of a mini car.

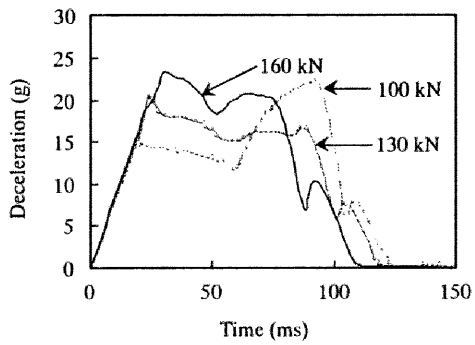

Figure 4.16. Time histories of the deceleration of a mini car (50 km/h).

The injury parameters of the driver in the mini car were also examined by the collapse force level of the underrun guard of the truck (Figure 4.17). All injury parameters are minimal at collapse force levels that differ at each velocity. The HIC and the chest acceleration (3ms) become minimal near the optimal force level. The chest deflection and the femur axial force also become minimal at this force level. This can be explained from the smallest deformation of the mini car at the optimal force level. If we compare the femur force in case of 50 and 60 km/h, the underrun guard at 50 km/h is more effective than at 60 km/h. This result shows that the underrun guard of the truck can reduce the number of minor injuries to the femur as well as severe injuries. Furthermore, the underrun guard of the truck combined with the optimum restraint system of a car can reduce the number of injuries.

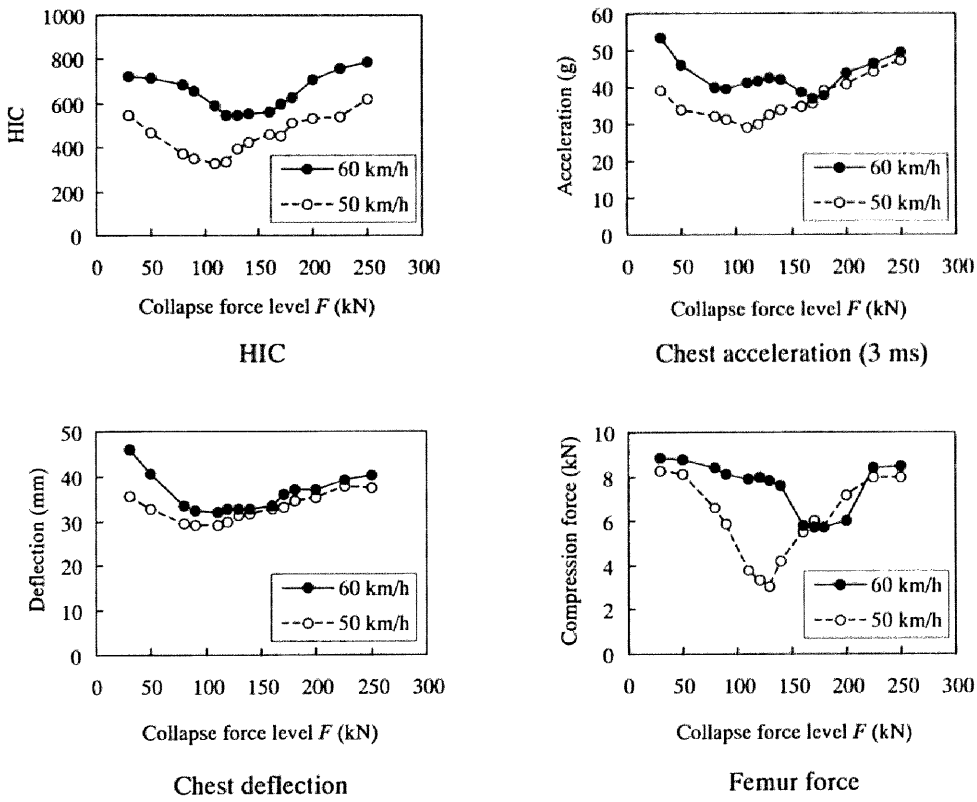

Figure 4.17. Injury parameters of driver in the mini car.

4.4. DISCUSSION

The aggressivity of trucks caused by mass and the geometry differences was evaluated by focusing on the Japan traffic situations by using accident data. The underrun guard of trucks was examined on the basis of a mathematical simulation.

In a car-to-truck collision, truck mass has a large effect on the injury severity of the driver in the car. When the truck mass is more than 5 tons, this injury risk does not change much.

As shown in Section 4.2, the aggressivity of large truck was estimated to be very high in terms of the vehicle itself and human factors. This situation has not changed since 1989. Only the self-protection of passenger cars has been improved. In Japan, the high aggressivity of trucks and the poor self-protection of mini cars should be considered to obtain the total compatibility in vehicle-to-vehicle collisions.

In many car-to-truck collisions, the frame of the trucks does not make contact with a car because the overlap ratio of the truck is less than 1/3. Cars underride the truck due to the stiffness and height difference of the bumpers. The intrusion into the compartment of a car due to underride is one of the causes of injury to the driver in the car.

In order to improve truck aggressivity, the underrun guard was examined using MADYMO. The stiffness effect analysis of the underrun guard showed that there is an optimal force level that can minimise the deceleration and deformation of the colliding car. In this optimal force level, injury risks to the driver in the car also become minimal. It should be noted that this optimum force level depends on the crash velocity. The effective underrun guard should be investigated in order to reduce the injury risk to the driver in cars with various sizes and for a wide range of velocity.

Japan Automobile Manufactures Association (JAMA) has guidelines on crash safety of trucks and buses. The trucks and buses of GVW less than 20 tons are tested by a full rigid barrier crash. This crash test aims at self-protection of the truck, and so the injury parameters of the dummy in the truck are measured. Such a full rigid barrier test will lead to a stiff front structure of the truck. Bumper height and inhomogeneous lateral stiffness of the truck that cause underride of cars will not be improved. Therefore, this guideline will lead to more incompatible trucks. In Japan, more drivers are killed in car-to-truck collision than truck-to-truck collision. Therefore, it is not the improvement in the self-protection but the improvement in the partner-protection of trucks by the underrun guard that will reduce the total number of fatalities.

5. CAR-PEDESTRIAN IMPACT

5.1. INTRODUCTION

The concept of compatibility can be extended to the vehicle-pedestrian impacts since the crash partners in these cases are very different from one another. Similarly to the compatibility between cars, the incompatibility of the mass, stiffness and geometry (shape) between a human and a vehicle induces serious injury to the pedestrian.

The current modern cars are different in shape from those of 10 years old. Many current cars have a short hood length with a rounded wedge shape. Consequently, the injury types of the pedestrian have become different. The vehicle fleet has also changed: the number of sedans is decreasing whereas that of new types of vehicles such as the mini van is increasing.

In this study, the compatibility between vehicles and pedestrians is investigated. The influences of the vehicle shapes on the pedestrian injuries are examined by accident analysis and mathematical simulations. The injury risks to pedestrians are compared for two different car shapes such as the bonnet-type car and the van. The human head is the most critical body part injured in pedestrian accidents. As the pedestrian head contacts with various parts of the cars depending on the vehicle shape and pedestrian height, the headform impact tests are conducted to clarify the head injury risk.

First, the accident analyses will be conducted and injury risks for two contrary vehicle shapes such as the bonnet-type car and the van will be examined in Section 5.2. Second, a pedestrian model are developed and applied to vehicle-pedestrian impact in order to clarify the influence of those vehicle shapes on the pedestrian behavior and injury parameters (Section 5.3). The results of these simulations are compared with those of accident analyses. In Section 5.4, the headform impact tests are conducted and the injury risks to the head are evaluated for various areas of the front of the car including the windscreen and the A pillar. Finally Section 5.5 discusses the results of the car-pedestrian impacts.

5.2. ACCIDENT ANALYSIS

We investigate the vehicle-pedestrian impacts using the current accident data. The macro and micro accident databases of ITARDA are used for this analysis. The macro accident data is based on police reports which offer the largest numbers of data from the whole of Japan. On the other hand, the micro accident data is based on the in-depth investigation of limited number of accidents collected by ITARDA. Using both types of data, information on current pedestrian accidents can be obtained. In this study, the influence of vehicle shapes on the causes and patterns of pedestrian injuries is also examined.

5.2.1. Macro Data Analysis

The probability of fatal injury to pedestrians of different ages was compared for 1988 and 1997 as shown in Figure 5.1. The probability of fatal injury slightly decreases from 1988 to 1997. Taking account of the decrease in the traveling velocity from 1997 to 1988, it can be concluded that the pedestrian safety has not been improved much. Figure 5.1 also indicates that the injury risk to the pedestrian increases strongly with age. From 1997 to 1988, the number of pedestrian fatalities decreased from 2967 to 2643. Among them, the number of pedestrian fatalities aged 65 or more increased from 1381 to 1566. Due to the increase of the ratio of elderly people in Japan, the protection of pedestrians, particularly for elderly people, is becoming important.

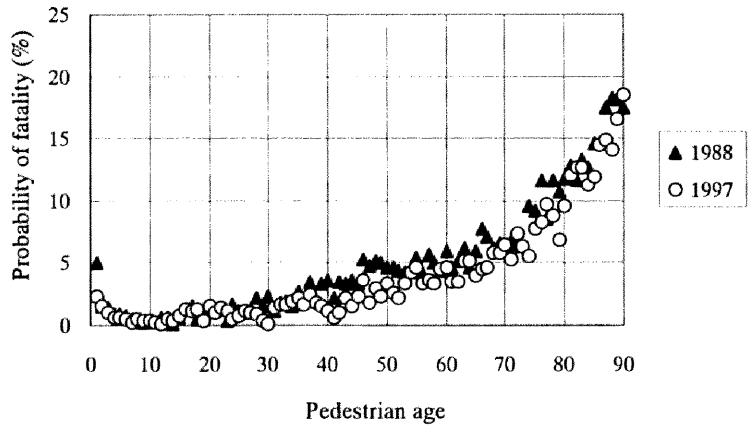

Figure 5.1. The probability of fatality of pedestrian in Japan for 1988 and 1997.

Vehicle mass

The compatibility of cars with pedestrians is related to the mass, stiffness and geometry of the car. It has been reported that the vehicle mass will have no effect on the pedestrian injury since the vehicle is much heavier than pedestrian [Evans 1991b].

In order to confirm this assumption, we examine the relationship between car mass and pedestrian fatality rate for a bonnet-type car. Figure 5.2 shows the pedestrian fatality rate and car mass classified by travelling velocity. As the car velocity has a large effe,,ct on the pedestrian injury, the pedestrian fatality rate increases with car velocity. Whereas, over the same range of car velocity, the fatality rate is almost constant when the car mass is less than 1400 kg. The mass of the car is much larger than those of pedestrian. Thus, in this range of car mass, the fatality rate of the pedestrians is not affected by car mass. However, when the car mass is greater than 1400 kg, the fatality rate increases. This is because SUV occupies large portion of heavy cars. It can be concluded that not the mass but the geometry and stiffness incompatibility of the SUV causes the high fatality rate among pedestrians.

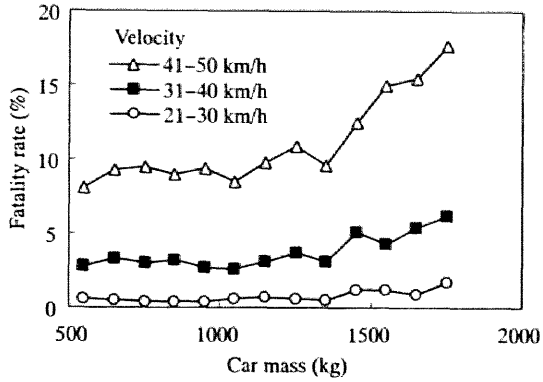

Figure 5.2. Pedestrian fatality rate and car mass classified by the travelling velocity for a bonnet-type car. The front site of the car impacted a pedestrian (1994-1996).

Car shape and pedestrian injury

From 1992 to 1996, 14761 pedestrians were killed in traffic accidents. Among them, 1041 (7.1%) pedestrian fatalities were struck by mini cars, 6646 (45.0%) by bonnet-type cars, 3628 (24.5%) by vans and 965 (6.5%) by large-sized vehicles. In order to examine the injury risks of the injury regions by vehicle class, the number of the fatalities and the severe injuries per 1000 accidents were analyzed (Figure 5.3). Only the most severely injured body region was considered. Vehicles were divided by classes; mini car, small sedan, medium sedan, large sedan, sports and specialty car, wagon, van and SUV. In order to reduce the influence of the impact velocity and the variation of pedestrian height, the accident data was limited so that the level of travelling velocity was less than 40 km/h and the pedestrian age was 13 years old or older. Using this method, the influences of vehicle shapes on the pedestrian injuries can be clarified.

It is observed from Figure 5.3 that the head is a dominant body region in fatalities for all car classes. The number of fatalities due to head and chest injuries is about double for van than for bonnet-type cars (mini, small, medium, large sedan, sports & specialty and wagon). In a serious injury, the number of head and chest injures which can be a cause of death is larger for a van than for a bonnet-type car. Therefore, the front shape of a van seems to be more aggressive for a pedestrian than that of a bonnet-type car. Whereas, the shape of a bonnet-type car is aggressive in relation to pedestrian legs because the number of serious leg injuries is large in crashes with this type of car. Though leg injuries are not so important in terms of threat to life, they often result in long term disability. Thus, the leg protection should be considered for the bonnet-type car.

The risk of head injury to a pedestrian when struck by a mini car is higher than for other bonnet-type cars. The SUV has high aggressivity in relation to the head and chest of the pedestrian due to the height of the hood edge and bumper and the high stiffness of the vehicle body. As the body front shape affects the distribution of injured body regions of the pedestrian, modification of the shape of the car front can be effective in increasing the compatibility between cars and pedestrians.

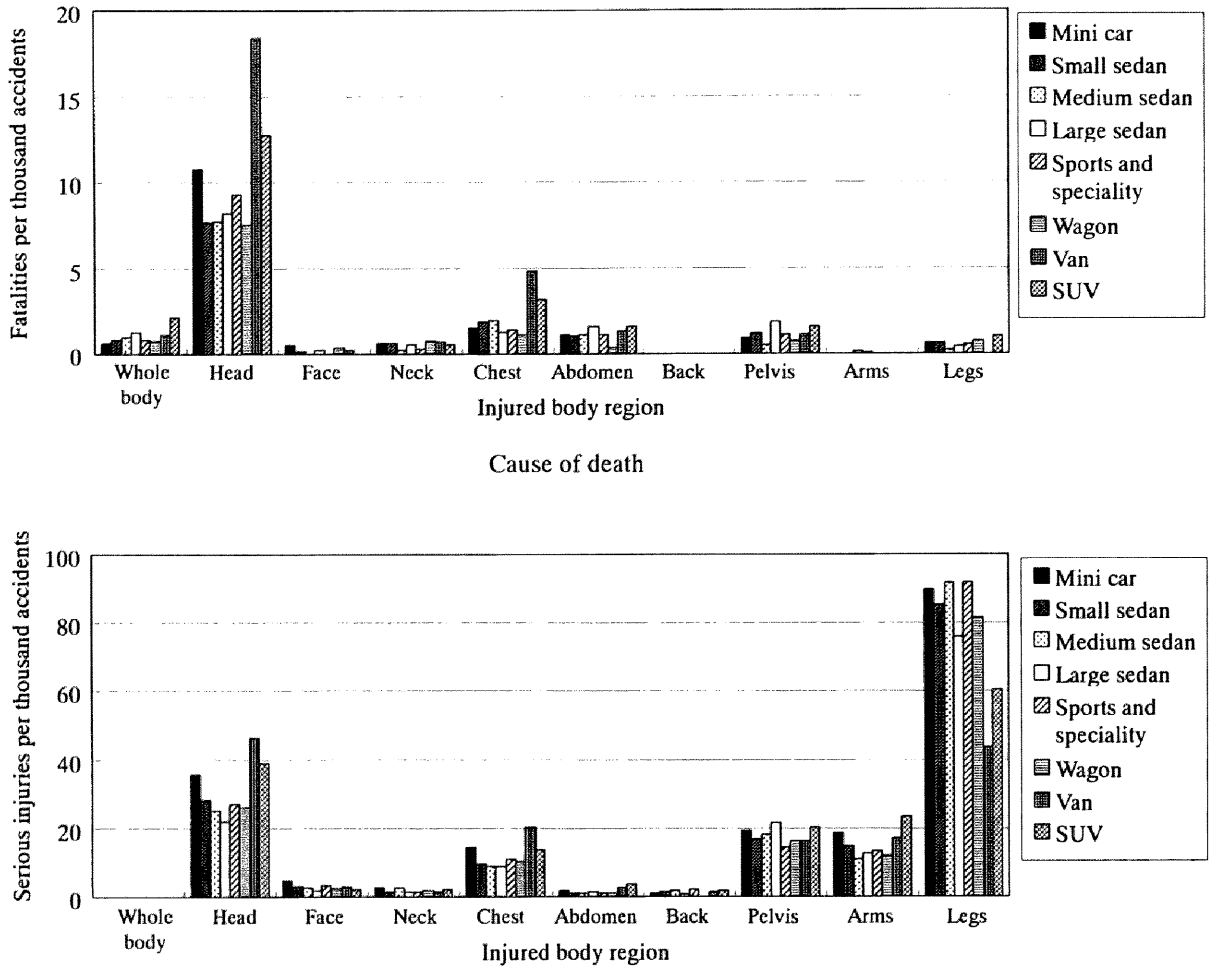

Figure 5.3. Distribution of pedestrian injuries per thousand accidents by body region, car shape and injury severity for the travelling velocity ≤ 40 km/h and pedestrian aged 13 or more. The front site of the car impacted on pedestrian (1994-1996).

5.2.2. Micro Data Analysis

To get a better understanding of injury causes and types, another data set, the micro data, are used for analysis. This micro accident data of pedestrian (1993-1997) are collected by the ITARDA [ITARDA, TSNRI, Nagoya University 1999a], which consists of in-depth investigations of a limited numbers of accident in Tsukuba area. In this database, the number of selected pedestrian accidents is 104.

Impact velocity and pedestrian injury

The injury of pedestrians becomes more severe as the impact velocity of the vehicle increases. The cumulative distributions of the impact velocity for bonnet-type cars and vans were examined for injury severity (MAIS 1,2, or MAIS 3-6). This is shown in Figure 5.4. When struck by the bonnet-type cars, the impact velocity at a cumulative frequency of 50% is about 40 km/h for the severe injury (MAIS 3-6), while this velocity is about 25 km/h for the minor injury (MAIS 1, 2). In the case of a van, on the

other hand, the velocity of severe injury is 25 km/h, and that for the minor injury is 15 km/h, respectively. The impact velocity of the 50% cumulative frequency of vans is much lower than that of bonnet-type cars for both injury severities. According to these results, it is confirmed that the pedestrian injury is likely to be severe when struck by a van, even though the impact velocity is lower than that of bonnet-type cars.

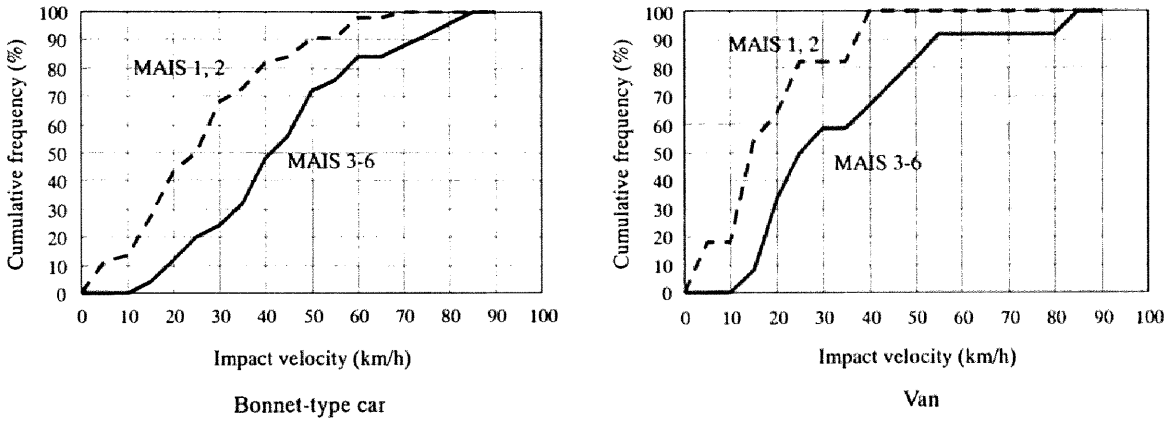

Figure 5.4. Vehicle shape and impact velocity

Head contact location

The head contact positions were examined for a bonnet-type car and van. This analysis may show the effects of various vehicle front shapes on the head impact positions and on the potential head injury risk to the pedestrian. The head injuries sustained by the contact with vehicle body were counted whereas those in contact with the ground were omitted.

There were 69 cases of pedestrian accidents with bonnet-type cars excluding the SUV in the micro data. Among them we chose 17 accidents, in which the head injuries occurred by direct contact with vehicle body and the head contact positions were apparent. Head contact positions are shown in Figure 5.5 with indication of the pedestrian height and the injury severity. The most frequent head contact positions are the lower part of the windscreen and its vicinity; the windscreen frame, cowl and A pillar. Thus, to protect pedestrians, the aggressivity of those areas should be considered. In addition, the accidents often occurred on the left side of the cars.

Furthermore, there were 18 pedestrian accidents with vans. Six accidents among them where the head contact position is clear are shown in Figure 5.5. There were four fatalities where the head hit the windscreen frame and A pillar. For short pedestrians whose height was less than 150 cm, the heads hit the front panel because their heads did not reach the windscreen. From Figure 5.5, the frequency of the head contact with the stiff parts such as the front panel and the windscreen frame in the accidents with a van is higher than that of a bonnet-type car. In other words, the micro data analysis confirmed that there was a high risk of sustaining head injuries in accidents with those vehicles.

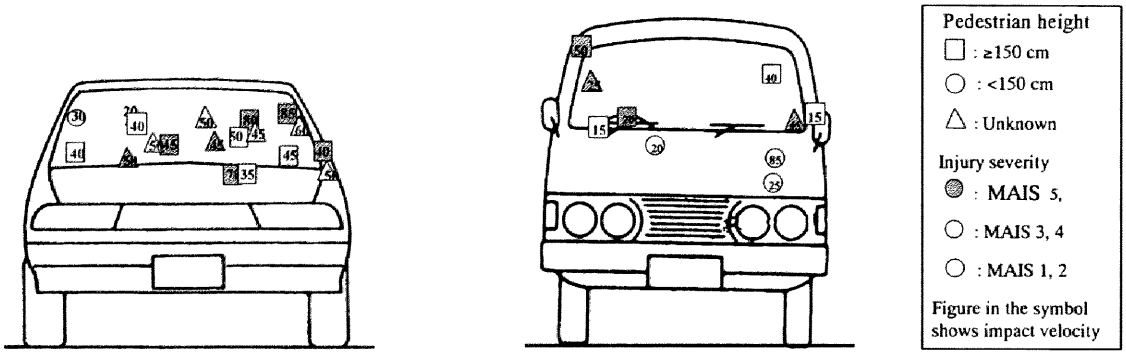

Bonnet-type car

Van

Figure 5.5. Head impact position

Wrap around distance

When a pedestrian is struck by a vehicle, the pedestrian wraps around the front of the vehicle. The location of the head impact is approximately estimated by the wrap around distance (WAD), which is the length measured along the vehicle profile from the ground to the head contact point (Figure 5.6). The WAD gives us important information about vehicle body parts where the head makes impact.

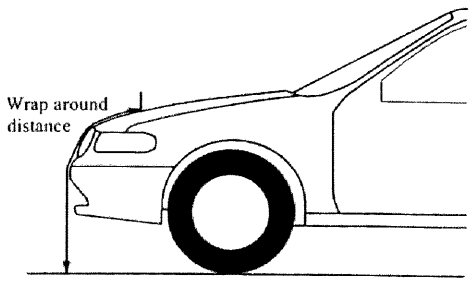

Figure 5.6. Wrap around distance (WAD)

The WAD has a close relation with standing height of the pedestrian. Figure 5.7 shows the relation between the pedestrian height and the WAD of two vehicle types; a bonnet-type car and a van. The WAD increases with the pedestrian height. The WAD is larger than the pedestrian height when the pedestrian is involved in an accident with a bonnet-type car. However in the case of a van, the WAD approximately equals the pedestrian height. Therefore, if the pedestrian height is available, the head contact position can be estimated easily in accidents with a van and we can predict the zones where it is necessary to take countermeasures and to perform tests for the pedestrian protection.

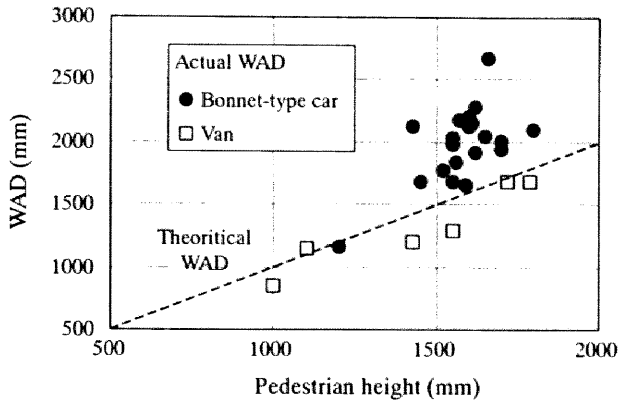

Figure 5.7. Pedestrian height and WAD.

Head injuries and their causes

As discussed above, head injury severity varies with impact location of the vehicle. The causes of injury (including the ground) in accidents with bonnet-type cars are shown in Figure 5.8, and those with vans are shown in Figure 5.9.

Head injuries occurred due to the impact against the vehicle body in accidents with bonnet-type cars in 9 cases (50%) with severe and fatal injuries (AIS 3-6), and in 22 cases (54%) with minor injuries (AIS 1, 2). The windscreen frame and A pillar have a high potential to cause severe head injury (17%) followed by the hood (11%) and the fender (6%). As for the minor injuries, the windscreen occupied the highest frequency (32%) among the injury causes of all the vehicle parts. There are three cases where the windscreen caused serious injuries to the head, however, the impact location was close to the windscreen frame. The A pillar, hood and fender lead to severe injury to the head. Thus, for a reduction of head injury severity, vehicle body parts such as the A pillar, hood and fender, should be considered to enhance the pedestrian protection. On the other hand, the ground caused severe injury to the head in 17% of the cases, and may be one of the head contact locations with a high frequency. In the case of minor injuries, the ground was the most frequent cause of injury (41%). Countermeasures for head injuries due to the ground are difficult to take, which reflects the limitation of pedestrian protection only from the design of car body.

In the case of the van, due to the head impact on the vehicle, 10 cases (83%) sustained serious and fatal injury, and 8 cases (38%) had minor injuries. The front panel (42%) and windscreen frame (17%) were the main injury causes for the severe and fatal injuries. In the case of the minor injuries, the windscreen shows the highest frequency of the injury cause. Furthermore, there were two cases (17%) of serious and fatal injuries and five cases (38%) of minor injury due to contact with the ground. For vans, the front panel should be considered to improve pedestrian protection.

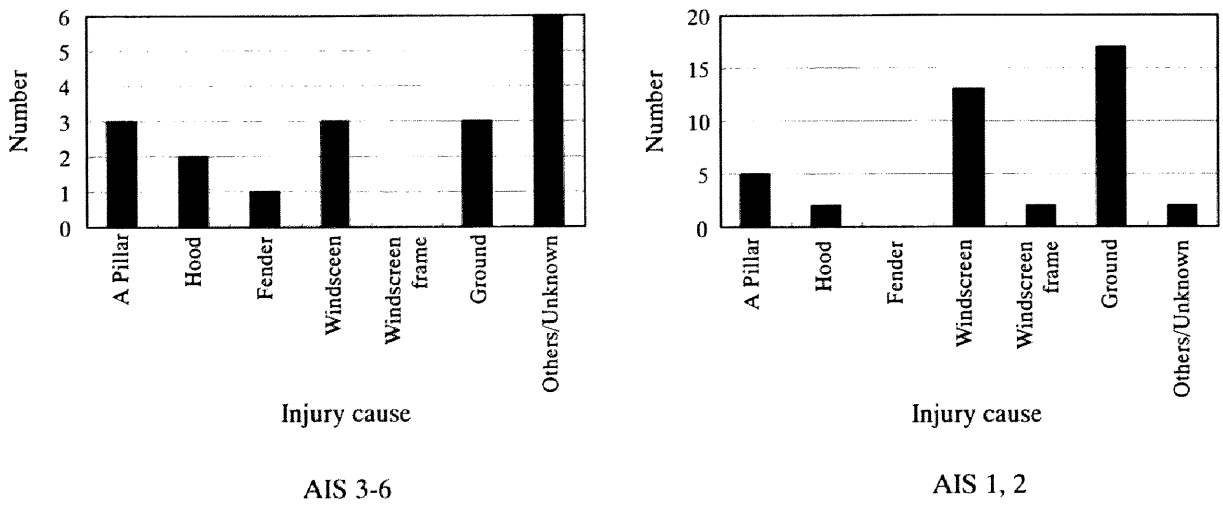

Figure 5.8. Causes of head injury (bonnet-type car)

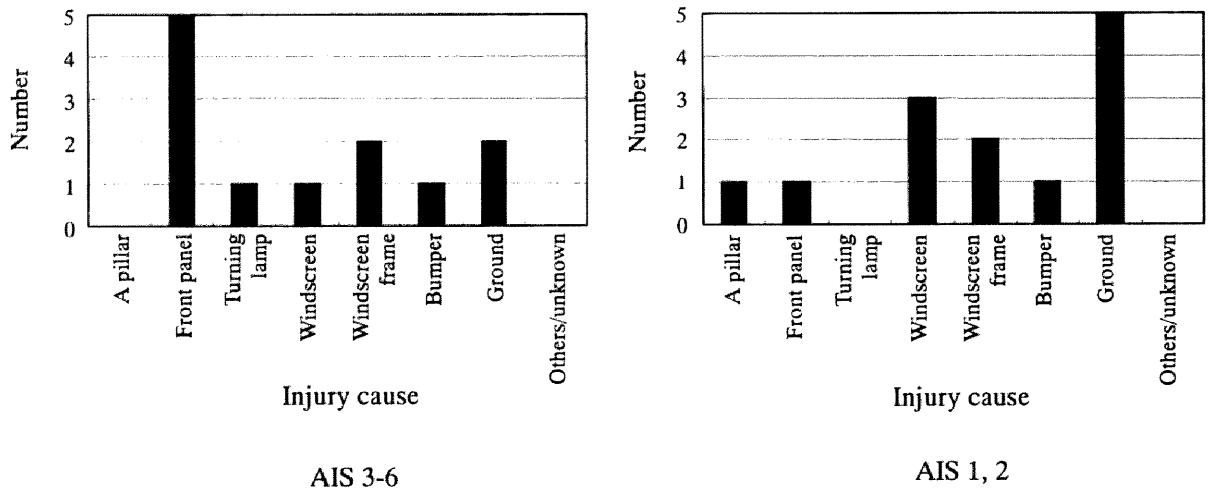

Figure 5.9. Causes of head injury (van).

Various types of head injuries occur in the accidents. Figure 5.10 shows the distribution of head injury classified by the injury causes, the injury types and the injury severity (AIS 3-6 and AIS 1,2).

Brain injury is a main cause of the severe and the fatal head injuries (AIS 3-6). On the other hand, for the minor injuries (AIS 1, 2), the percentages of bruises and lacerations are high. Especially, in contact with the windscreen, the pedestrian is likely to sustain bruise and laceration unless impact locations are near the windscreen frame. Skull fractures occur frequently when a pedestrian's head contacts with a stiff part such as an A pillar, windscreen frame or the ground.

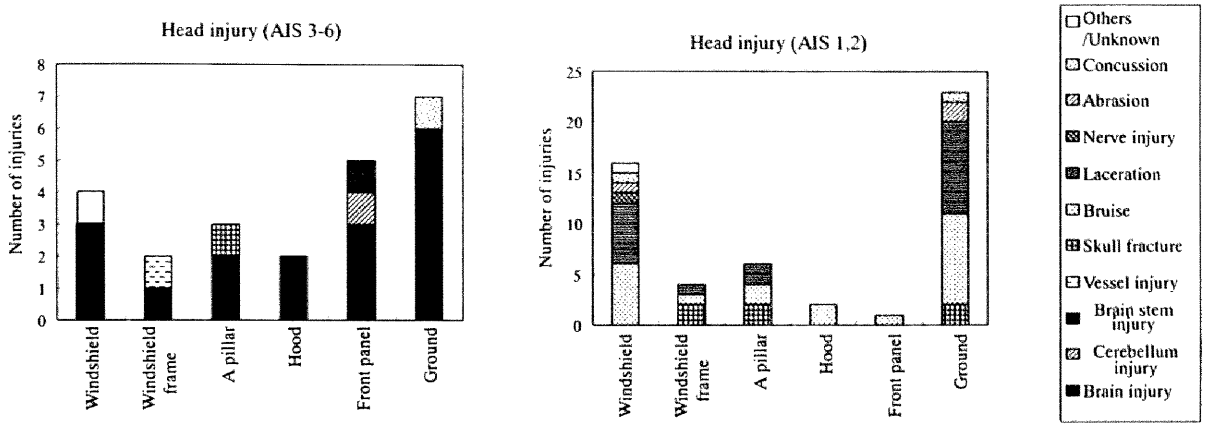

Figure 5.10. Head injury types and injury cause.

Case study

Some typical accidents where pedestrians sustained injury to the head in contact with different areas of the car body were examined. Three accidents presented are with bonnet-type cars, and impact locations were the windscreen, the lower area of the windscreen and the A pillar respectively.

In the accidents shown in Figure 5.11, a pedestrian (male, 46 years old, height unknown) was hit by a bonnet-type car with an impact velocity of 20 km/h. The head contacted the windscreen. As the deformation of the windscreen, made of laminated glass, was large (60 mm) there was only minor injury to the head (AIS 1, headache or dizziness). The kinetic energy of the head was absorbed by the large deformation of the windscreen.

A pedestrian (female, 64 years old, height 152 cm) was struck by a bonnet-type car at an impact velocity of 35 km/h. The head hit the windscreen close to the windscreen frame (Figure 5.12). The area of spider webbed marking is smaller to that when the contact is in the center of the windscreen as shown in Figure 5.11. In this accident, the deformation of the windscreen (laminated glass) was small (10 mm) and the energy absorption of the car at impact was small. Therefore, the pedestrian sustained the serious injury of subarachnoid hemorrhage (AIS 3), oculomotor nerve NFS (AIS 2) and laceration (AIS 1). By comparing the results of Figure 5.11 with Figure 5.12, it was observed that the windscreen has different force-deformation characteristics, which cause various injury patterns to the head.

In the accident shown in Figure 5.13, a pedestrian (male, 31 years old, height 162 cm) was hit by a bonnet-type car at an impact velocity of 55 km/h. The head made contact with the A pillar and the windscreen, and the deformation of the A pillar was small (5 mm). The pedestrian sustained diffuse axonal injury (AIS 5), epidural hematoma (AIS 4) and skull fractures (AIS 2).

From the results of these accidents, it is clear that the injury patterns of the head depends on the stiffness of the contacted parts of the car. The head injury risk is low when contact is with the windscreen, however, even if contact will be the windscreen, when the region is close to the frame or A pillar, serious injuries to the head can occur.

Figure 5.11. Head contact with driver side windscreen.

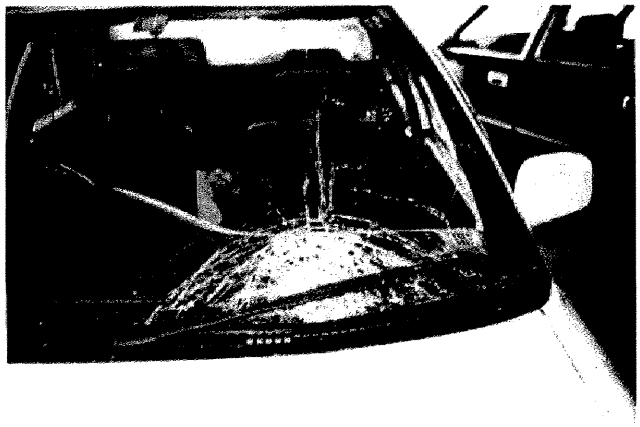

Figure 5.12. Head contact with lower area of windscreen. Both the windscreen and cowl top were deformed.

Figure 5.13. Deformation of A pillar by head impact. Both the windscreen and A pillar hit the head.

5.3. MATHEMATICAL SIMULATION

Accident analysis in previous section indicated that the vehicle shape has large influences on the pedestrian injury risk. Thus, mathematical simulations were performed and injury mechanisms are discussed for three types of vehicles such as the mini car, the medium car and the van.

5.3.1. Model Development

The pedestrian model used in the mathematical simulations is based on the human-body model which was developed by Yang et al. (1997). This is a multi-body simulation model which consists of ellipsoids and joints. Similarly to the original model, joint characteristics are based on the human body, and contact interactions between human body and car were obtained from experiments [Ishikawa et. al 1993b]. Figure 5.14 shows this model.

In Japan, many elderly people with heights ranging from 140 cm to 165 cm are involved in pedestrian accidents [Yoshida et al. 1998]. This height is lower than that of the AM50 (American Male 50 percentile, 175 cm, 75 kg), which is commonly referred in the field of the crash safety. Therefore, a pedestrian model has been developed by focusing on an average Japanese male aged 60 to 69 whose standing height is 161.3 cm and weight is 59.0 kg [Management and Coordination Agency of Japan 1997]. The sizes, masses and inertia of the body segments of the pedestrian model are calculated using GEBOD (Generator of Body Data). This model is called JE60 in this study. The model consists of 21 ellipsoids, 2 planes and 12 spring-damper elements. This pedestrian model was validated using cadaver tests from the literature [Ishikawa et al. 1993b].

The vehicle models consist of the bumper, hood edge, hood and windscreen. The bumper, hood edge and hood are represented by ellipsoids, and the windscreen by a plane. The impact velocity in the simulation is 40 km/h.

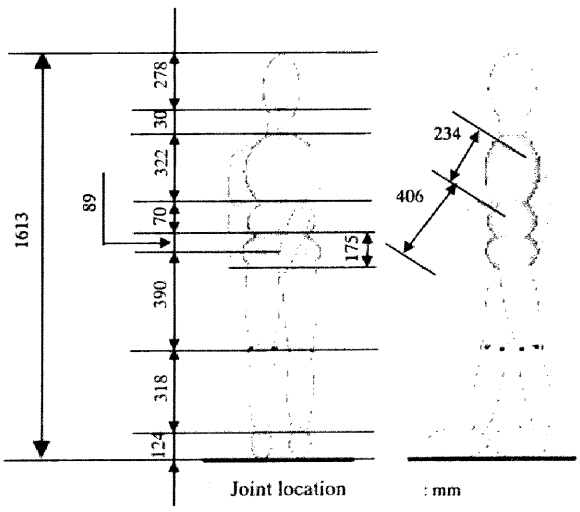

Body segment	mass (kg)
Head	4.7
Neck	1.1
Chest	14.7
Abdomen	3.4
Pelvis	9.7
Upper arms	3.2
Lower arms	3.6
Upper legs	11.9
Lower legs	5.5
Feet	1.3
Total	59.0

Figure 5.14. Pedestrian model (JE60).

5.3.2. Simulation Results

The pedestrian shows various kinematics in impact with different vehicle shapes, as shown in Figures 5.15, 5.16 and 5.17. When a pedestrian is struck by a mini car or a medium sedan, the bumper hits the leg and the hood edge hits the thigh, and then the upper torso of the pedestrian rotates toward the hood of the car. The pedestrian's head contacts the lower region of the windscreen at 118 ms when hit by a mini car, and the hood rear area at 97 ms when hit by medium car. With a van, the whole body of the pedestrian is struck by the vehicle front almost at the same time. The chest contacts the upper part of the front panel, the head contacts the lower part of the windscreen at 41 ms, and then the whole pedestrian body is projected ahead of the vehicle.

It was found that the pedestrian kinematics, when struck by a vehicle, consist of the translational and rotational movement of the pedestrian. In the case of a bonnet type car such as a mini car and a medium sedan, the pedestrian upper body rotates and this rotational movement is dominant. Whereas with a van, the translational movement is dominant, and the pedestrian is pushed in front of the vehicle as shown in Figure 5.17.

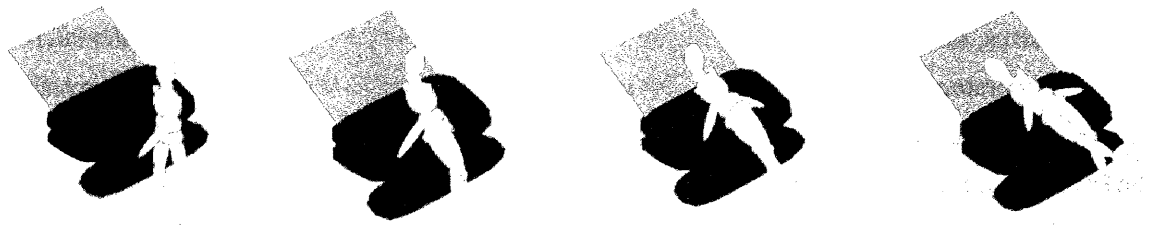

Figure 5.15. Pedestrian kinematics (mini car, JE60)

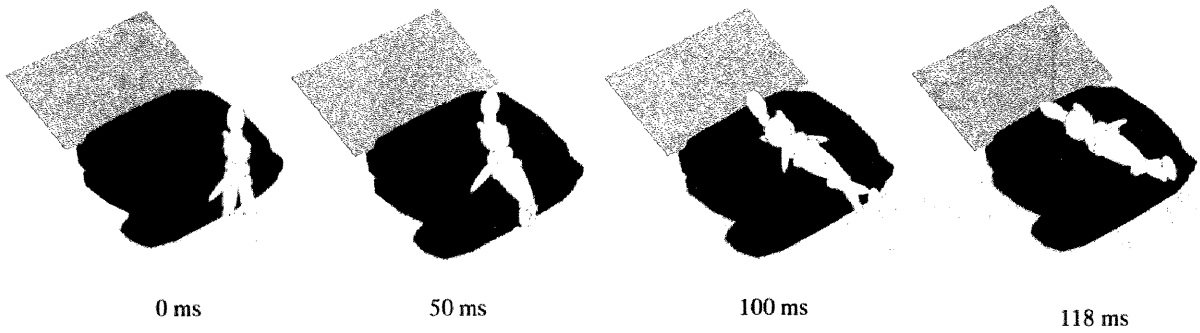

Figure 5.16. Pedestrian kinematics (medium car, JE60).

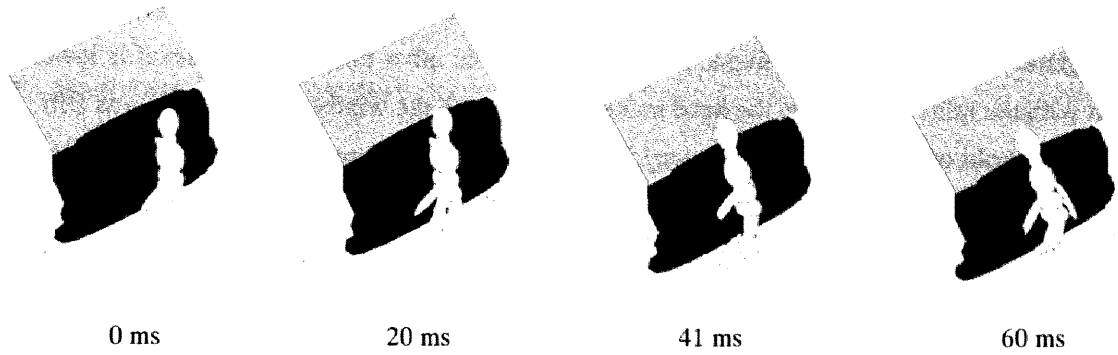

Figure 5.17. Pedestrian kinematics (van, JE60).

The head impact velocity as well as the force-deformation characteristics of impact location affect the head injury risk. The heads resultant velocity relative to the vehicle is shown in Figure 5.18. Because the translational movement is dominant in pedestrian kinematics in a van impact, the head resultant velocity relative to the vehicle decreases consistently after the impact. The head contacts the vehicle at a velocity of 9.6 m/s that is lower than initial velocity. In the case of the bonnet-type car and the mini-car, both influences of translational and rotational movement are large.

In the first phase, the head resultant velocity increases due to the rotational movement of the upper body, then it decreases due to the translational movement of the whole body. The head resultant velocity in contact with a car is 12.0 m/s for a mini-car and 9.6 m/s for a medium sedan. The head resultant velocity of the bonnet-type car and the mini car is higher than that of the van. Based upon the mathematical simulations, it is found that the head resultant velocity depends on the shape of vehicles.

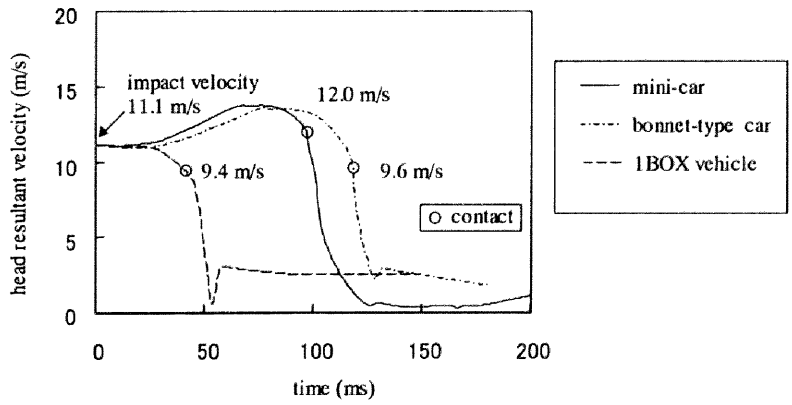

Figure 5.18. Head resultant velocity to the vehicle (JE60).

The pedestrian injury parameters such as the HIC, acceleration of the chest, pelvis and upper leg (maximum acceleration of duration time 3 ms) are shown in Figure 5.19. For the impact with the van, the HIC level is the highest because the head makes contact with the windscreen frame which is a stiff

structure. This result of high HIC level in the simulation is consistent with that of the accident analysis that the injury risk is high when impacted by a van. On the other hand, the HIC level is lower in the impact with the mini car because the head makes contact with the windscreen which is less stiff.

The threshold of the severe chest injury is 60g for the chest acceleration. As observed in Figure 5.19, the chest accelerations in all simulations are less than 60g. However, the chest acceleration on impact with the van is twice as high as that with other vehicle types. This result agrees with that of the accident analysis that the chest injury risk is higher when struck by a van. The pelvis acceleration on impact with the van is the highest, though this level is lower than the injury threshold (80g). The acceleration of the upper leg when struck by a bonnet-type car is higher than that when struck by a van. This result is also consistent with that of the accident analysis that the leg injury risk is higher when struck by a bonnet-type car.

In summary, the risk of head injury depends on the impact velocity of the head and the stiffness of the vehicle structure where head made contact. Furthermore, the head impact velocity and position of the vehicle are affected by the vehicle shape because the pedestrian kinematics depend on it. The results of the accident analysis that the bonnet-type car induces high injury risk to the leg and the van induce high injury risk to the head and chest, agree with those from the mathematical simulations.

Fundamentally, these simulations are able to predict the head contact position and the injury risk to the pedestrian. However, these simulations could not confirm the high injury risk to the head of the pedestrian when struck by a mini car. As the head can contact with various locations of the car, it is necessary to evaluate the head injury risks in the case of impact onto these areas.

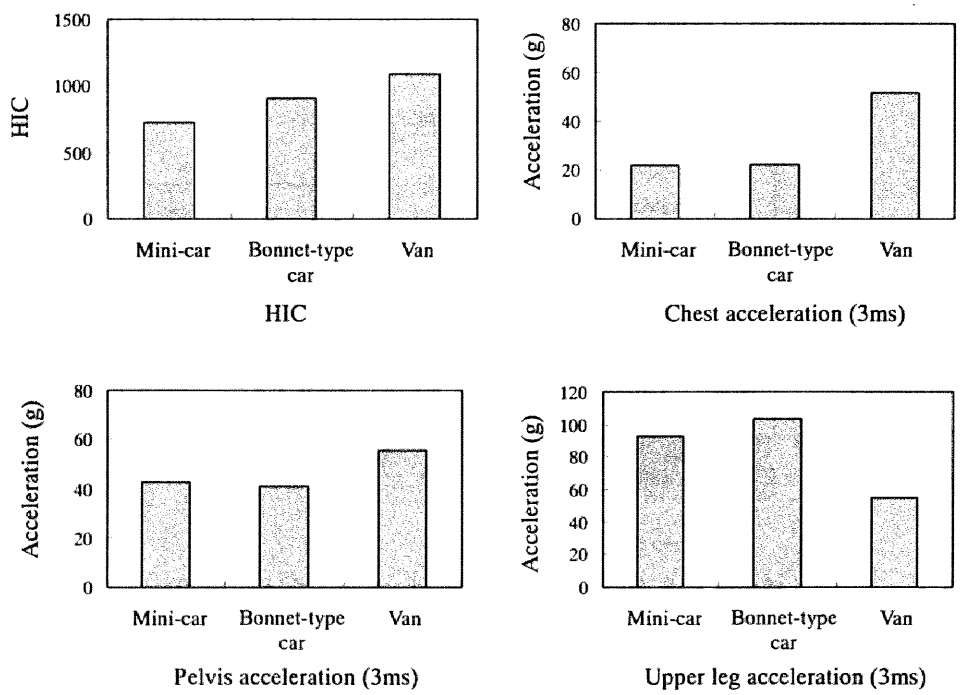

Figure 5.19. Pedestrian injury parameter (JE60).

5.4. HEAD IMPACT TEST

5.4.1. Headform Impact Test Methodology

The head injury risk depends on the stiffness of the vehicle as well as on the impact velocity of the head. The pedestrian head impacts various locations of the vehicle with different stiffness. Therefore, the headform impact tests were carried out to evaluate the injury risk to the pedestrian head for impact on the car frontal areas. The adult headform impactor prescribed in the proposed EEVC pedestrian test procedure [EEVC 1994] was used (Figure 5.20). The outer layer of the adult headform impactor is composed of a skin and sphere, and the mass is 4.8 kg. The acceleration is measured at its center of gravity. The impact velocity is 40 km/h and the impact angle is 65° from the horizontal plane. In order to clarify the injury risk to the head due to different body regions of the car, various impact positions such as the hood top (WAD is 1500 or more), cowl, fender and the lower area of the windscreen were impacted. In the area of the windscreen, the impact positions were varied by the distance from the windscreen frame and A pillar. The Head Injury Criteria (HIC 36 ms), acceleration-time histories and force-deformation characteristics are measured at each area of the car.

The velocity has a large effect on the injury risk to the pedestrian. The results of simulation showed that the pedestrian head hit the windscreen of the mini car at a higher velocity than the medium sedan where the head hit the hood (see Figure 5.18). Therefore, we performed the impact tests onto the hood and windscreen at different impact velocities of 30, 40 and 50 km/h, and the HIC values are compared.

The same types of sub-compact cars (Toyota Collora AE91) were used in the tests. The windscreen of this car is of laminated safety glass, which consists of three layers; i.e. an outer glass layer, a Polywinyl Butyral (PVB) interlayer and an inner glass layer. The thickness of the outer and inner glass is 2.3 mm, respectively, and that of the interlayer is 0.76 mm, which is the most commonly used specifications for the windscreen. The headform impact tests onto the windscreen is shown in Figure 5.21.

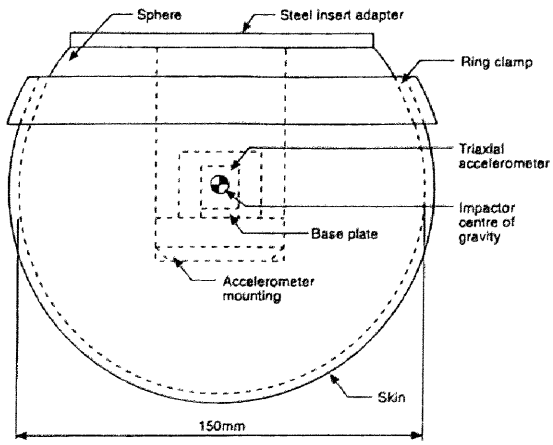

Figure 5.20 Adult head impactor [EEVC 1994]

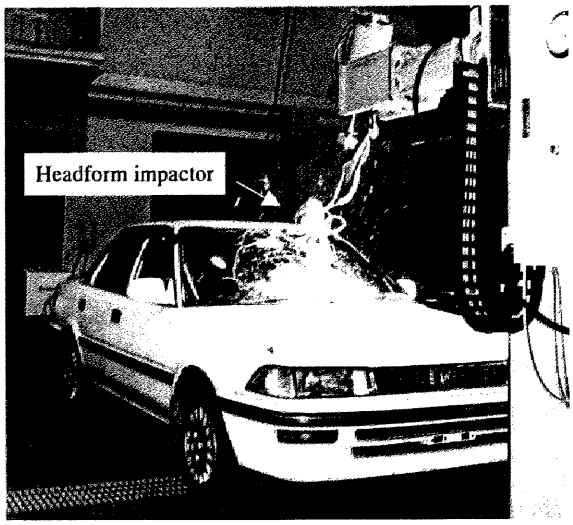

Figure 5.21. Head impact test on the windscreen.

5.4.2. Test Results

Impact location and injury risk

The impact locations and the test results are shown in Figure 5.22 and Table 5.1, respectively. The 36 impact tests were carried out on the hood, fender, cowl, windscreen, windscreen frame and A pillar. In the hood, cowl and fender area that is prescribed in the EU test method, the HICs for only two locations (experimental No. 3 and 4 in Figure 5.22) are less than the injury threshold (HIC 1000). The rear hood and hood/fender areas produce high HICs. The HICs are extremely high and greater than 5000 in the locations of the hood hinge, the hood at the hood stopper, the corner of the windscreen frame and the bottom of the A pillar.

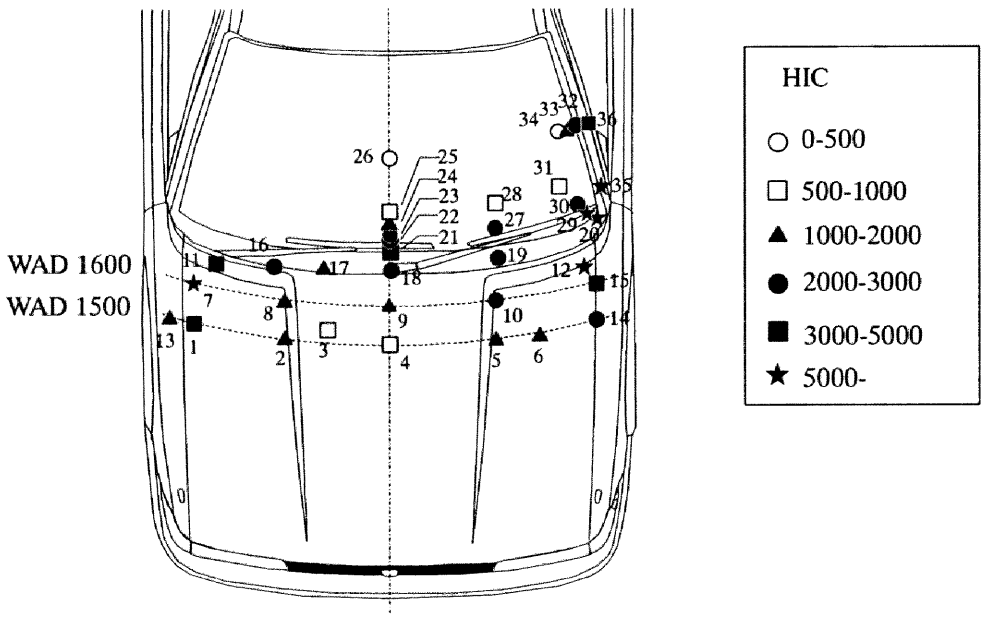

Figure 5.22. Distributions of HIC and impact location by the impact position for the tested car (40 km/h).

Table 5.1. The HIC (36 ms) at impact locations (40 km/h)

No.	Impact location	HIC	No.	Impact location	HIC	No.	Impact location	HIC
1	Hood	4071	13	Fender	1489	25	Windscreen	947
2	Hood	1131	14	Hood/Fender	2934	26	Windscreen (center)	426
3	Hood	795	15	Hood/Fender	4143	27	Windscreen	2236
4	Hood	805	16	Hood/Cowl	2435	28	Windscreen	710
5	Hood	1105	17	Cowl	1733	29	Windscreen	5133
6	Hood	1984	18	Cowl (wiper pivot)	2256	30	Windscreen	2730
7	Hood (hinge)	6663	19	Cowl	2875	31	Windscreen	850
8	Hood	1548	20	Windscreen frame/A pillar	6892	32	Windscreen/A pillar	2990
9	Hood	1064	21	Windscreen frame	3228	33	Windscreen	2232
10	Hood	2003	22	Windscreen	2270	34	Windscreen	451
11	Hood (wiper pivot)	4706	23	Windscreen	2284	35	A pillar	5240
12	Hood (hood stopper)	7770	24	Windscreen	2126	36	A pillar	4158

The car body shows various force-deformation characteristics when hit by the headform. Figure 5.23 shows the force-deformation characteristics of the main locations of the car. In the hood region, the force has a peak at deformation of 25 mm, and after the hood reinforcement separates from the hood, the force shows a plateau. However, the hood at the hinge and the hood stopper leads to the high force levels of 20 kN. In the cowl area, the force increases consistently, whereas at the wiper pivot, the force is high due to the deformation of the wiper pivot axis. The A pillar has a constant force level due to the collapse of its box shape, but its force levels are high enough to cause serious injuries to the head.

In addition to the baseline force-deformation characteristics of each car body structure, it was found that the local high stiffness of the hood hinge, hood stopper and wiper pivot had a large effect on the force-deformation characteristics and the HIC in headform impacts.

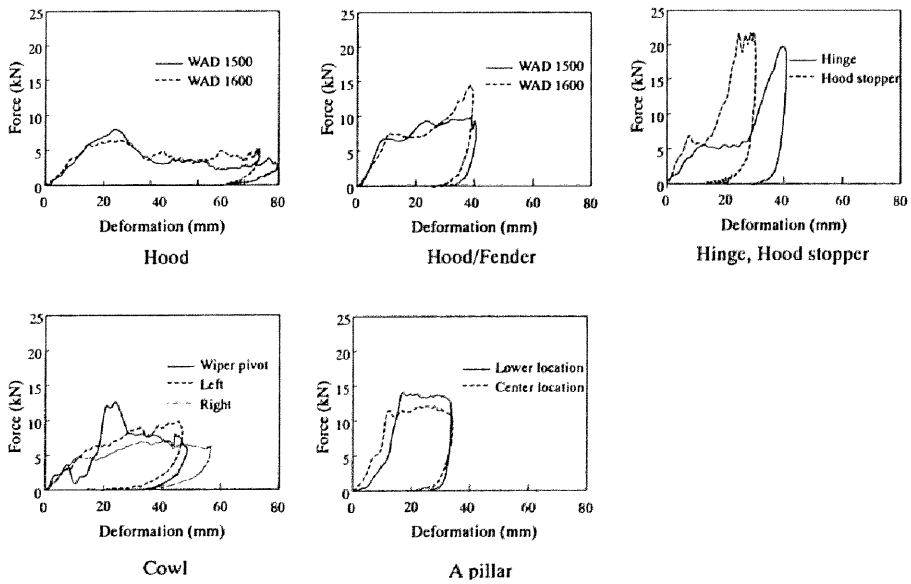

Figure 5.23. Force-deformation characteristics of the car from headform impact tests (40 km/h).

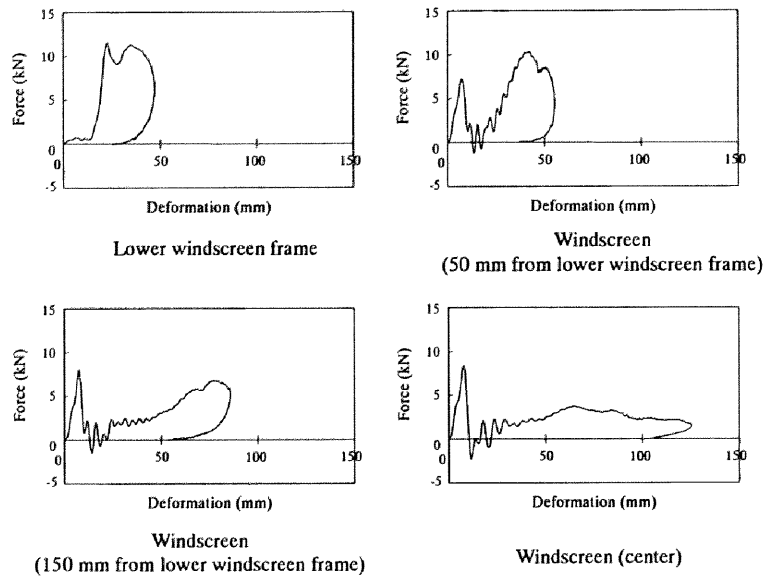

Figure 5.24. Force-deformation characteristics of the windscreen from headform impact tests (40 km/h).

The force-deformation characteristics were compared at the lower windscreen frame, 50, 150 mm above the lower windscreen frame, and at the windscreen center (Figure 5.24). In the windscreen area which is 50 mm above the lower windscreen frame, the force shows the inertial spike of about 7.5 kN in the initial phase when the glass breaks. After that, the force increases, and the force-deformation curve is similar to that of the windscreen frame. For the impact on the center of the windscreen, the initial spike of the glass breaking is followed by a low plateau force of about 3 kN. This plateau force level is due to stretching of the PVB interlayer of the HPR glass. In this area, the effect of the stiffness of the lower windscreen frame on the force-characteristics is small. These results show that the force-deformation characteristics of the windscreen are mainly affected by those of windscreen frame.

The bonded width of the windscreen and lower windscreen frame is larger than that of the A pillar. This difference of the boundary conditions between the windscreen frame and the A pillar affects the HIC value in the windscreen area. Figure 5.25 shows the relation between the HIC and the distance from the windscreen boundary for three paths.

The HIC value has a maximum at the windscreen boundary for all paths, and it decreases with distance from the boundary. The inclination of decrease of the HIC varies with each boundary. The HIC value decreases gradually with the distance from the lower windscreen frame and it reaches less than 1000 at a location of 190 mm above the lower windscreen frame. This can be attributable to that the bonded width is large around the lower windscreen frame. It is also due to the fact that the oblique impact angle and the interaction force experienced by the impactor with the windscreen frame are large. Whereas for the A pillar, the HIC decreases abruptly. As the windscreen bonded area to the A pillar is small, the deformation of the windscreen becomes large in such a way that the windscreen boundary of the A pillar works like a hinged joint. The corner of the windscreen boundary is so stiff that the HIC in the windscreen around this corner leads to high value. The HIC of path C has a similar

tendency to that of path A when the distance from the lower windscreen frame is over 100 mm, which means that the influence of the boundary by the A pillar is small in this region.

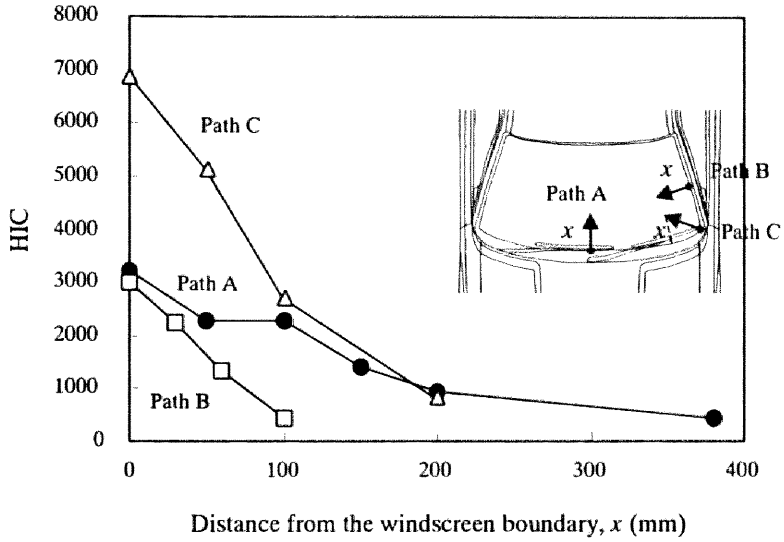

Figure 5.25. The relation between the HIC and the distance from the windscreen boundary for the tested car (40 km/h). The path A is from the lower windscreen frame, the path B is from the A pillar, and the path C is from the corner of the windscreen. For path C, the lateral axis indicates the distance from the lower windscreen frame.

The HIC near the windscreen boundary depends on the stiffness of the boundary structures. A contour map on the windscreen is drawn based on the test results (Figure 5.26). The region where the HIC value is below the injury threshold (1000) occupies a large proportion in the windscreen.

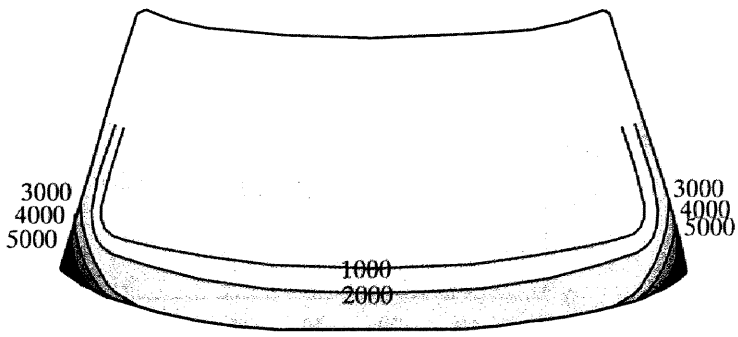

Figure 5.26. The HIC in the windscreen region in the headform impact tests for the tested car (40 km/h)

If we determine the head impact test procedure for the windscreen, it is sufficient to test near the boundary of the windscreen, and the center area of windscreen need not be tested. This is because the HIC has a maximum at the boundary of the windscreen. It is necessary to take into consideration that the HIC has a highest value at the lower corner of windscreen boundary.

The HIC is greater than the injury threshold (HIC 1000) in the area of the windscreen where the distance from the lower windscreen frame is less than 190 mm. Therefore, it is important to design the rear area of the hood to prevent head contact with the lower windscreen area. The A pillar is so stiff that the HIC in contact with the windscreen around the A pillar becomes high. It is difficult to change the stiffness of the A pillar, thus one solution may be that the location of the A pillar be changed to the side so that the head can not make contact with this structure while taking the visibility of the driver into consideration.

Impact velocity and injury risk

In order to clarify the effects of impact velocity, the relation between impact velocity and the HICs were examined for the hood and the center of the windscreen by the impact tests. The results are shown in Figure 5.27. The hood produces linear increase of the HIC with increasing impact velocity, and the HIC value exceeds 1000 at 50 km/h. Although the impact velocity is 50 km/h on the windscreen, the interlayer of the windscreen is torn (there was no penetration of the headform), which results in a HIC value less than injury threshold. The fragments of the broken glass become larger with higher impact velocity.

The head of the pedestrian hits the windscreen at a higher velocity than on the hood because the pedestrian head rotates toward the car and contacts the windscreen during this rotation. As the HIC for contact with the windscreen is still less than the injury threshold even at the impact velocity of 50 km/h, it is considered that in car-pedestrian impacts the injury risk to the head is low in the center of the windscreen.

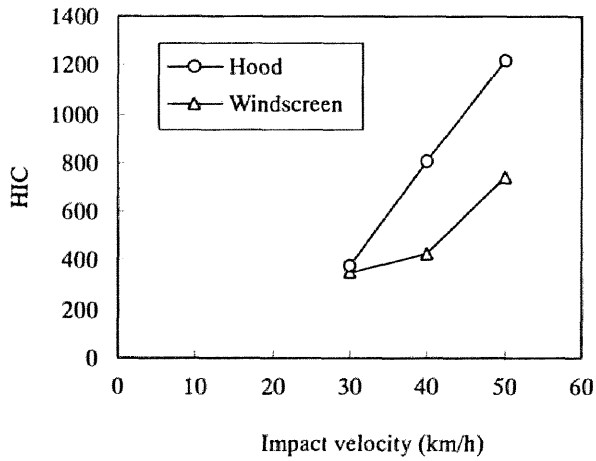

Figure 5.27. The effect of the impact velocity on the HIC for the tested car.

5.4.3. HIC and Dynamic Deformation

The deformation necessary to keep the HIC below 1000 is important in order that a car may be designed to reduce the likelihood of pedestrian head injuries. MacLaughlin et al. (1990) found in headform impact tests onto the hood top (37 km/h) that the HIC is related to the dynamic deformation. Their study was concerned only with the hood top, and this relation has not been analyzed theoretically. In the following, this relation was examined based on theoretical analysis as well as impact tests for the windscreen and the hood top.

Theoretical HIC

Here we examine the relation between the HIC and dynamic deformation based on the approximation of the acceleration curve. Let the deceleration-time history of the headform $\alpha(t)$ [m/s^2] be approximated based on the curve of second degree of time t (see Figure 5.28):

$$\alpha(t) = -a\,t\,(t - 2t_0) \tag{4.1}$$

where a is coefficient for curve fitting, and t_0 is the time when the deceleration becomes a maximum.

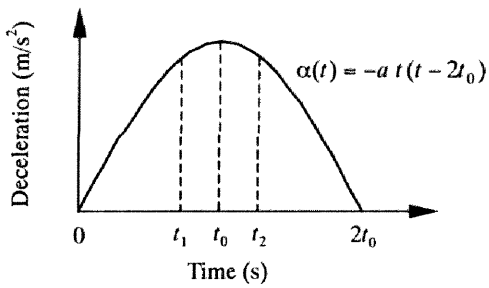

Figure 5.28. The model of headform deceleration.

The velocity of the headform impactor $v(t)$ [m/s] is given by:

$$\begin{aligned} v(t) &= v_0 + \int_0^t a\,t'(t' - 2t_0)\,dt' \\ &= v_0 + \left(\frac{t^3}{3} - t_0 t^2\right) a \end{aligned} \tag{4.2}$$

where v_0 is initial velocity. The velocity becomes zero when $t = t_0$. Thus using Eq. (4.2), the coefficient a is expressed using v_0 and t_0 as follows:

$$a = \frac{3v_0}{2t_0^3}. \tag{4.3}$$

Integration of Eq. (4.2) yields the displacement of the impactor $x(t)$ [m]:

$$x(t) = v_0 t + \left(\frac{t^4}{12} - \frac{t_0 t^3}{3} \right) a \tag{4.4}$$

The displacement has a maximum x_d [m] when $t = t_0$:

$$x_d = x(t_0) = v_0 t_0 - \frac{t_0^4}{4} a = \frac{3}{8} v_0 t_0 \tag{4.5}$$

According to its definition (see Eq. (2.14)), the HIC is calculated using deceleration as follows:

$$\mathrm{HIC} = \max_{0 \le t_1 \le t_2 \le 2t_0} \left[\left\{ \frac{1}{t_2 - t_1} \int_{t_1}^{t_2} \frac{\alpha(t)}{g} dt \right\}^{2.5} (t_2 - t_1) \right] \tag{4-6}$$

where g is the acceleration of gravity (=9.81 m/s^2). By introducing the variable $\tau = t - t_0$, the HIC can be computed as follows:

$$\mathrm{HIC} = \max_{0 \le t_1 \le t_0} \left[\left\{ \frac{1}{t_1} \int_0^{t_1} \frac{a(\tau^2 - t_0^2)}{g} d\tau \right\}^{2.5} (2t_1) \right] \tag{4.7}$$

$$= \sqrt{2} \left(\frac{5}{6} a \right)^{2.5} t_0^6 . \tag{4.8}$$

By using Eqs (4.3), (4.5) and (4.8), the relation between the HIC and dynamic deformation is obtained as:

$$\mathrm{HIC} = 2^{-9} 3^{1.5} 5^{2.5} g^{-2.5} v_0^4 x_d^{-1.5} = 0.001882 v_0^4 x_d^{-1.5} . \tag{4.9}$$

We call this calculated value the *theoretical HIC*. The theoretical HIC increases markedly with velocity (v_0), and decreases with dynamic deformation (x_d). The HIC value is below 1000 if

$$x_d > 0.0934 \text{ m} \tag{4.10}$$

Based on this analysis, a dynamic deformation of 93.4 mm can make the HIC value less than the injury threshold.

Experimental Results

The HIC results obtained from the headform impact test onto the car body (excluding the windscreen) and windscreen are shown as a function of dynamic deformation in Figure 5.29. The HIC correlates well with the dynamic deformation of the car body and windscreen. The HIC of the windscreen is larger than that of the car body. This tendency is apparent for HIC values below 3000. It can be considered that the high HIC of the windscreen is due to the inertial spike of the acceleration in the initial phase. Figure 5.29 also shows that the theoretical HIC calculated using Eq. (4.8) agrees with the headform test results.

The approximation curves were calculated for the windscreen and the car body and are shown in Figure 5.29. Based on these approximation curves, a HIC value of 1000 is associated with a dynamic deformation value of 76 mm for the car body, and 89 mm for the windscreen, respectively. In order to reduce the HIC below 1000, dynamic deformations greater than those values are necessary.

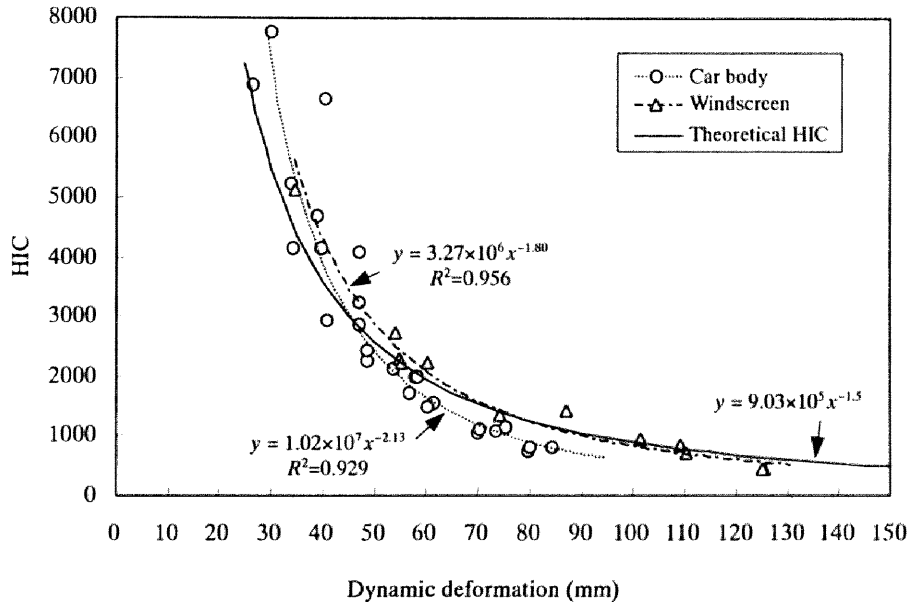

Figure 5.29. HIC versus dynamic deformation in headform impact tests for tested car (40 km/h).

5.5. DISCUSSION

The injury risks to the pedestrian were examined based on the accident analyses, simulations and impact tests. From the accident analysis using macro data, it was shown that the shapes of the vehicle have a large influence on injury risk of the pedestrian. When the pedestrians are struck by bonnet-type cars, the pedestrians tend to have serious injuries to their legs. In impact against vans, the pedestrians are at high risk to serious and fatal injury to the heads and thoraxes. The probability of severe injuries to the pedestrian is higher for a van than for a bonnet-type car.

Accident analysis using micro data indicated that when the pedestrians are struck by bonnet-type cars, severe head injuries are caused by the A pillar, the windscreen close to the frame and the hood. Stiff structures such as the windscreen frame and the A pillar have a high potential to cause serious injury to the head which can cause skull fracture in addition to brain injury. In van-pedestrian impacts, the windscreen frame and front panel can induce severe head injuries. The energy absorption characteristics of these structures should be examined for reduction of severe head injuries. It was also confirmed from the micro data that the probability of severe injuries to the pedestrian is higher for a

van than for a bonnet-type car. One reason for this high injury risk is that the pedestrian head is apt to hit the stiff structures like the windscreen frame and the frame in the front panel in impact against a van.

From the mathematical simulations, it was elucidated that the pedestrian behavior is influenced by the vehicle shape. Consequently, the impact locations and velocities of the pedestrian's body vary. The injury risks are compared for two opposite vehicle shapes of a bonnet-type car and a van. The acceleration of the upper leg is high in bonnet-type car impacts, while that of the chest and HIC is high in van impacts. These results agreed with accident analysis for body regions likely to be injured by these vehicle types.

Based on the micro accident data, the impact locations of the pedestrian head have been found to have shifted from the car front towards the windscreen area because of the short and steep bonnets of the modern cars. Therefore, the headform impact tests were also carried out for various locations of the car including the windscreen. The cowl, rear hood, hood/fender and A pillar produced high HIC values. The HICs were extremely high at the hood hinge and hood stopper. The windscreen center produces low HIC even at a high velocity of 50 km/h, whereas the HIC value becomes high for the windscreen close to the frame. Thus, for reduction of the likelihood and the severity of the head injury, it can be effective to design a car so that the pedestrian head contacts the windscreen center region in the case of an accident.

The dynamic deformation required for a HIC value below 1000 is 76 mm for the car body, and 89 mm for the windscreen. However, it will be difficult to ensure this deformation for stiff parts of the car such as the A pillar, cowl and windscreen boundary. One feasible solution will be to design a car body so that the pedestrian head does not contact these regions on impact. For example, it is possible that the cowl and windscreen frame be covered by the hood panel, and the A pillar is located to the side and rear compared with the current car.

Accident analysis using macro data indicated that in impact with a mini car, the head injury risk to the pedestrian is high (see Figure 5.3). This high injury risk to the head could not be reproduced by the mathematical simulation because the head made contact with windscreen. The headform impact tests showed that the HIC values are high near the windscreen boundary. As the mini car has a small windscreen area, the pedestrian has a high risk of contact onto the windscreen boundary. In particular, the head of shorter pedestrians can make contact with the lower windscreen region. This could be the reason for high injury risk to the pedestrian head in accidents with mini cars.

6. CONCLUSIONS AND REMARKS

6.1. GENERAL DISCUSSION

We will now carry out a general discussion on the total compatibility based on the results obtained in this study.

Self-protection of the car has been considered to be most important in injury control strategies, and it has saved many lives. However, since seatbelts and airbags have been installed in cars, it will be difficult to make significant improvement of self-protection. On the other hand, partner-protection is a new concept for an injury control strategy and has great potential to reduce the total number of fatalities. Therefore, compatibility should be one of the injury control strategies. From Chapter 4, comparison of the accident data between 1989 and 1997 shows that, though the level of self-protection of the passenger has improved, partner-protection remains at the same level. This concept of partner-protection can be applied not only in car-to-car collisions but also in car-to-truck collisions and pedestrian impacts.

Due to the different fleet of vehicles, the compatibility situation varies from country to country. In the US, the aggressivity of the LTV is the most important. However, according to the results of Chapters 2 and 3, the low self-protection of the mini car and high aggressivity of the truck is the most significant problem in Japan. Therefore, different strategies are necessary for compatibility in each country.

In Japan, mini cars occupy about 14% of the passenger car market, and this ratio is increasing. If all drivers of mini-passenger cars were to trade their current cars for small cars weighing 701-800 kg, the number of drivers seriously and fatally injured in car-to-car frontal collision accidents would fall by 108 from 2,645 per year, based on a calculation in Section 2.5 using the numerical distribution of passenger cars. Considering the economical side of the problems, it seems to be reasonable that mini cars should be made safer and compatible with large cars rather than replacing them with small or medium cars.

In two-vehicle collisions, mass difference has the largest effect on the compatibility, however, modification of stiffness and restraint system can reduce this incompatibility. The size of cars also affects the injury risk to the driver due to compartment intrusion. Geometry incompatibility can make the improvement of the stiffness and restraint system invalid. Thus, the geometry incompatibility is also a basic factor for consideration.

There may be two methods for improving the compatibility of the mini car according to the simulation presented in Chapter 2. The first method is to stiffen the mini car along with an optimized restraint system. Though this stiff mini car accomplishes a high level of self-protection, some side effects should be considered when introducing such a car. Due to the high acceleration of this type of a

car, the injury risk to the driver will be higher when the cars are involved in a collisions beyond the concept of the design, i.e. out-of-position occupants, unbelted drivers and elderly drivers. As was pointed out in Section 2.3, in the case where the airbag does not deploy, like a low velocity crash or oblique crash, the driver in this stiff mini car is at higher risk to injury than an ordinary mini car. The aggressivity of this stiff mini car should also be considered. The injury risk to the pedestrian can be high. Based on the headform impact, it was found that the dynamic deformation of 89 mm is necessary for the head injury risk to be less than the injury threshold. Even for a mini car, this crush space can be fitted under the hood. Designing a car with a large windscreen area can also reduce the injury risk to the pedestrian.

The second method is to improve the partner-protection of the large car which collides with a mini car. A large car should become less-stiff in order to enhance the partner-protection. This situation will reduce the driver injury risk in a large car for a single car crash to within the range of crash severity where the compartment intrusion is small. However, in severe crashes where the intrusion becomes large, the injury risk to the legs of the driver in a large car can be high. This injury risk can be controlled more easily than that of the mini car.

The partner-protection of the road environment should be modified to protect the drivers in mini cars as well as large cars. It is effective for the reduction of the driver injury risk in a single car crash if the roadside objects absorb sufficient energy to prevent compartment intrusion into the car. Not only should the guardrail be installed around stiff slender objects such as bridge structures and walls, but also the energy absorption of the guardrail has to be improved because guardrails are not optimized for this purpose.

Since the current test procedures of crashes into a fixed barrier are designed to evaluate the self-protection of the car, we found in Chapter 3 that they cannot evaluate the compatibility of the car, even if the impact velocity is varied. In order to evaluate the compatibility performance correctly, it is necessary that the MDB crash test procedure is introduced. Based on this test procedure, the self- and partner-protection of the vehicle should be evaluated. If the performances of self- and partner-protection is within a certain range, the vehicles with extremely low self-protection or high aggressivity will be eliminated.

Although vehicle mass has little effect in the crash test into a fixed barrier, the simulation and test results in Chapter 3 showed that it has a large effect on the injury parameters of the driver dummy in the MDB crash test. Therefore, this test procedure has the possibility to change the size of cars in the car population, especially when the injury risks to the drivers in mini cars are passed on to users via the NCAP tests. Accordingly, it is important to decide the levels of self and partner-protection in this test procedure. The limits of the minimum and maximum sizes of the cars depend on these levels. One strategy is to fix the levels of self and partner-protection based on the average car like a medium sedan. As the number of the average cars is the largest, modifications will be necessary mainly for mini and large cars. To get the same levels of self- and partner-protection as the average car, a mini car can be stiffened and incorporate an optimum restraint system and the stiffness of the large car can be reduced.

As this level will be decided on the current average car, the size of mini cars will be larger and that of large cars will be smaller.

Another strategy is to decide the compatibility levels based on the mini cars. Small, medium and large cars should include crush space for a mini car. However, for a car designed based on this strategy, it will be difficult to ensure self-protection in a crash with a truck. In this strategy, it is necessary to separate the traffic flow between cars and trucks which is not realistic. Considering the total cost and benefits, it will be reasonable to design cars based on the first strategy where all cars have a similar level of self- and partner-protection to that of the current average car.

As was described in Chapter 4, since the outcome of car-truck collisions are sometimes so severe and there are a large number of deaths in these collisions, the improvement of truck aggressivity may be most effective for reducing the total number of fatalities. The aggressivity of the truck also has to be reduced not only for the mini car but also for the less-stiff large car that was found to be more compatible with the mini car. However, JAMA introduced the guidelines on full rigid barrier crash tests for the truck, which may lead to stiffer front structures of the truck. Only self-protection of the truck is considered in that guideline, therefore, the geometry of the truck will not be improved. This kind of crash test will lead to a low level of partner-protection. The total compatibility can not be accomplished unless all the vehicles are designed considering the compatibility of the average car.

In designing a compatible vehicle, the pedestrian protection also has to be considered. Pedestrian kinematics are affected by vehicle shape, and the injury risk is also affected by vehicle shape as well as the vehicle stiffness. As the HIC values in contact with the windscreen are low except close to the frame, designing a car so that the pedestrian head hits this area will be effective for reducing the injury severity of the pedestrian. Thus, a wide windscreen area is recommended. This kind of design can also be useful for protection of cyclists.

In the traffic situation in Japan, compatibility can be improved significantly by introducing stiff mini cars with optimum restraint systems, large cars and trucks with low aggressivity, and vehicles with pedestrian protection.

6.2. CONCLUSIONS

There have been many research projects which investigate vehicle compatibility. However, they were based only on one method such as accident analysis or computer simulation. Accident analysis makes the current situation clear. From computer simulation, it is possible to examine the injury risk, injury mechanism and its countermeasures. In order to examine and understand the vehicle compatibility, both accident analysis and computer simulation should be performed.

This thesis discussed the total compatibility of cars, trucks and pedestrian for various crash configurations by using accident analyses, experiment and computer simulations. It was found from

accident data that in Japanese traffic, the mini car and the truck have the most significant problems of compatibility.

Mathematical models to evaluate the vehicle compatibility in car-to-car, car-to-truck and car-to-pedestrian impacts were developed. By using these models, the injury risk to the driver could be clarified in various crash configurations where the influences of acceleration and intrusion are large. The injury risk to the pedestrian was also investigated using mathematical simulations.

The main results of each chapter can be summarized as follows:

In Chapter 1, the literature of vehicle compatibility was reviewed. The vehicle compatibility should be investigated in each country since the vehicle compatibility is related to vehicle size and population.

In Chapter 2, by the use of the accident data, the aspects of car compatibility in Japan were discussed for car-to-car frontal, side and single-car collisions. By using computer simulations, it was found that a high injury risk to the driver in a mini car was related to its high acceleration and large intrusion, and furthermore countermeasures to improve the compatibility of a mini car were proposed. The results of the analyses are summarized as follows:

(1) From accident analysis, the absolute injury rate of the driver in car-to-car frontal collisions was formulated using the average mass of the car. A car with a mass of 1150 kg is the most compatible among the current car population in Japan. This compatible car mass coincides with the average mass of cars.

(2) In car-to-car frontal and side collisions, the SUV and the mini car are the least compatible car types with high and low aggressivity to other cars, respectively. The medium sedan and the wagon are considered compatible cars in car-to-car frontal and side collisions.

(3) A mathematical model that can evaluate the effect of acceleration- and intrusion-related injury parameters of the driver was developed. This model was found to be useful to evaluate the compatibility of the car.

(4) Simulations to investigate the safety of the driver in a mini car were performed by using MADYMO for crashes into a rigid barrier and into a large car. The crash test of a mini car into a rigid barrier was found to be insufficient to assure the safety in a crash into a large car. This is because in a crash into a rigid barrier the acceleration greatly influences the risk of injury to the driver of a mini car, whereas in a crash with a large car the effect of intrusion as well as acceleration is large.

(5) The countermeasures for the safety of the mini car in car-to-car frontal collisions were suggested based on MADYMO simulations. Firstly, the combination of the restraint systems in conjunction with high stiffness of the mini car provides good protection for the driver in either crashes into a rigid barrier or into a large car. Secondly, when a large car has additional crush space, it is

effective for reduction of the injury risk to the driver in the mini car in both cases where a mini car is stiff and less-stiff.

(6) The guardrail is the most compatible fixed object struck by a single car. It can reduce the fatality rate on the prefecture roads by about 60%. If the other fixed objects in the road environment are equipped with a guardrail, many drivers' lives could be saved.

In Chapter 3, crash test procedures to evaluate the compatibility of the car in car-to-car frontal crashes were examined from accident analysis, computer simulations and crash tests. The results are summarized as follows:

(7) Based on the accident data, the overlap ratio of 40% of the car and impact angle of 0 degrees are recommended to evaluate the risk of serious injuries to the driver in car-to-car frontal collisions in Japan.

(8) According to the data of the NCAP test, it was confirmed that a full rigid barrier crash test and an offset deformable crash test can evaluate the different features of crashworthiness. The acceleration-related injury parameters in the full rigid barrier crash test are proportional to those in the offset deformable crash test, whereas the intrusion-related injury parameters are in inversely proportional.

(9) From the MADYMO simulations, it was found that the single-crash car test, such as the full and offset barrier crash, can not evaluate the injury risk to the driver in car-to-car collisions, even though the impact velocity is changed according to car mass. Only the MDB crash test procedures will be able to reproduce the injury risk of the driver in car-to-car collisions.

(10) The MDB crash test was carried out by using a small car at a velocity of 112 km/h. Both acceleration and intrusion-related injury parameters of a driver in the small car become large. These values are higher than those in a full rigid barrier crash and an ODB crash tests using the same type of car.

In Chapter 4, the aggressivity of the truck caused by the mass and the geometry difference was evaluated for Japan traffic situations. To reduce the aggressivity of the truck, the front underrun guard of the truck was examined using a mathematical simulation. The conclusions are as follows:

(11) In a car-to-truck collision, when the truck mass is less than 5 tons, the injury risk of the driver in passenger cars increases with the truck mass. When the truck mass is more than 5 tons, this injury risk does not change much.

(12) The aggressivity of the large truck was estimated to be very high in terms of the vehicle itself and the human factors. This situation has not changed since 1989. Only self-protection of passenger cars has been improved. In Japan, the high aggressivity of the truck and the poor self-protection of the mini car should be considered in seeking to obtain the total compatibility in vehicle-to-vehicle collisions.

(13) In many car-to-truck collisions, the frame of the truck does not make contact with the car because the overlap ratio of the truck is less than 1/3. The cars are apt to underide the truck due to the stiffness and the height difference of the bumper.

(14) In order to improve truck aggressivity, the effect of the underrun guard was examined by using a simulation. Stiffness effect analysis of the underrun guard showed that there is an optimal force level that can minimise the deceleration, deformation and injury risks to the driver of the mini car. It should be noted that this optimum force level depends on the crash velocity.

In Chapter 6, the compatibility between vehicle and pedestrian was examined based on the accident analyses, simulations and impact tests.

(15) From accident analysis, it was found that when the pedestrians are struck by bonnet-type cars, the pedestrians tend to sustain serious injuries to their legs. In impact with vans the pedestrians are at high risks of serious and fatal injury to their head and thorax. The probability of severe injuries to the pedestrian is higher for a van than for a bonnet-type car. This is because in van-pedestrian impacts, the head of the pedestrian hits a stiff location such as the windshield frame and A pillar.

(16) Accident analysis showed that the impact locations of the pedestrian head are now shifted from the car bonnet to the windscreen area. The windscreen does not cause serious injury to the pedestrians head. The stiff structures such as the windshield frame and A pillar have a high potential to cause serious head injury.

(17) The mathematical simulation showed that the acceleration of the upper leg was found to be high in a bonnet-type car impact, while that of the chest and the HIC is high in a van impact. These results are consistent with accident analysis for body regions likely to be injured by these vehicle types.

(18) Based on the results of the headform impact tests, the HIC value was found to be high at the hood hinge, hood stopper and A pillar. The distribution of the HIC value in the windscreen was obtained from this test.

(19) The relation between the HIC and dynamic deformation was formulated based on the approximation of the acceleration curve. This result was confirmed by impact tests. In order to reduce the HIC below 1000, dynamic deformations greater than 89 mm are necessary for the windscreen and greater than 76 mm for the car body.

(20) For reduction of the likelihood and the severity of the head injury, it is effective to design a car so that the pedestrian head make contact with the windscreen center region.

This thesis clarified the importance of partner-protection as well as self-protection for compatibility. Increasing the number of compatible vehicles in Japan seems to be the most effective strategy for significant reduction of traffic fatalities and injuries in the future.

ACKNOWLEDGEMENTS

This research was carried out at the Department of Mechanical Engineering, Graduate School of Engineering, Nagoya University, Nagoya, Japan, as well as the Traffic Safety and Nuisance Research Institute, Japanese Ministry of Transport. I would like to thank everyone who has helped and supported me throughout this research, especially:

Dr. Janusz Kajzer, Visiting Professor, Department of Mechanical Engineering, Graduate School of Engineering, Nagoya University, my supervisor, for his enlightening supervision and stimulating discussion throughout my study;

Professor Sumio Murakami, Department of Mechano-Informatics and Systems, Graduate School of Engineering, Nagoya University, for his encouragement, and for giving me the opportunity of studying at the Nagoya University.

Professor Eiichi Tanaka, Department of Mechanical Engineering, Graduate School of Engineering, Nagoya University, for his valuable suggestions and discussions throughout my study.

Professor Nobutada Ohno, Department of Micro System Engineering, Graduate School of Engineering, Nagoya University, for reviewing this thesis and for his helpful suggestions.

Mr. Sota Yamamoto, Research Associate, Department of Mechanical Engineers, Nagoya University, for his support and kindness.

Dr. Hirotoshi Ishikawa, Project manager, Japan Automobile Research Institute, for introducing me to study under the direction of Professor Dr. Kajzer, and also for his suggestions on this thesis.

Mr. Yoshihiro Nanto, Director General, Traffic Safety and Nuisance Research Institute, Japanese Ministry of Transport, for his suggestions and kindness, for encouraging me to go to the Nagoya University.

Mr. Atsunari Hirota, Director, Automotive Technology Division, Traffic Safety and Nuisance Research Institute, Japanese Ministry of Transport, for his advice in the field of car safety.

Mr. Hideki Yonezawa, Senior Research Engineer, Traffic Safety and Nuisance Research Institute, Japanese Ministry of Transport, for his suggestions and support.

Mr. Haruo Omae, Project manager, Japan Automobile Research Institute, for fruitful discussions of crash tests.

Mr. Yoshiji Kadatani, Honda R&D CO., LTD., for the discussion and suggestion on the subject of vehicle compatibility.

Ms. Satoko Ito, Institute for Traffic Research and Analysis, for her favour and suggestions for accident data collection.

Dr. Andrew Sowdon, Ship Research Institute, Japanese Ministry of Transport, for kind revision of the English text of this thesis.

REFERENCES

Adalian, C., Russo, J, Césari, D., Desfontaines, H., "Improvement of Car-to-Truck Compatibility in Head-on Collisions, 16th ESV, Paper Number 98-S4-O12, 1998.

Akiyama, A., Yoshida, S., Matsuhashi, T., Rangarajan, N., Shams, T., Ishikawa, H., Konosu, A., "Development of Simulation Model and Pedestrian Dummy", SAE Paper 1999-01-0082, Advances in Safety Technology 1999, 1999.

Aldman, B., Gustaffson, H., Nygren, A., Tingvall, C., Wersall, J., "Injuries to Car Occupants – Some Aspects of the Interior Safety and Cars", Folksam, Stockholm, 1984.

Appel, H., "Optimal Deformation Characteristics of Front Rear and Side Structure of Motor Vehicles in Mixed Traffic", 2nd ESV, 1971.

Appel, H., "Compatibility, Guideline for Passive Safety, for Active Safety and Even for the Total Transportation System, FISITA 1996.

Banthia, V. K., Miller, J. M., Valisetty, R. R, Winter, E.F.M, "Lightweighting of Cars with Aluminum for Better Crashworthiness", SAE Paper 930494.

Bloch J A., "Introduction of Compatibility in the Development of a Frontal Impact Test Procedure", 14th ESV, Paper Number 94-S4-O15, 1994

Bloch J A., Chevalier M C., "In-Depth Analysis of Offset Frontal Crash Tests in view of External Aggressivity", 14th ESV, Paper Number 94-S4-O15, 1996.

Buzeman, D., "Car Compatibility in Frontal Crashes", Thesis for the degree of Doctor in Philosophy, Chalmers University of Technology, Göteborg, Sweden, 1998a.

Buzeman, G. D., Viano, C. D., Lövsund. P., "Injury Probability and Injury Risk in Frontal Crashes: Effects of Sorting Techniqes on Priorities for Offset Testing", Accident Analysis and Prevention, Vol. 30, No. 5, pp. 583-595, 1998b.

Cameron, M., Mach, T., Neiger, D., Graham, A., Ramsay, R., Pappas, M., Haley, J., "Vehicle Crashworthiness Ratings from Victoria and New South Wales Crash Data", Road & Transport Research, Vol. 1, No.3, 4-18, 1992.

Campbell, B. J., Reinfurt, D. W., "Relationship between Driver Crash Injury and Passenger Car Weight", Highway Safety Research Centre, University of North Carolina, Chapel Hill, North Carolina, 1973.

Cavallero et al.: Improvement of Pedestrian Safety: Influence of Shape of Passenger Car-Front Structures Upon Pedestrian Kinematics and Injuries", SAE Paper 830624, 1983

Chillon, G., "The Importance of Vehicle Aggressiveness in the Case of a Transversal Impact", 1st ESV, 1971.

Dalmotas, D. J., "Injury Mechanisms to Occupants Restrained by Three-Point Seat Belts in Side Impacts", SAE Paper 830462, 1983.

Deloffre, P., Dubos, A., Muhlke, C., "Crash Compatibility of the Renulat Vehicle Range: Application of Numerical Simulation to a Car to Truck Front Crash", F98T130, FISITA, 1998.

EEVC, "Proposal for Methods to Evaluate Pedestrian Protection for Passenger Cars", EEVC Working Group 10 Report, 1994.

EEVC, "Improved test methods to evaluate pedestrian protection afforded by passenger cars", EEVC Working Group 17 Report, 1998.

Emori, I., "Analytical approach to automobile collisions", SAE Paper 680016, Society of Automotive Engineers, 1968.

Ernst, G. Brühning, E., Glaeser, K.P., Schmid, M., "Compatibility Problems of Small and Large Passenger Cars in Head-on Collisions", 13th ESV, 91-S1-O-12, 1991.

Evans, L., "Car mass and Likelihood of Occupant Fatality", SAE Paper 82007, Society of Automotive Engineers, 1982.

Evans, L., "Accident Involvement Rate and Car Size", General Motors Research Laboratories, Research Publication GMR-4453, Michigan, USA, 1983.

Evans, L., Waisielewski, P.F., "Serious or Fatal Driver Injury Rate Versus Car Mass in Head-on Crashes between Cars of Similar Mass", Accident Analysis and Prevention 19, pp.119-131, 1987.

Evans, L. and Frick, M., C.: "Driver Fatality Risk in Two-Car Crashes – Dependence on Masses of Driven and Striking Car," 13th ESV, 1991a.

Evans, L., *Traffic Safety and the Driver*, Van Nostrand Reinhold, New York, 1991b.

Evans, L. Frick, M. C., "Car mass and fatality risk – has the relationship changed?", 36th Annual Proceedings Association for the Advancement of Automotive Medicine, October 5-7, Portland, Oregon, AAAM, pp. 83-93, 1992a.

Evans, L. and Frick, M. C., "Car size or mass – which has greater influence on fatality risk?", American Journal of Public Health Vol. 82,. 1992b, pp. 1105-1112.

Evans, L., "Light versus heavier vehicles: increased weight equals increased safety", Search, Vol. 27, No. 2, General Motors Research Laboratories, Michigan, USA, 1-4, 1992c.

Evans, L. and Frick, M. C., "Mass Ratio and Relative Driver Fatality Risk in Two-Vehicle Crashes". Accident Analysis & Prevention. Volume 25, No.2,. pp. 213–224, 1993.

Evans, L., "Driver Injury and Fatality Risk in Two-Car Crashes Versus Mass Ratio Inferred Using Newtonian Mechanics". Accident Analysis & Prevention. Volume 26. No. 5. pp. 609-616, 1994.

Filders, B. N., Lee, S. J., Lane J. C., "Vehicle Mass, Size and Safety", Report No. CR 133, 56p, Federal Office of Road Safety.

Fontaine, H., "Car Characteristics and Safety", VTI Rapport, 380A, 106-18, 1992.

Frei, P., Kaeser, R., Hafner, R., Schmid, M., Dragon, A., Wingeier, L., Muser H, M., Niedere, F., P., Waltz, H, F., "Crashworthiness and compatibility of low mass vehicles in collisions", SAE Paper 970122, 1997.

Gabler, C. H. and Hollowell, T. W., "NTHSA's Vehicle Aggressivity and Compatibility Research Program", 16th ESV, Paper Number 98-S3-O-01, 1998.

Grime G., Hutchinson T. P., "The Influence of Vehicle Weight on the Risk of Injury to Drivers", 9th ESV, 1982.

Hackney, J. R., Kahane, C. J., Chan, R., "Activities of the New Car Assessment Program in the United States, " 15th ESV, 1996.

Harris, J., "A Study of Test Methods to Evaluate Pedestrian Protection for Cars", 12th ESV, pp. 1217-1225, 1989.

Higuchi, K., Akiyama, A., The Effect of the Vehicle Structure's Characteristics on Pedestrian Behavior, 13th ESV, 1991.

Huddon, W., Baker, S., Injury Control. In: Clark, D., MacMahon, C. (edis), Preventive and Community Medicine, Little Brown and Co., 1981.

IHRA Pedestrian, Current Situation of Pedestrian Accident in Japan, 1997.

IIHS, "Crashworthiness", Brochure on frontal offset crash test performance, Insurance Institute for Highway Safety, North Glebe Road, Arlington, VA, November 1995.

IIHS, Crash Test Report, 1997.

IIHS, Status Report, "Crash Compatibility", Vol. 33, No. 1, February 14, 1998.

Injury in America: A Continuing Pubic Health Problem. Washington, DC: Committee on Trauma Research, Commission on Life Siences, National Research Council and Institute of Medicine, 1985.

IRF, *World Road Statistics*, Geneva, International Road Federation, 1995.

Ishikawa, H., "Kinematics of Automobile Collision – Analytical Formulars for One Dimensional Impact", Journal of Japan Automobile Research Institute, Inc., Vol. 12, No. 10, p.25-32, 1990 (in Japanese).

Ishikawa, H., Yamazaki, K., Ono, K. Sasaki, A., "Current Situation of Pedestrian Accidents and Research into Pedestrian Protection in Japan", 13th ESV, pp. 281-293, 1991.

Ishikawa, H., "Impact Model for Accident Reconstruction", SAE Paper 930654, Society of Automotive Engineers, 1993a.

Ishikawa, H., Kajzer, J., Schroeder, G., "Computer Simulation of Impact Response of the Human Body in Car-Pedestrian Accidents", SAE Paper 933129,1993b.

Ishikawa H., Digges, K., Ennis J., "Restitution coefficients and delta-V in offset frontal collisions", Proceeding of JSAE Autumn Convention, 9540075, Beppu, Society of Automotive Engineers of Japan, 1995 (in Japanese).

ISO, Road Vehicles – Frontal fixed barrier or pole impact test procedure, ISO/DIS 3560, TC22/SC10/WG1 N422, 1998

ISO, Compatibility Testing Procedure, ISO/TC22/SC10/WG1 N440, 1999.

ITARDA, *The Analysis Result of Relationship between Traffic Accident, Driver and Vehicle*, 1996 (in Japanese).

ITARDA, *Report of In-Depth Accident Analysis, 1996 Edition* 1997 (in Japanese).

ITARDA, *Statistics of Traffic 1997 Edition*, 1998 (in Japanese).

ITARDA, Traffic Safety and Nuisance Research Institute, Nagoya University, *Reduction of Injury Severity of Pedestrians in Vehicle-Pedestrian Accidents*, Report of Joint Research, ITARDA, 1999a (in Japanese).

ITARDA, *Report of In-Depth Accident Analysis, 1997 Edition* 1999b (in Japanese).

Joksch, H. C., Thoren S., "Car Size and Occupant Fatality Risk, Adjusted for Differences in Drivers and Driving Conditions, CEM Report 4308-754, Foundation for Traffic Safety, 1984.

Joksch, H. C., "Velocity Change and Fatality Risk in a Crash – a Rule of Thumb", Accident Analysis & Prevention. Volume 25. No. 1. pp. 103-104, 1993.

Joksch, H., Massie D., Pichler, R., "Vehicle Aggressivity: Fleet Characterization Using Traffic Collision Data", National Highway Traffic Safety Administration, DOT HS 808 679, 1998.

Kaeser R., Walz H., F., Brunner, A., "Collsion safety of a hard shell low mass vehicle", International Conference on Biomechanics of Impacts (IRCOBI), Verona, 1992.

Kaeser, R., Muser, M. Spiess, O., Frei, P., Guenat, M. J. Wingeier, L., "Passive safety potential of low mass vehicles", International Conference on Biomechanics of Impacts (IRCOBI), Brunnen, 1995.

Kahane, C. J., Hackney, J. R., Berkowitz, A. M., "Correlation of Vehicle Performance in the New Car Assessment Program with Fatality Risk in Actual Head-on Collisions", 14th ESV Conference, pp. 1388-1403, 1994.

Kahane, C. J., "Relationship between Vehicle Size and Fatality Risk in Model Year 1985-93 Passenger and Light Trucks", DOT HS 808 570, 1997.

Kallina, I., "Aspects of Car Crash Safety", The 5th Daimler-Benz Seminar, Tokyo, November, 1998.

Krafft M., Nygren C., Tingvall C., "Rear Seat Occupant Protection. A Study of Children and Adults in the Rear Seat of Cars in Relation to Restraint Use and Car Characteristics", 12th ESV, p. 1145-9, 1989.

Kubota, M., Kokubu Yoshiharu, "Crash Energy Absorption Characteristics Classified by Front Shapes of Vehicles", Journal of Japan Automobile Research Institute, Inc., Vol. 17, No. 1, pp.19-22, 1995.

Lowne, R. W., "EEVC Working Group 11 Report on the Development of a Frontal Impact Test Procedure", 14th ESV, 1994.

MacLaughlin, T. F., Kessler, J. W., "Test Procedure – Pedestrian Head Impact Against Centeral Hood", SAE Paper No. 902315, Society of Automotive Engineers, 1990.

Management and Coordination Agency of Japan, Statistics Bureau and Statistics Center, *Japan Statistics*, 1997 (in Japanese).

Marumo, N., Aya, N., Takahashi, K., Nosho, H., "Compatibility between Different-Sized Vehicles on Crash Survivability", 3rd ESV, 1974.

Matsumoto H., Sakaida M., Kurimoto K., "A parametric evaluation of vehicle crash performance", SAE Paper 900465, Society of Automotive Engineer, 1990.

Mendis, K., Mani, A., "Concept to Reduce Heavy Truck Aggressivity in Truck-to-Car Collisions, 15th ESV, Paper Number 96-S4-O-14, 1996.

Mertz, H. J., Injury Assessment Values Used to Evaluate Hybrid III Response Measurements, NHTSA Docket 74-14, Notice 32, 1984.

Ministry of Transport, ASV Phase 2 (1996-2000), 1997.

Mizuno, K., Yonezawa, H., "The Effect of Vehicle Mass in Car-to-Car Collisions", SAE Paper 960441, Society of Automotive Engineers, 1996.

Morris, A. et al., Mechanisms of Fractures in Ankle and Hind-Foot Injuries to Front Seat Car Occupants, SAE Paper 973328, Society of Automotive Engineers, 1997.

Muser, M., Krabbel, G., Prescher, V., Dragon, A., Walz, F., Nieder, P., "Advanced energy absorbing components for improved effectiveness of low mass vehicle restraint systems", International Conference on Biomechanics of Impacts (IRCOBI), Dublin, 1996.

NHTSA, "Pedestrian Injury Reduction Research", Report to the Congress, 1993.

NHTSA, "Report on International Harmonized Research Agenda", Proceedings of 15th International Technical Conference on Enhanced Safety Vehicles, DOT HS 808 465, pp. 2082－2124, 1996.

NHTSA, "Status Report on Establishing a Federal Motor Vehicle Safety Standard for Frontal Offset Crash Testing", Report to Congress, 1997.

NHTSA, "Overview of Vehicle Compatibility/LTV issues", DOT HS 808 689, NHTSA, 1998.

O'Neill, B., Lund, A. K., Zuby, D. S., Preuss, C. A., "Offset Frontal Impacts – A comparison of Real World Crashes with Laboratory Tests, 14th ESV Conference, Paper No. 94-S4-O-19, 1994.

Otsubusin, A., Green, J., "An Analytical Assessment of Pedestrian Head Impact Protection", 16th ESV, Paper Number 98-S10-W17, 1998.

Partyka, S. C., "Registration-based Fatality Rates by Car Size from 1978 through 1987", NHTSA, report DOT HS 807 444, pp. 45-72, 1989.

Planath-Skogsmo, I., Nilsson, R., "Frontal Crash Tests – A Comparison of Method", 38th Stapp Car Crash Conference Proceedings, 1994.

Prasad, P., Smorgonsky, L., "Comparative Evaluation of Various Impact Test Procedures", SAE Paper 950646, Society of Automotive Engineers, 1995.

Ragland L. C., "Offset Test Procedure Development and Comparison", 16th ESV, Paper Number 98-S1-O03, 1998.

Ragland C., Dalrymple G., "Overlap Car-to-Car Tests Compared to Car-to-Half Barrier and Car-to-Full Barrier Tests", 13th ESV Conference, Paper No. S9-W-31, 1991.

Sakimura, M., "Compatibility of Car-to-car collision safety", Journal of Japan Automobile Research Institute, Inc., Vol. 2, No. 6, pp.161-166, 1980 (in Japanese).

Sakurai, T., Aoki, T., "On the safety body structure of finite element method analysis", 12th ESV, pp.327-333, NHTSA, 1989.

Shearlaw, A., Thomas, P., "Vehicle to Vehicle Compatibility in Real World Accidents", 15th ESV, Paper Number 96-S4-O-04, 1996.

Schimmelpfenning, H., K., "The Gliding Zone", 15th ESV, Paper Number 96-S4-O-06, 1996.

Sugimoto, T., Kadotani, Y., Ohmura, S., "The Offset Crash Test –A Comparative Analysis of Test Methods", 16th ESV, Paper Number 98-S1-O08, 1998.

Tarrière, C., Morvan, Y., Steyer, C., Bellot, D., "Accident Research and Experimental Data Useful for an Understanding of the Influence of Car Structural Incompatibility on the Risk of Accident Injury", 14th ESV, Paper No. 94-S4-O-14, 1994a.

Tarrière, C., "Car Safety and Ratings: Comparative Study on Facts and Practices – Proposals", Proceedings of IRCOBI Conference on Biomechanics, Lyon, pp. 205-216, 1994b.

Tarrière, "Compatibility Issues and Vulnerable Uses", *Crashworthiness of Transportation Systems: Structural Impact and Occupant Protection*, Kluwer Academic Publishers, pp. 139-170, 1997.

Thomas, C., Faverjon, G., Henry, C., Le Coz Y. J., Got, C., Patel A., "The Problem of Compatibility in Car-to-Car Collisions", Proceeding of the 34th Annual Conference of the Association for the Advancement of Automotive medicine, pp. 253-267, 1990.

Thomas, P., "Real World Collisions and Appropriate Barrier Tests", Proceeding of 14th ESV, pp. 1450-1460, Paper No. 94-S8-W-19, 1994.

Trinca, G. W., Johnston, I.R., Campbell B. J., Haight, F. A., Knight, P. R., Mackay, G. M., McLean, A.J., Petrucelli, E., "Reducing Traffic Injury – A Global Challenge", Royal Australasian College of Suregeons, ISBN 0 909844 20 8, 1988.

Vallet G. et al., "A Contribution to the Analysis of the Aggressivity in Frontal Collision", 14th ESV, 1994.

Ventre P., "Homogenous Safety Amid Heterogeneous Car Population", 3rd ESV, 1972.

Versace, J., "A Review of the Severity Index", SAE Paper 710881, 15th Stapp Car Crash Conference, Society of Automotive Engineers, 1971.

Volksworgen AG, "Research Safety Vehicle – Phase I Volume 3 of 3", NHTSA, DOT HS-801 626, 1975.

Waltz, H., F., Kaeser, R., Nieder, P. "Occupant and exterior safety of low mass cars (LMC)", International Conference on Biomechanics of Impacts (IRCOBI), Berlin, 1991.

Watanabe, K., Yamaguchi, T., "Analysis of Factors Affecting Dummy Readings in Side Impact Tests, 12 the ESV, 1989.

Wood P. D., Mooney S., Doody, M., Ríordáin, "The Influence of Car Crush Behavior on Frontal Collision Safety and on the Car Size Effect", SAE Paper 930893, Society of Automotive Engineers, 1993.

Wykes J., Edward M., Hobbs, C., Compatibility Requirements for Cars in Frontal and Side Impact, 16th ESV Conference, Paper No. 98-S3-O04, 1998.

Yamanaka, A., Nagaike, N., "The Crash Test of Medium Duty Truck", 17th FISITA, 1978.

Yonezawa, H., Toyofuku, Y., Mizuno, K., Irie, Y.: Experimental Study on Absorbed Energy of Side Structure of Passenger Cars by 90-degrees Side Impact Test, 14th ESV Conference, Paper No. 94-S6-O-06 1994.

Yoshida, S., Matsuhasi, T., "Simulation System of Car-Pedestrian Accident to Evaluate Car Structure", PUCA '98, Proceedings Volume 1, pp. 285-288, 1998 (in Japanese).

PUBLICATIONS

This thesis is based on the following papers which are published in journals.

1. Mizuno, K., Yonezawa, H., "The Effect of Vehicle Mass in Car-to-Car Collisions", SAE Paper 960441, 1996 SAE Transactions Vol. 15, Journal of Passenger Cars, Section 6, pp. 395-403, Society of Automotive Engineers, 1997.
   [Sections 2.2.2, 2.2.5 and 2.4.2 are based on this paper.]

2. Mizuno, K., Umeda, T., Yonezawa, H., "The Relationship Between Car Size and Occupant Injury in Traffic Accidents in Japan", SAE Paper 970123, 1997 SAE Transactions Vol. 16, Journal of Passenger Cars, Section 6, pp. 199-213, Society of Automotive Engineers, 1998.
   [Sections 2.2.1, 2.4.1 and 2.5 are based on this paper.]

3. Mizuno, K., Kajzer, J., "Compatibility Problems in Frontal, Side, Single Car Collisions and Car-to-Pedestrian Accidents in Japan", International Journal of Accident Analysis & Prevention, Vol. 31, No.4, pp.89-99, 1999.
   [Sections 2.2.3, 2.2.4 and 5.2.1 are based on this paper.]

4. Mizuno, K., Kajzer, J., "Compatibility Analysis of Mini Cars in Frontal Collisions Using MADYMO", International Journal of Crashworthiness, Vol. 3, No. 2, pp.123-134, Woodhead Publishing Ltd., 1998.
   [Section 2.3 is based on this paper.]

5. Mizuno, K. and Kajzer, J., "The Compatibility Analysis of Automobile Collisions Using Accident Data and Simulation", Transaction of Japan Society of Mechanical Engineers, Series C, Vol. 65, No. 631, pp. 245-252, 1999 (in Japanese).
   [Section 2.3 is based on this paper.]

6. Mizuno, K. and Kajzer, J., "The Potential of Single-Car Crash Tests to Replace Car-to-Car Crash Test", Transaction of Society of Automotive Engineers of Japan (in Japanese, submitted).
   [Chapter 3 is based on this paper.]

7. Mizuno, K., Kajzer, J., Aiba, T., "The Influence of Vehicle Shape on Injury in Pedestrian-Vehicle Impact", Transaction of Society of Automotive Engineers of Japan (in Japanese, accepted).
   [Sections 5.2.2 and 5.3 are based on this paper.]

8. Mizuno, K., Yonezawa, H., Kajzer, J., "The Relation Between Head Injury and Impact Location in Pedestrian-Car Impacts", Transaction of Society of Automotive Engineers of Japan (in Japanese, accepted).
   [Section 5.4 is based on this paper.]